

DISSERTATION

**A novel three-body R -matrix
formalism for breakup reactions in
light nuclear systems**

Ausgeführt zum Zwecke der Erlangung des akademischen Grades eines
Doktors der technischen Wissenschaften unter der Leitung von

Univ.Prof. Dipl.-Ing. Dr.techn. Helmut Leeb

E 141

Atominstitut

eingereicht an der Technischen Universität Wien
Fakultät für Physik

von

Dipl.-Ing. Benedikt Raab, BSc

██

██

Wien, am 6.7.2022

.....

eigenhändige Unterschrift

Meinen Eltern

Summary

A good knowledge of nuclear reaction cross sections is an important prerequisite not only for the design of nuclear devices and the development of novel nuclear technologies, e.g. nuclear fusion on a large scale, but also for several applications, e.g. materials science, nuclear medicine, geology and space research. Hence, there is a worldwide effort to establish nuclear data libraries which represent our best knowledge of reaction cross sections. At present several evaluated nuclear data libraries exist containing the best quantitative knowledge of nuclear reaction data for a wide range of nuclei and projectiles. Especially for neutron-induced reaction cross sections of medium and heavy nuclei the libraries provide excellent descriptions of cross sections up to neutron energies of 200 MeV.

At low incident energies the reaction cross sections exhibit striking resonance structures associated with many-nucleon effects. These phenomena cannot be properly reproduced by (semi-)microscopic nuclear models. Usually R -matrix theory is applied to obtain a sufficiently accurate and consistent, but phenomenological description of the resonance region. However, the concept of standard R -matrix theory is only based on two-particle reaction channels. Three- and many-particle channels cannot be described by standard R -matrix theory and are usually treated in an approximative way, e.g. by sequential processes. In light nuclear systems, however, breakup reactions can even occur at low incident energies and often have a significant share on the reaction cross section. Consequently approximations become increasingly inadequate and there is a need for an exact treatment in the frame of R -matrix theory.

In this PhD thesis a novel R -matrix formalism for three-body reactions is presented. The first idea of such an R -matrix method was proposed by W. Glöckle based on the Faddeev equations and restricted to three identical particles in the exit channel. This model has been generalized to arbitrary particle masses and interactions in a previous work. In this PhD thesis essential modifications were performed in order to make the formalism applicable to realistic nuclear systems. A numerical implementation was successfully elaborated and first demonstrated on the neutron+deuteron system. Also the neutron+ ^9Be system was studied in the frame of the three-body R -matrix. The results for both systems are presented in the final chapter of this thesis.

Kurzfassung

Eine gute und zuverlässige Kenntnis nuklearer Reaktionsdaten ist unabdingbar für die Auslegung und das Design nuklearer Geräte und die Entwicklung neuer nuklearer Technologien wie Kernfusion in großtechnischem Maßstab. Darüber hinaus ist diese wichtig für weitere Anwendungen in den Bereichen wie Materialwissenschaft, Nuklearmedizin, Geologie und Raumfahrt. Aus diesem Grund besteht ein weltweites Bestreben zur Schaffung nuklearer Datenbanken, die den besten Kenntnisstand über Reaktionswirkungsquerschnitte enthalten. Derzeit existiert eine Zahl nuklearer Datenbanken, in denen der aktuell beste Wissensstand über eine Vielzahl nuklearer Reaktionen enthalten ist. Speziell für Neutronen-induzierte Reaktionen mittelschwerer und schwerer Kerne liegen profunde Daten der Wirkungsquerschnitte von Neutronenenergien bis 200 MeV vor.

Im niedrigen Energiebereich weisen die Reaktionswirkungsquerschnitte markante Resonanzstrukturen auf, die auf Vielteilcheneffekte zurückzuführen sind. Diese Strukturen können durch (semi-)mikroskopische Modelle nicht zufriedenstellend reproduziert werden. Daher wird im genannten Energiebereich hauptsächlich die R -matrix Theorie zur Beschreibung herangezogen. Sie bietet eine hinreichend genaue und konsistente, jedoch phänomenologische Beschreibung des Resonanzbereiches. Die Standardmethode der R -matrix Theorie beruht auf zwei-Teilchen Reaktionskanälen. Drei- oder Mehrteilchen-Reaktionskanäle werden üblicherweise approximativ behandelt, beispielsweise im Rahmen von sequentiellen Prozessen. Da jedoch in leichten nuklearen Systemen schon bei niedrigen Einfallenergien Aufbruchwirkungsquerschnitte einen signifikanten Anteil am Reaktionswirkungsquerschnitt haben können, sind solche approximative Methoden inadäquat. Daher besteht die Notwendigkeit einer exakten Behandlung dieser Reaktionen im Rahmen der R -matrix Theorie.

In dieser Dissertation wird eine neue R -matrix Methode zur Behandlung von dreikörper Kanälen präsentiert. Ein erster Ansatz einer solchen Methode wurde zuerst von Walter Glöckle vorgelegt, basierend auf den Faddeev-Gleichungen und beschränkt auf drei identische Teilchenmassen im Ausgangskanal. Dieses Modell konnte in einer vorangegangenen Arbeit auf beliebige Massen und Wechselwirkungen verallgemeinert werden. In der vorliegenden Arbeit wurden essentielle Modifikationen durchgeführt, um den Formalismus auf reale nukleare Systeme anwendbar zu machen. Eine numerische Umsetzung konnte erfolgreich ausgearbeitet und am Neutron+Deuteron System erst-

mals angewandt werden. Auch das Neutron+⁹Be System wurde im Rahmen der drei-Körper *R*-matrix studiert. Die Resultate beider Systeme werden im abschließenden Kapitel dieser Dissertation präsentiert.

Contents

1	Introduction	1
2	Basics principals of standard R-matrix theory	4
2.1	Basics of scattering theory	5
2.2	Standard R -matrix theory	11
3	Introduction into the 3-body problem in the frame of R-matrix theory	17
3.1	The general difficulty	17
3.2	Sequential Approach	18
4	Faddeev equations for three-body systems	20
4.1	Description of the three-body system	20
4.2	Faddeev equations	22
4.2.1	Lippmann-Schwinger equation	23
4.3	Faddeev equations for the T -operator	26
4.4	Faddeev equations for the resolvent and scattering states	29
5	A novel three-body R-matrix formalism	32
5.1	Faddeev equations and asymptotic wave functions	32
5.2	Derivation of the generalized three-body R -matrix formalism	42
5.2.1	Division of the Jacobi-coordinate space	42
5.2.2	Equations of three-body R -matrix theory	45
5.3	Formulation of a new applicable R -matrix method	52
5.4	Calculation of cross sections	59
6	Numerical implementation	64
6.1	Setting up a system of linear equations for $c_\mu^{(i)}$	64
6.2	Stability of the algorithm	68
7	Results	72
7.1	The neutron+deuteron system	72
7.2	Application of the novel formalism on the neutron+deuteron system . .	75
7.2.1	Pauli principle and consequences	75
7.2.2	Basis states	76

7.3	Results for the neutron+deuteron system	80
7.4	The problem of the continuity of flux	85
7.5	The neutron+ ⁹ Be system	95
7.5.1	Basis states	98
7.6	Results for the neutron+ ⁹ Be system	102
8	Conclusion and Outlook	108
	Appendix	112
A	Partial integration of Eq. (5.58)	112
B	Experimental data for the neutron+deuteron system	116
B.1	Breakup cross section	116
B.2	Elastic cross section	118
	Bibliography	119

1 Introduction

Reliable data of nuclear reactions are a crucial prerequisite in various scientific fields, especially for the construction and design of nuclear devices such as fusion or fission reactors. Therefore, there is a worldwide effort to obtain consistent and reliable sets of reaction data which represent our best knowledge of the reactions. In order to create such data sets all available experimental data of a certain group of reactions are retrieved [1] and an assessment of their quality is performed. In a further step these data undergo an evaluation process frequently based on Bayesian statistics which allows one to consistently combine these data with a-priori knowledge mostly given in terms of nuclear model calculations. This so-called "Evaluation Process" yields evaluated data sets with information also in energy regions where no measured data exist and the associated uncertainties. Finally, the evaluated data sets are collected in "Nuclear Data Libraries" [2, 3, 4] using the ENDF-format [5]. The evaluation process is well established for medium and heavy nuclear systems at energies above the resonance regime, but exhibits some problems in the resonance regime at low energies. First, there is a lack of a-priori knowledge because there are no microscopically-based nuclear models available which provide a quantitative description. Another open problem is the difficulty to establish reliable uncertainties associated with resonances. A first approach was given in [6].

At present reaction cross sections are usually described by R -matrix theory [7]. In general a phenomenological R -matrix description is used where the parameters (poles and widths) are adjusted in order to obtain the best agreement of the R -matrix model with experimental data. The phenomenological R -matrix does not contain microscopic information on the n -body structure and consequently it is limited in its predictive power. Alternatively the calculable R -matrix is based on a Hamiltonian with a microscopic potential, but similarly to other methods one cannot account for the complexity of the n -body system thus missing a quantitative description of the resonance regime. Both the phenomenological and the calculable R -matrix theory are originally designed for two-body channels only. Hence, when dealing with light nuclear systems there arises another difficulty namely the appearance of breakup channels even at low incident energies. Due to the lack of a corresponding R -matrix theory these many-particle channels have usually been treated in an approximative way using for instance sequential approach models [8]. However, in many light nuclear systems of interest, e.g. in

fusion research, breakup processes occur in the low energy range of a few MeV and have a significant share on the total reaction cross section. For such dominant breakup channels the validity of sequential approaches (Sec. 3.2) is questionable. In order to include dominant breakup channels in a consistent R -matrix analysis an extension of the R -matrix formalism to not-binary channels is required.

The focus of the present thesis is the extension of the R -matrix formalism to three-body breakup channels. They represent, apart from capture channels, a significant fraction of non-binary channels in the low energy regime of light nuclear systems. Furthermore there exists an exact quantum mechanical description of three-body problems via the Faddeev equations [9]. In 1974 W. Glöckle [10] presented a first proposal of a three-body R -matrix formalism for particles of equal masses based on the Faddeev equations. This concept could be successfully generalized to particles with different masses in [11] and thus became applicable to a wider range of nuclear systems. However, we are not aware of any demonstration or application of this method.

The developments of the R -matrix formalism in the present thesis started from the idea of Glöckle [10] to enter division in the Jacobi-coordinates. This assumption bypasses a conceptual problem hampering a straightforward extension of standard R -matrix theory to three- and many-body channels. In course of the developments in the present thesis significant modifications of the formalism apart from the generalization to different masses were required in order to obtain a working tool for an R -matrix type description for breakup channels. The new formalism was numerically implemented and successfully applied to experimental data of breakup reactions.

The present thesis is structured essentially in three parts. After this brief introduction chapters 2, 3 and 4 constitute the first part which gives a concise introduction into the theoretical basics required for the further developments. In chapter 2 the basis of standard R -matrix theory is revisited together with the most important quantities and relationships of scattering theory. In chapter 3 the difficulty of an extension of the standard R -matrix concept to three- and more-body channels is outlined. Furthermore, a frequently used approximative method, i.e. the sequential approach is sketched without details. Chapter 4 gives an introduction into the Faddeev equations and provides all basic definitions and relationships required for the development of the novel R -matrix formalism.

The second part comprising chapters 5 and 6 is the central part of this thesis and gives a detailed description of the formal developments (chapter 5) and numerical

implementation (chapter 6). It provides the details of the derivation of the complex set of equations and its transfer into a uniquely solvable system of linear equations for the expansion coefficients of the interior wave function and the T -amplitudes from which the breakup, the elastic scattering cross section and the rearrangement cross sections can be directly calculated.

The first applications of the three-body R -matrix formalism to real systems are subject of chapter 7, the third part. As a first application the neutron+deuteron system is considered which is the simplest and most genuine nuclear three-body system without further structures. The calculated results for the breakup reaction and for elastic scattering will be compared to experimental data. Also the optical theorem will be considered and possible algorithm errors will be specified. In the next step the three-body R -matrix is applied on the neutron+ ${}^9\text{Be}$ system. In this nuclear system the breakup reaction occurs at incident energies of about 1.6 MeV and has a significant share on the total cross section. It is of great importance in fusion devices since it serves as a neutron multiplier for tritium breeding. Therefore, a good knowledge of the neutron-induced reaction cross sections of ${}^9\text{Be}$ is important for the design and operation of fusion facilities in order to optimize the facility regarding maintenance, safety and production rate. Compared to the neutron+deuteron system there arise some more difficulties since the ground state of ${}^9\text{Be}$ is $J^\pi = 3/2^-$ and a pure s-wave description is no longer sufficient. Again the calculated results will be presented together with measured data sets.

Finally, in chapter 8, a summary and outlook on further applications and combinations with standard two-body R -matrix theory will be given.

2 Basics principals of standard R -matrix theory

Standard R -matrix theory is formulated for reactions of particle systems for which non-relativistic quantum mechanics is applicable. Hence creation and destruction processes of particles are excluded. In order to treat the dynamics of an N -nucleon system in the frame of R -matrix theory one assumes a space-fixed finite *channel surface* that confines the microscopic nuclear interactions into an interior region (Fig. 1). The lack

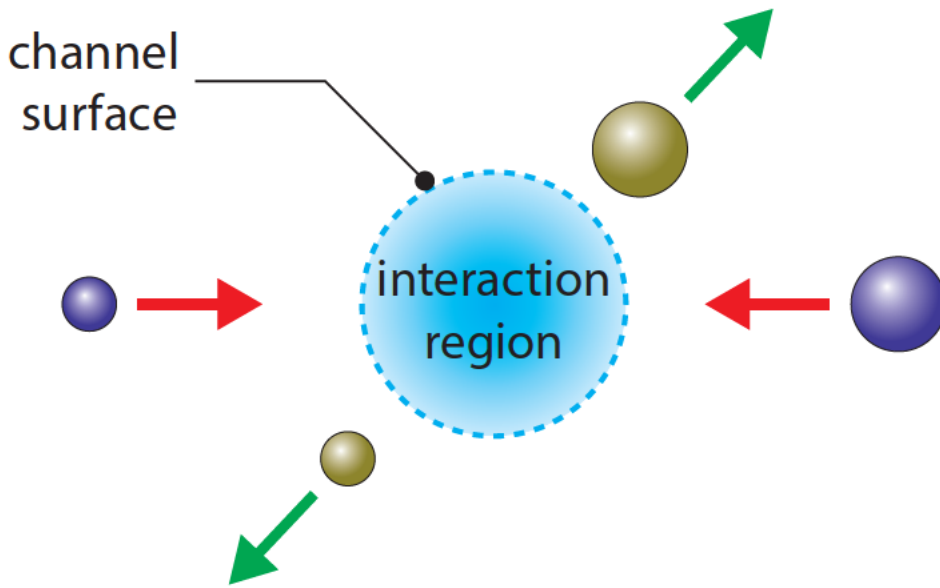


Figure 1: Division of space assumed by standard R -matrix theory at the example of a two-body reaction in the cm-system.

of detailed knowledge of the complex many-body wave function in this area is effectively described by an expansion over a set of basis states which is matched at the channel surface to the external region where no mutual polarization of the objects occur. The problem of a projectile interacting with a single nucleon or a nucleus of N nucleons is thus transferred to an effective two-body problem. Therefore it is convenient to change to the center of mass system. As a consequence in the external region all quantities (potential, wave functions etc.) are given in terms of the distance r between the two objects of the channel and the center of mass motion vanishes.

A comprehensive and detailed description of the R -matrix formalism is given by Lane and Thomas [8]. In the following a brief sketch of scattering theory and standard two-body R -matrix theory following [12] and [13] will be given. These relations will be

relevant for the further developments regarding three-body channels.

2.1 Basics of scattering theory

The starting point is a simple single-channel problem governed by a central potential $V(r)$ and described by the radial Schrödinger equation

$$(T_\ell + V(r) - E) u_\ell(r) = 0 \quad (2.1)$$

with the kinetic energy operator

$$T_\ell = -\frac{\hbar^2}{2\mu} \left(\frac{d^2}{dr^2} - \frac{\ell(\ell+1)}{r^2} \right). \quad (2.2)$$

Here, E is the total energy of the system, ℓ the orbital momentum quantum number and μ is the reduced mass of the channel.

We consider the eigenstates $\phi_\alpha(t)$ of the free Hamiltonian $H_0 = T_\ell$

$$H_0 |\phi_\alpha(t)\rangle = i\hbar \frac{\partial}{\partial t} |\phi_\alpha(t)\rangle \quad (2.3)$$

and $\psi_\alpha(t)$ of the interaction Hamiltonian $H = T_\ell + V(r)$

$$H |\psi_\alpha(t)\rangle = i\hbar \frac{\partial}{\partial t} |\psi_\alpha(t)\rangle. \quad (2.4)$$

The time evolution under H of $\psi_\alpha^{(\pm)}(t)$ is given by

$$\psi_\alpha^{(\pm)}(t) = U(t, t') \psi_\alpha^{(\pm)}(t') \quad (2.5)$$

with the time evolution operator

$$U(t, t') = e^{-i/\hbar H(t-t')}. \quad (2.6)$$

In infinite past or future depending if one considers outgoing (+) or incoming (-) solutions $\psi_\alpha^{(\pm)}$ equals ϕ_α so that we can write

$$\psi_\alpha^{(\pm)}(t) = U(t, t') \psi_\alpha^{(\pm)}(t') = \lim_{t' \rightarrow \mp\infty} U(t, t') \phi_\alpha(t'), \quad (2.7)$$

or equivalently, using the Green's function,

$$\psi_{\alpha}^{(+)}(t) = i \lim_{t' \rightarrow -\infty} G^{(+)}(t, t') \phi_{\alpha}(t'). \quad (2.8)$$

The Green's functions G is defined by

$$(E - H)G = \mathbb{1}. \quad (2.9)$$

Similarly we have a Green's function G_0 associated with the free Hamiltonian H_0

$$(E - H_0)G_0 = \mathbb{1}. \quad (2.10)$$

Considering the relationship

$$G_0(E - H)G = G_0(E - H_0 - V)G = G_0(E - H_0)G - G_0VG = G - G_0VG \quad (2.11)$$

one obtains

$$G = G_0 + G_0VG \quad (2.12)$$

which is the Dyson equation. Plugging Eq. (2.12) into Eq. (2.8) yields under the assumption of an instantaneous interaction

$$\psi_{\alpha}^{(+)}(t) = i \lim_{t' \rightarrow -\infty} G_0^{(+)}(t, t') \phi_{\alpha}(t') + i \lim_{t' \rightarrow -\infty} \int dt'' G_0^{(+)}(t, t'') V(t'') G^{(+)}(t'', t') \phi_{\alpha}(t') \quad (2.13)$$

and with

$$i \lim_{t' \rightarrow -\infty} G^{(+)}(t'', t') \phi_{\alpha}(t') = \psi_{\alpha}^{(+)}(t'') \quad (2.14)$$

we finally get the Lippmann-Schwinger equation

$$\psi_{\alpha}^{(+)}(t) = \phi_{\alpha}(t) + \int dt'' G_0^{(+)}(t, t'') V(t'') \psi_{\alpha}^{(+)}(t''). \quad (2.15)$$

As already mentioned above one boundary condition of the scattering problem is the equivalence of $\psi_{\alpha}^{(+)}$ with the free state ϕ_{α} in infinite past, i.e.

$$\lim_{t \rightarrow -\infty} [e^{-i/\hbar H t} \psi_{\alpha}^{(+)}(t) - e^{-i/\hbar H_0 t} \phi_{\alpha}(t)] = 0. \quad (2.16)$$

This leads to the relationship

$$\psi_{\alpha}^{(+)}(t' = 0) = \lim_{t \rightarrow -\infty} (e^{i/hHt} e^{-i/hH_0 t}) \phi_{\alpha}(t' = 0) = \Omega^{(+)} \phi_{\alpha}(t' = 0), \quad (2.17)$$

with $\Omega = \lim_{t \rightarrow -\infty} (e^{i/hHt} e^{-i/hH_0 t})$ is the so-called Møller operator or wave operator. The free states build up the complete Hilbert space, while the scattering states form a subspace which excludes the part formed by the bound states. Therefore the Møller operator is an isometric operator satisfying the relations

$$\Omega^{(+)\dagger} \Omega^{(+)} = \Omega^{(-)\dagger} \Omega^{(-)} = \mathbf{1} \quad (2.18)$$

and

$$\Omega^{(+)} \Omega^{(+)\dagger} = \Omega^{(-)} \Omega^{(-)\dagger} = \mathbf{1} - \sum_n \psi_n \psi_n^{\dagger}, \quad (2.19)$$

where ψ_n denotes the bound states sustained by H . The second term on the right hand side of Eq. (2.19) is denoted as defect. In the absence of bound states Ω is unitary. The second form of the Dyson equation (2.12) reads

$$G = G_0 + GVG_0. \quad (2.20)$$

This expression can be applied onto a free state in order to obtain a scattering state

$$\begin{aligned} \psi^{(+)}(E, \alpha) &= \lim_{\epsilon \rightarrow 0^+} [\pm i\epsilon(E + i\epsilon - H)^{-1}] \phi(E, \alpha) = G^{(+)}(E) \phi(E, \alpha) \\ &= \phi(E, \alpha) + G^{(+)}(E) V \phi(E, \alpha) = [\mathbf{1} + G^{(+)}(E) V] \phi(E, \alpha), \end{aligned} \quad (2.21)$$

where the energy dependent Green's function results from the transformation

$$G_0^{(\pm)}(E) = \frac{1}{\hbar} \int_{-\infty}^{\infty} dt e^{iEt/\hbar} G_0^{(\pm)}(t) \quad (2.22)$$

Comparing Eq. (2.21) with Eq. (2.17) one finds a relationship between the Møller operator and the Green's function

$$\Omega^{(+)} = \mathbf{1} + G^{(+)}(E) V. \quad (2.23)$$

One of the most important quantities in scattering theory is the S -matrix. It is calculated as the overlap of the plane wave $\psi_{\beta}^{(-)}(t)$, which in infinite future has the set of quantum numbers β , with $\psi_{\alpha}^{(+)}(t)$, which is a plane wave with quantum numbers α

in the infinite past. Hence,

$$\begin{aligned} S_{\beta\alpha} &= \langle \psi_{\beta}^{(-)}(t) | \psi_{\alpha}^{(+)}(t) \rangle = \langle \Omega^{(-)} \phi_{\beta}(t) | \Omega^{(+)} \phi_{\alpha}(t) \rangle = \langle \phi_{\beta}(t) | (\Omega^{(-)})^{\dagger} \Omega^{(+)} | \phi_{\alpha}(t) \rangle \\ &= \langle \phi_{\beta}(t) | S | \phi_{\alpha}(t) \rangle, \end{aligned} \quad (2.24)$$

where the definition of $\Omega^{(\pm)}$ from Eq. (2.17) was used. With Eq. (2.24) the S -matrix can be expressed via the Møller operator

$$S = (\Omega^{(-)})^{\dagger} \Omega^{(+)} . \quad (2.25)$$

The S -matrix is unitary

$$S^{\dagger} S = \mathbb{1} \quad (2.26)$$

which means that its domain and codomain are identical. In angular momentum representation and for spherical symmetric potentials the S -matrix can be written as

$$\langle \ell' m' | \hat{S} | \ell m \rangle = \delta_{\ell' \ell} \delta_{m' m} S_{\ell} = \delta_{\ell' \ell} \delta_{m' m} e^{2i\delta_{\ell}}, \quad (2.27)$$

where δ_{ℓ} is the phase shift in the ℓ^{th} partial wave.

Another essential quantity is the transition- or T -matrix defined by

$$T_{\beta\alpha} = \langle \phi(E_{\beta}, \beta) | V | \psi^{(+)}(E_{\alpha}, \alpha) \rangle \quad (2.28)$$

Using relation (2.21) one obtains

$$T_{\beta\alpha} = \langle \phi(E_{\beta}, \beta) | V + VG^{(+)}V | \phi(E_{\alpha}, \alpha) \rangle \quad (2.29)$$

and consequently the (two-body) T -operator is

$$T(E) = V + VG^{(+)}(E)V . \quad (2.30)$$

If we consider the T -matrix element (2.29) we can distinguish three different cases. First if the energies E_{α}, E_{β} and E are all different from each other it is the *off-shell* T -matrix. Second if two of the three energies are equal and the third one is not, it is called *half off-shell* T -matrix. And finally if all energies are equal it is the *on-shell* T -matrix. The *on-shell* quantities will be important for the following three-body formalism and therefore we will proceed with these quantities.

The on-shell part \tilde{S} of the S -matrix is obtained by

$$S_{\beta\alpha} = \delta(\vec{k}_b - \vec{k}_a) \tilde{S}_{\beta\alpha} = \frac{\hbar^2}{\mu k_a} \delta(E_\beta - E_\alpha) \tilde{S}_{\beta\alpha}, \quad (2.31)$$

with the reduced mass μ of the two collision partners and the relative wave vector k_a . The on shell S -matrix is related to the T -matrix via

$$\tilde{S}_{\beta\alpha} = \delta(\Omega_b - \Omega_a) - i\mu k_a \frac{2\pi}{\hbar^2} T_{\beta\alpha}. \quad (2.32)$$

Analogously one can define an on-shell T -matrix \tilde{T} as

$$\tilde{T}_{\beta\alpha} = \mu k_a \frac{1}{\hbar^2} T_{\beta\alpha} \quad (2.33)$$

and relation (2.32) becomes

$$\tilde{S}_{\beta\alpha} = \delta(\Omega_b - \Omega_a) - 2\pi i \tilde{T}_{\beta\alpha} \quad (2.34)$$

or in operator notation

$$S = \mathbb{1} - 2\pi i T \quad (2.35)$$

valid on the energy shell.

With the nomenclature $\beta = \vec{k}'$ and $\alpha = \vec{k}$ we have

$$\langle \phi(\vec{k}') | V | \psi^{(+)}(\vec{k}) \rangle = \langle \phi(\vec{k}') | \hat{T} | \phi(\vec{k}) \rangle = T_{\vec{k}'\vec{k}}. \quad (2.36)$$

The unitary relation for the on-shell S -matrix reads

$$\int d\Omega'' \tilde{S}_{\vec{k}''\vec{k}'}^* \tilde{S}_{\vec{k}''\vec{k}} = \delta(\Omega' - \Omega). \quad (2.37)$$

Starting from this relation and using Eq. (2.32) we get (with $E'' = E' = E$)

$$\begin{aligned}
\delta(\Omega' - \Omega) &= \int d\Omega'' \tilde{S}_{\vec{k}'\vec{k}'}^* \tilde{S}_{\vec{k}''\vec{k}} \\
&= \int d\Omega'' \left[\delta(\Omega'' - \Omega') - i\mu k \frac{2\pi}{\hbar^2} T_{\vec{k}''\vec{k}'} \right]^* \left[\delta(\Omega'' - \Omega) - i\mu k \frac{2\pi}{\hbar^2} T_{\vec{k}''\vec{k}} \right] \\
&= \delta(\Omega' - \Omega) - i\mu k \frac{2\pi}{\hbar^2} [T_{\vec{k}'\vec{k}} - T_{\vec{k}\vec{k}'}^*] + \left(\mu k \frac{2\pi}{\hbar^2} \right)^2 \int d\Omega'' T_{\vec{k}'\vec{k}'}^* T_{\vec{k}''\vec{k}} \\
&\Rightarrow i\mu k \frac{2\pi}{\hbar^2} [T_{\vec{k}'\vec{k}} - T_{\vec{k}\vec{k}'}^*] = \left(\mu k \frac{2\pi}{\hbar^2} \right)^2 \int d\Omega'' T_{\vec{k}'\vec{k}'}^* T_{\vec{k}''\vec{k}}.
\end{aligned} \tag{2.38}$$

On the energy shell $\vec{k}' = \vec{k}$ and thus

$$\begin{aligned}
i[T_{\vec{k}\vec{k}} - T_{\vec{k}\vec{k}}^*] &= \mu k \frac{2\pi}{\hbar^2} \int d\Omega'' T_{\vec{k}''\vec{k}}^* T_{\vec{k}''\vec{k}} \\
-2 \operatorname{Im} T_{\vec{k}\vec{k}} &= \mu k \frac{2\pi}{\hbar^2} \int d\Omega'' |T_{\vec{k}''\vec{k}}|^2
\end{aligned} \tag{2.39}$$

which is the optical theorem in terms of the T -amplitudes. Using the on-shell T -elements from Eq. (2.33) with the same nomenclature $\beta = \vec{k}'$ and $\alpha = \vec{k}$ reading

$$\tilde{T}_{\vec{k}'\vec{k}} = \mu k \frac{1}{\hbar^2} T_{\vec{k}'\vec{k}} \tag{2.40}$$

and inserting this expression into the optical theorem (2.39) yields

$$\begin{aligned}
-2 \frac{\hbar^2}{\mu k} \operatorname{Im} \tilde{T} &= 2\pi \frac{\hbar^2}{\mu k} \int d\Omega'' |\tilde{T}_{\vec{k}''\vec{k}}|^2 \\
\operatorname{Im} \tilde{T} &= -\pi \int d\Omega'' |\tilde{T}_{\vec{k}''\vec{k}}|^2
\end{aligned} \tag{2.41}$$

which is the optical theorem in terms of the on-shell T -amplitudes.

The T -matrix is a crucial quantity for all scattering processes because it grasps the effect of the interaction. Hence, it provides the necessary input for the determination of the elastic cross section [20]

$$\sigma_{elastic} = \left(\frac{2\pi}{\hbar} \right)^4 \mu^2 \int d^2\hat{k}' |T_{\vec{k}'\vec{k}}|^2 \tag{2.42}$$

where μ is the reduced mass of projectile and target. The T -matrix elements are

directly proportional to the scattering amplitude $f_{\vec{k}}^{(+)}(\hat{r})$,

$$f_{\vec{k}}^{(+)}(\hat{r}) = -\mu \left(\frac{2\pi}{\hbar^2} \right)^2 T_{\vec{k}\hat{r}\vec{k}} = -\frac{4\pi^2}{\hbar^2} \frac{\tilde{T}_{\vec{k}\hat{r}\vec{k}}}{k}, \quad (2.43)$$

and the elastic cross section is calculated according to

$$\sigma_{elastic} = \int d\hat{r} \left| f_{\vec{k}}^{(+)}(\hat{r}) \right|^2 = \mu^2 \left(\frac{2\pi}{\hbar^2} \right)^4 \int d\hat{r} |T_{\vec{k}\hat{r}\vec{k}}|^2 = \frac{16\pi^4}{\hbar^4 k^2} \int d\hat{r} \left| \tilde{T}_{\vec{k}\hat{r}\vec{k}} \right|^2. \quad (2.44)$$

2.2 Standard R -matrix theory

The potential $V(r)$ in Eq. (2.1) is usually composed of a Coulomb part of infinite range and a short-ranged nuclear part. Introducing a matching radius a sufficiently large that the nuclear part is negligible defines a proper channel surface and thus the separation of the space into an internal and an external region. In the external region the form of the radial wave function $u_\ell(r)$ is well known and given in terms of the S -matrix element $S_\ell(E)$ from Eq. (2.27) which in R -matrix theory is usually denoted by $U_\ell(E)$, i.e.

$$u_\ell^{ext}(r) = C_\ell [I_\ell(kr) - U_\ell \cdot O_\ell(kr)] \quad \text{for } r \geq a, \quad (2.45)$$

where $k = \sqrt{2\mu E/\hbar^2}$. The incoming function

$$I_\ell = G_\ell - iF_\ell \quad (2.46)$$

and outgoing function

$$O_\ell = G_\ell + iF_\ell \quad (2.47)$$

are defined in terms of the regular and irregular Coulomb functions F_ℓ and G_ℓ , respectively. The regular Coulomb functions F_ℓ vanish at the origin and are asymptotically normalized as

$$F_\ell(\eta, kr) \xrightarrow{kr \rightarrow \infty} \sin(kr - 1/2\ell\pi - \eta \ln(2kr) + \sigma_\ell), \quad (2.48)$$

whereas the irregular Coulomb functions G_ℓ are unbound at the origin (except for $\ell = \eta = 0$) and have the asymptotic form

$$G_\ell(\eta, kr) \xrightarrow{kr \rightarrow \infty} \cos(kr - 1/2\ell\pi - \eta \ln(2kr) + \sigma_\ell). \quad (2.49)$$

The Coulomb phase shift σ_ℓ is given as

$$\sigma_\ell = \arg \Gamma(\ell + 1 + i\eta) \quad (2.50)$$

with the Euler function

$$\Gamma(z) = \int_0^\infty x^{z-1} e^{-x} dx \quad (2.51)$$

for $\text{Re}(z) > 0$.

In the asymptotic region the functions I_ℓ and O_ℓ represent incoming and outgoing waves, respectively. The behavior is directly reflected in the asymptotic form,

$$I_\ell(\eta, kr) \xrightarrow{kr \rightarrow \infty} \exp[-i(kr - 1/2\ell\pi - \eta \ln(2kr) + \sigma_\ell)] \quad (2.52)$$

and

$$O_\ell(\eta, kr) \xrightarrow{kr \rightarrow \infty} \exp[i(kr - 1/2\ell\pi - \eta \ln(2kr) + \sigma_\ell)]. \quad (2.53)$$

In the case of at least one of the two particles being neutral the regular and irregular Coulomb functions simplify to $F_\ell(0, kr) = kr j_\ell(kr)$ and $G_\ell(0, kr) = kr n_\ell(kr)$ with $j_\ell(kr)$ and $n_\ell(kr)$ being the spherical Bessel and Neumann functions.

In the internal region the radial wave function $u_\ell(r)$ is represented by an expansion over a finite set of N linearly independent basis functions, $\varphi_j(r), j = 1, \dots, N$,

$$u_\ell^{\text{int}}(r) = \sum_{j=1}^N c_j \varphi_j(r). \quad (2.54)$$

In order to describe a physical solution the basis functions φ_j must vanish at $r = 0$, but they must not satisfy specific boundary conditions at the matching radius $r = a$.

A solution of Eq. (2.1), i.e. the radial wave function $u_\ell(r)$ and its derivative $u'_\ell(r)$, must be continuous at each r -value in the domain $r \in [0, \infty[$ and especially at the matching radius a . The matching of the external wave function u_ℓ^{ext} , Eq. (2.45), and the internal wave function u_ℓ^{int} , Eq. (2.54), at the channel surface provides a boundary condition, which is conveniently expressed by the definition of the R -matrix $R_\ell(E)$,

$$u_\ell(r = a) = R_\ell(E) [a u'_\ell(r = a) - B u_\ell(r = a)], \quad (2.55)$$

where B is a dimensionless boundary parameter. The inverse of the R -matrix is directly

related to the logarithmic derivative of the wave function at the matching radius,

$$R_\ell^{-1}(E) = a \frac{u'_\ell(a)}{u_\ell(a)} - B. \quad (2.56)$$

The R -matrix takes a particularly convenient form for a Hamiltonian which is hermitian on the domain of the internal region $r \in [0, a]$. This is not satisfied for the Hamiltonian of Eq. (2.1), but can easily be restored by introducing the Bloch operator [17],

$$\hat{L} = \frac{\hbar^2}{2\mu} \delta(r - a) \left(\frac{d}{dr} - \frac{B}{r} \right) \quad (2.57)$$

into the Schrödinger equation. This leads to the Bloch-Schrödinger equation,

$$\left[\left(T_\ell + \hat{L} - E \right) + V(r) \right] u_\ell^{\text{int}}(r) = \hat{L} u_\ell^{\text{ext}}(r). \quad (2.58)$$

Using Eq. (2.54) and Eq. (2.45) for the radial wave function $u_\ell(r)$ in Eq. (2.58) and projecting Eq. (2.58) on the set of basis states at $r = a$ yields the matrix equation

$$\sum_{j=1}^N \langle \varphi_i | \hat{C}_\ell(E, B) | \varphi_j \rangle c_j = \frac{\hbar^2}{2a\mu} \varphi_i(a) \left[a \cdot u_\ell^{\prime \text{ext}}(a) - B \cdot u_\ell^{\text{ext}}(a) \right], \quad i = 1, \dots, N \quad (2.59)$$

where $\hat{C}(E, B)$ is defined by

$$\hat{C}(E, B) = T_\ell + \hat{L} - E + V(r). \quad (2.60)$$

It is important to remark that Eq. (2.59) implies that the solution of the Bloch-Schrödinger equation is fully determined by the internal region, while the right-hand side of Eq. (2.58) contains only values of the channel surface. The expansion coefficients c_j are obtained by solving the system of linear equations (2.59)

$$c_j = \frac{\hbar^2}{2a\mu} \sum_{i=1}^N \varphi_i(a) (C^{-1})_{ij} \left[a \cdot u_\ell^{\prime \text{ext}}(a) - B \cdot u_\ell^{\text{ext}}(a) \right], \quad (2.61)$$

with

$$C_{ij} = \langle \varphi_i | C(E, B) | \varphi_j \rangle. \quad (2.62)$$

Introducing these coefficients (2.61) into Eq. (2.54) at $r = a$ gives

$$u_l(a) = \frac{\hbar^2}{2a\mu} \sum_{j=1}^N \varphi_j(a) \sum_{i=1}^N \varphi_i(a) (C^{-1})_{ij} [a \cdot u_\ell^{\text{ext}}(a) - B \cdot u_\ell^{\text{ext}}(a)] \quad (2.63)$$

and with the definition of the R -matrix in Eq. (2.55)

$$R_\ell(E, B) = \frac{\hbar^2}{2a\mu} \sum_{j=1}^N \sum_{i=1}^N \varphi_i(a) (C^{-1})_{ij} \varphi_j(a). \quad (2.64)$$

Assuming that the basis functions $\varphi_i(r)$ are orthonormal the matrix C^{-1} can be written in its spectral representation

$$[C(E, B)]^{-1} = \sum_{n=1}^N \frac{\vec{v}_{n\ell} \vec{v}_{n\ell}^T}{E_{n\ell} - E} \quad (2.65)$$

with the eigenvalues $E_{n\ell}$ and the corresponding eigenvectors $\vec{v}_{n\ell}$,

$$C(0, B) \vec{v}_{n\ell} = E_{n\ell} \vec{v}_{n\ell}. \quad (2.66)$$

The eigenvectors fulfill the condition $\vec{v}_{n\ell}^T \vec{v}_{n'\ell} = \delta_{nn'}$. Inserting expression (2.66) into Eq. (2.64) yields the spectral representation of the R -matrix,

$$R_\ell(E, B) = \sum_{n=1}^{\infty} \frac{\gamma_{n\ell}^2}{E_{n\ell} - E}. \quad (2.67)$$

In a complete basis the energies $E_{n\ell}$ are exact eigenvalues of the Hamilton operator $H_\ell = T_\ell + V(r) + \hat{L}(B)$. The quantities $\gamma_{n\ell}$ are denoted as "reduced width amplitudes" and $\gamma_{n\ell}^2$ reduced widths. They are connected to the basis functions at the matching radius a

$$\gamma_{n\ell} = \left(\frac{\hbar^2}{2\mu a} \right)^{1/2} \Phi_{n\ell}(a), \quad (2.68)$$

with

$$\Phi_{n\ell}(r) = \sum_{i=1}^N v_{n\ell,i} \varphi_i(r). \quad (2.69)$$

Here, $v_{n\ell,i}$ denotes the i -th component of the eigenvector $\vec{v}_{n\ell}$. However, within the frame of phenomenological R -matrix theory the form (2.67) is replaced by a finite

sum and well suited to fit a certain number of pole and widths parameters to measured data. Once fitted to available experimental reaction data in a certain energy region the R -matrix provides a tool for calculating consistently different observables for a large energy range, e.g. the phase shift

$$\tan(\delta_\ell) = \frac{ka R_\ell(E) F'_\ell(\eta, ka) - F_\ell(\eta, ka)}{ka R_\ell(E) G'_\ell(\eta, ka) - G_\ell(\eta, ka)} \quad (2.70)$$

and all observables derived from it.

With the external wave function (2.45), its derivative and the definition of the R -matrix, Eq. (2.56), the scattering matrix U_ℓ can be expressed in terms of the R -matrix as follows

$$U_\ell = e^{2i\phi_\ell} \frac{1 - (L_\ell^* - B)R_\ell(E, B)}{1 - (L_\ell - B)R_\ell(E, B)}, \quad (2.71)$$

where

$$L_\ell = ka \frac{O'_\ell(ka)}{O_\ell(ka)} \quad (2.72)$$

is the dimensionless logarithmic derivative of O_ℓ in Eq. (2.47) at the channel radius a , L^* denotes the complex conjugate of L and

$$\phi_\ell = -\arctan[F_\ell(ka)/G_\ell(ka)] \quad (2.73)$$

is the hard-sphere phase shift.

Using the relationship between the R -matrices with different B -values,

$$\frac{1}{R_\ell(E, 0)} = \frac{1}{R_\ell(E, B)} + B, \quad (2.74)$$

one can show that Eq. (2.71) is independent of the boundary parameter B which is a physical requirement that the scattering matrix U_ℓ must not depend on the parameter B .

The single-channel case where the R -matrix is a number can be generalized to a multi-channel system based on the matrix equation

$$\sum_d [(T_c + E_c - E) \delta_{cd} + V_{cd}] u_d = 0, \quad (2.75)$$

where c, d, \dots denote the different channels. E_c is a diagonal matrix which contains for each channel the threshold where it energetically opens. Again in order to restore

hermiticity on the interval $[0, a]$ a Bloch operator \hat{L}_c is introduced for each channel c ,

$$\hat{L}_c = \frac{\hbar^2}{2\mu_c} \delta(r - a_c) \left(\frac{d}{dr} - B_c \right). \quad (2.76)$$

In analogy to the single channel system the Bloch-Schrödinger equation of the coupled channel system is projected onto the basis states yielding

$$\sum_d \langle \varphi_i | \hat{C}_{c,d}(E, B) | \varphi_j \rangle c_{d,j} = \sum_d \frac{\hbar^2}{2a\mu_d} \varphi_i(a) \times [a \cdot u_d^{\text{ext}}(a) - B_d \cdot u_d^{\text{ext}}(a)]. \quad (2.77)$$

The summation on the right hand side is performed over all involved channels and contains only quantities of the external regions. This allows a clear separation into an internal and external region. Finally one ends up with a generalized form of the R -matrix for the multi-channel case

$$R_{cc'}(E, B) = \sum_{n=1}^{\infty} \frac{\gamma_{nc} \gamma_{nc'}}{E_n - E}. \quad (2.78)$$

Here, $R_{cc'}$ is a matrix of dimension $N_c \times N_c$ with N_c being the number of reaction channels at energy E . This form of the R -matrix plays an important role in phenomenological R -matrix analyses of experimental data where it provides a simultaneous consistent description for all the reaction channels. To that end Eq. (2.78) is used with a finite number of poles at real energies E_n and widths γ_{nc} and $\gamma_{nc'}$ which are fitted to experimental data in the desired energy region. Poles that are located outside this energy region are accounted for by so called background poles which influence the cross section in the considered energy range by shifting its ground level. Because of rotational invariance and the properties of the nuclear and the Coulomb force the total angular momentum J and parity π are conserved quantities. Consequently the R -matrix must be considered for a given J^π and must include all sub-channels coupling to the channel J^π . The R -matrices for different J^π are in this case disjunct.

3 Introduction into the 3-body problem in the frame of R -matrix theory

3.1 The general difficulty

In nuclear collisions breakup channels with three outgoing particles may occur at rather low energies in the resonance region, especially in light nuclear systems.

Albeit total energy and momentum must always be conserved in three-body kinetics there remains freedom in mutual directions and the partial kinetic energy of the three collision partners. Thus in a general three-body channel the external region in which no mutual polarization of the bodies occur cannot be fixed in space. This feature of three-body problems represents a severe obstacle for the extension of the R -matrix formalism to three- and many-body channels. Due to the lack of an interaction region confined in space the introduction of a channel surface is not possible. Therefore an extension of the R -matrix formalism to three- and many-body problems is not straightforward and requires major conceptual modifications. At present no generally applicable R -matrix formalism for three- and many-body channels is available.

In their seminal work on R -matrix theory Lane and Thomas [8] present some ideas on approximations which bypass the difficulty of defining a channel surface of the three-body problem. One possibility is the so-called sequential approach in which the three-body breakup is represented as a two-step process of binary reactions. More details on this approach and its validity are given in subsection 3.2. A second approach to account for non-binary channels is offered by the reduced R -matrix, a concept also first presented by Lane and Thomas [8]. In this case one considers an R -matrix analysis of an incomplete system, i.e. not all energetically open channels are included in the R -matrix analysis. Because of the loss of flux into ignored channels the S -matrix associated with the R -matrix analysis is not unitary. Hence, the defect of the unitarity is directly related with the total cross section for transitions into the ignored channels. This approach is frequently used to include capture reaction with the Reich-Moore approximation [14]. This method was not used for other channels, e.g. breakup channels, because of lack of proper parametrization for the reduced R -matrix. Recently, the nuclear data group at TU Wien developed R -matrix parametrizations suitable to account for breakup channels [15]. First reduced R -matrix analyses are currently in progress [16].

3.2 Sequential Approach

In nuclear collisions breakup channels with three outgoing nuclei may occur at rather low energies in the resonance region, especially in light nuclear systems. Therefore the description of breakup channels in R -matrix analyses of such nuclear systems is important. Being aware of the difficulty of R -matrix theory to describe systems with energetically open three- and many-body channels, the possibility of approximations was considered. In the following the sequential approach is sketched according to [13].

In the seminal work of Lane and Thomas [8] the treatment of breakup channels as a succession of two two-body disintegrations is worked out. This procedure is applicable if at least two of the three outgoing nuclei form a long-lived compound. In this case the wave function components in all unbound channels are negligible and an approximate finite channel surface can be given. Thus the breakup reaction appears as two successive two-body processes (see Fig. 2).

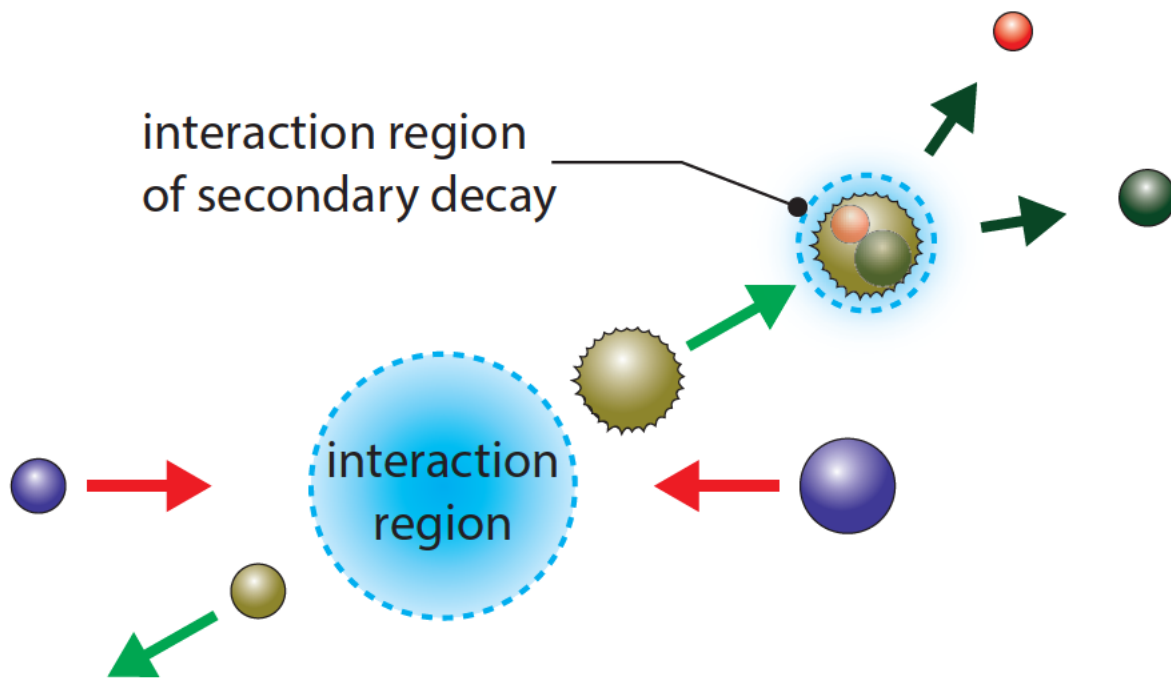


Figure 2: Illustration of a three-body breakup reaction involving a long-lived reaction product as two successive two-body processes in the C.M.-system.

The procedure has been worked out in detail in Ref. [8]. The key for the treatment of successive two-body reactions is the enumeration of the breakup channels. For a

given total energy E the energies E_α and E_β are given and consequently we know the energetically open unbound states (labeled by r) of the long-lived compound β . Thus the open states of β are given by $\psi_{c(E_\beta, r)}$ where the index c specifies the composition (α, β) of the nuclear system.

The inclusion of the successive breakup is easily implemented by substituting the \sum_c by $\sum_c \sum_r \int dE_\beta$ in all expressions. Thus the total asymptotic wave function of the system takes the form

$$\Psi_c \sim I_c - \sum_{c'} U_{c', c} O_{c'} - \sum_{c', r'} \int dE'_\beta U_{c'(E'_\beta, r'), c} O_{c'}, \quad (3.1)$$

where the first sum describes the two-body reaction into the composition (α, β) and the last sum gives the contribution of the subsequent decay of β . Using the collision matrix elements $U_{c'(E'_\beta, r'), c}$ one can evaluate the cross section of the breakup in the channel $c'(E'_\beta, r')$ and integrating over all admissible E'_β and summing over all open channel r' yields the cross section for given three end products.

4 Faddeev equations for three-body systems

The sequential approach discussed above is a reasonable approximation which is applicable if a long-lived nucleus is involved in the breakup reaction. A quantum mechanically exact treatment of three bodies exhibits the problem that the Lippmann-Schwinger equation (2.15) does not provide a unique solution [21]. This difficulty was solved by L. Faddeev [9] who set up a set of three equations which is the basis of W.Glöckle's proposal for a three-body R -matrix theory published in 1974 [10].

In this section a brief summary of Faddeev's three-body equations according to [11] is given followed by an introduction into the relations used by Glöckle for his formalism. In the next step the generalized formulæ derived in [11] are recapitulated and some essential modifications that make the formalism applicable to real nuclear systems are introduced. The result of this section is a system of three-body R -matrix equations ready for numerical implementation.

4.1 Description of the three-body system

A three-body problem composed of three nuclei with masses m_1 , m_2 and m_3 is governed by the total Hamiltonian,

$$H = \sum_{i=1}^3 \left(\frac{\vec{P}_i^2}{2m_i} + v_i \right) + (V_{ijn}), \quad (4.1)$$

where \vec{P}_i is the momentum of particle i , v_i the two-body interaction between particle j and n and V_{ijn} a three-body interaction which will be omitted in the following. It is convenient to change to Jacobi coordinates (Fig. 3) yielding the transformed Hamiltonian

$$H = \frac{\vec{p}_i^2}{2\mu_{jn}} + \frac{\vec{q}_i^2}{2\mu_{i(jn)}} + v_1 + v_2 + v_3 + \frac{\vec{P}_{CM}^2}{2(m_1 + m_2 + m_3)}. \quad (4.2)$$

The momenta \vec{p}_i and \vec{q}_i are associated with one of the Jacobi coordinate tuples (\vec{r}_i, \vec{R}_i) , $i = 1, 2, 3$. Latter are defined as

$$\vec{r}_1 = \vec{x}_2 - \vec{x}_3, \quad \vec{R}_1 = \vec{x}_1 - \frac{m_2\vec{x}_2 + m_3\vec{x}_3}{m_2 + m_3}, \quad (4.3)$$

$$\vec{r}_2 = \vec{x}_3 - \vec{x}_1, \quad \vec{R}_2 = \vec{x}_2 - \frac{m_3 \vec{x}_3 + m_1 \vec{x}_1}{m_1 + m_3}, \quad (4.4)$$

$$\vec{r}_3 = \vec{x}_1 - \vec{x}_2, \quad \vec{R}_3 = \vec{x}_3 - \frac{m_1 \vec{x}_1 + m_2 \vec{x}_2}{m_1 + m_2}, \quad (4.5)$$

where \vec{x}_i represent Cartesian coordinates. The momenta \vec{p}_i and \vec{q}_i in the Jacobi coordinate system are

$$\vec{p}_1 = \frac{1}{m_2 + m_3}(m_3 \vec{P}_2 - m_2 \vec{P}_3), \quad \vec{q}_1 = \frac{1}{m_1 + m_2 + m_3}[(m_2 + m_3) \vec{P}_1 - m_1(\vec{P}_2 + \vec{P}_3)], \quad (4.6)$$

$$\vec{p}_2 = \frac{1}{m_1 + m_3}(m_1 \vec{P}_3 - m_3 \vec{P}_1), \quad \vec{q}_2 = \frac{1}{m_1 + m_2 + m_3}[(m_1 + m_3) \vec{P}_2 - m_2(\vec{P}_1 + \vec{P}_3)], \quad (4.7)$$

$$\vec{p}_3 = \frac{1}{m_1 + m_2}(m_2 \vec{P}_1 - m_1 \vec{P}_2), \quad \vec{q}_3 = \frac{1}{m_1 + m_2 + m_3}[(m_1 + m_2) \vec{P}_3 - m_3(\vec{P}_1 + \vec{P}_2)]. \quad (4.8)$$

The potential v_i is the interaction between nuclei j and n (Fig. 3) and the associated reduced masses are

$$\mu_{jn} = \frac{m_j \cdot m_n}{m_j + m_n} \quad \text{and} \quad \mu_{i(jn)} = \frac{m_i \cdot (m_j + m_n)}{m_i + m_j + m_n}. \quad (4.9)$$

In the following considerations a vanishing center-of-mass motion is assumed, $\vec{P}_{CM} = 0$.

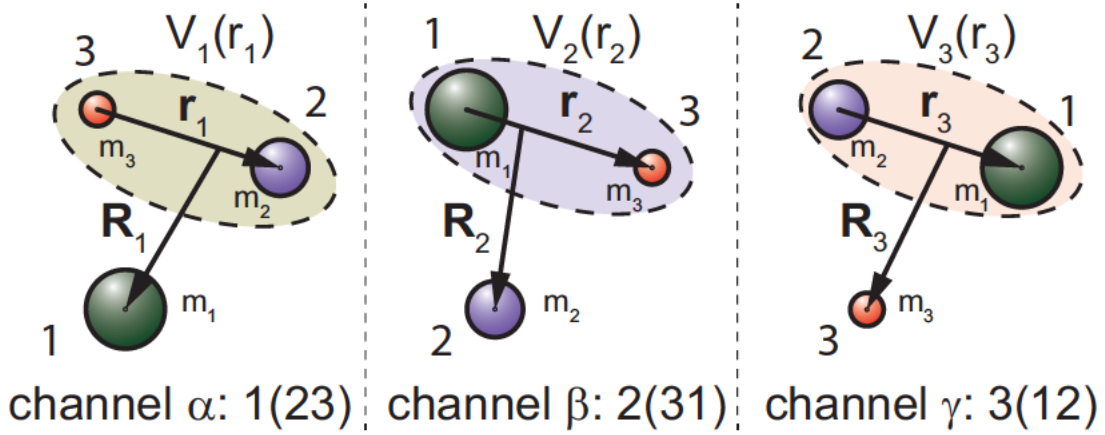


Figure 3: Jacobi coordinates and potentials in a three-body system

4.2 Faddeev equations

This subsection is focused on the path to the Faddeev equations for three-body systems reflecting mainly the derivation in [11]. In the following a system composed of three particles of different masses (m_1, m_2, m_3) interacting via two-body potentials is considered. Furthermore we assume that each subsystem of two particles sustains at least one bound state. Such a system may exhibit up to five types of exit channels,

- | | | |
|----|---|--|
| 1) | $1 \begin{pmatrix} 2 \\ 3 \end{pmatrix}$ | Final channel α : Elastic channel |
| 2) | $2 \begin{pmatrix} 3 \\ 1 \end{pmatrix}$ | Final channel β : Rearrangement channel |
| 3) | $3 \begin{pmatrix} 1 \\ 2 \end{pmatrix}$ | Final channel γ : Rearrangement channel |
| 4) | $1, 2, 3$ | Final channel 0 : Breakup channel |
| 5) | $\begin{pmatrix} 1 \\ 2 \\ 3 \end{pmatrix}$ | Final channel B : Bound channel |

The actual number of channels depends on the interaction and the involved particles/nuclei. Channel B which represents a three-particle bound state will not be considered in this thesis. The particles in brackets under 1), 2) and 3) interact via a two-body potential $v_{jn}(r_i) \equiv v_i(r_i)$ and form a bound state.

For each decomposition one can define a channel Hamilton operator

$$h_\alpha = \frac{\hat{p}_\alpha^2}{2\mu_\alpha} + \frac{\hat{q}_\alpha^2}{2M_\alpha} + v_\alpha, \quad \alpha = 1, 2, 3 \quad (4.10)$$

with the asymptotic channel states $|\phi_{\alpha m}\rangle$ as eigenfunctions,

$$h_\alpha |\phi_{\alpha m}\rangle = E_\alpha |\phi_{\alpha m}\rangle. \quad (4.11)$$

Here m denotes the m -th bound state of the corresponding subsystem. They are related to the total Hamilton operator according to

$$H = h_\alpha + \bar{V}_\alpha, \quad (4.12)$$

with the definition

$$\bar{V}_\alpha = V - v_\alpha = \sum_{\gamma \neq \alpha} v_\gamma. \quad (4.13)$$

For the following derivation two-particle operators are denoted by lowercase letters, whereas three-particle operators are represented by capital letters (except for channel Hamiltonians defined above). Each channel is characterized by an interaction between two-particles in a subsystem, which is expressed by the respective potentials v_α or v_i from above (Fig. 3). Since nuclear forces act at short ranges (< 2 fm) only the particles in the asymptotic area of the breakup channel can be assumed to be free (Fig. 4) and hence

$$v_0 \equiv 0. \quad (4.14)$$

This will change if more than one charged particle is involved because of the Coulomb interaction which is of infinite range. However, such systems will not be treated in this thesis.

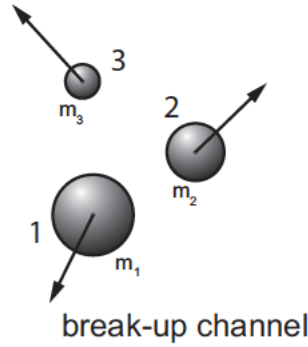


Figure 4: Breakup channel.

4.2.1 Lippmann-Schwinger equation

The Lippmann-Schwinger equation plays a central role in scattering theory. For two-body problems in Eq. (2.15) it provides a unique solution for the scattering problem. In the three-body case however, it must be extended to a set of three equations.

The full resolvent of the three-particle system $G(z)$ with $z = E \pm i\epsilon$ is defined as

$$G(z) \equiv (z - H)^{-1}. \quad (4.15)$$

Similarly to the two-body case one obtains two equations for $G(z)$ using the channel resolvent $g_\alpha(z) = (z - h_\alpha)^{-1}$,

$$G(z) = g_\alpha(z) + g_\alpha(z)\bar{V}_\alpha G(z) = g_\alpha(z) + G(z)\bar{V}_\alpha g_\alpha(z). \quad (4.16)$$

They can be verified by multiplying for instance the second equation in (4.16) by $G^{-1}(z)$ from the left and using the identity

$$\begin{aligned} g_\alpha^{-1}(z) - G^{-1}(z) &= z - h_\alpha - z - H = \bar{V}_\alpha \\ \Rightarrow G^{-1}(z) &= g_\alpha^{-1}(z) - \bar{V}_\alpha \end{aligned} \quad (4.17)$$

which yields

$$\begin{aligned} \mathbb{1} &= G^{-1}(z)g_\alpha(z) + \bar{V}_\alpha g_\alpha(z) \\ \mathbb{1} &= (g_\alpha^{-1}(z) - \bar{V}_\alpha)g_\alpha(z) + \bar{V}_\alpha g_\alpha(z) = \mathbb{1}. \end{aligned} \quad (4.18)$$

The scattering state in channel α is defined as

$$|\psi_{\alpha m}^{(\pm)}\rangle = \lim_{\epsilon \rightarrow 0} \pm i\epsilon G(E \pm i\epsilon)|\phi_{\alpha m}\rangle. \quad (4.19)$$

It is a three-particle wave packet with a subsystem of two particles being in their m -th bound state and the third one moving freely. Inserting the first resolvent equation (4.16) into Eq. (4.19) and after executing the limits leads to the Lippmann-Schwinger equation for a three-particle scattering state in channel α

$$|\psi_{\alpha m}^{(\pm)}\rangle = \lim_{\epsilon \rightarrow 0} \pm i\epsilon g_\alpha(z)|\phi_{\alpha m}\rangle + \lim_{\epsilon \rightarrow 0} \pm i\epsilon g_\alpha(z)\bar{V}_\alpha G(z)|\phi_{\alpha m}\rangle = |\phi_{\alpha m}\rangle + g_\alpha(E \pm i0)\bar{V}_\alpha|\psi_{\alpha m}^{(\pm)}\rangle. \quad (4.20)$$

$|\phi_{\alpha m}\rangle$ is an eigenstate of h_α and thus

$$\lim_{\epsilon \rightarrow 0} \pm i\epsilon g_\alpha(z)|\phi_{\alpha m}\rangle = \lim_{\epsilon \rightarrow 0} \pm i\epsilon(z - h_\alpha)^{-1}|\phi_{\alpha m}\rangle = \lim_{\epsilon \rightarrow 0} \frac{\pm i\epsilon}{E \pm i\epsilon - E_\alpha}|\phi_{\alpha m}\rangle = |\phi_{\alpha m}\rangle.$$

However, this equation exhibits a problem since it is not uniquely solvable. The reason is that the homogeneous equation

$$|\psi_{\alpha m}^{(\pm)}\rangle = g_\alpha(E \pm i0)\bar{V}_\alpha|\psi_{\alpha m}^{(\pm)}\rangle \quad (4.21)$$

has non-trivial solutions in the region of scattering energies, where $E > 0$. This can be shown by writing down the Lippmann-Schwinger equation (4.20) for the scattering

state of another channel $\beta \neq \alpha$,

$$|\psi_{\beta n}^{(\pm)}\rangle = \lim_{\epsilon \rightarrow 0} \pm i\epsilon g_{\alpha}(z)|\phi_{\beta n}\rangle + \lim_{\epsilon \rightarrow 0} \pm i\epsilon g_{\alpha}(z)\bar{V}_{\alpha}G(z)|\phi_{\beta n}\rangle = g_{\alpha}(E \pm i0)\bar{V}_{\alpha}|\psi_{\beta n}^{(\pm)}\rangle. \quad (4.22)$$

Since $|\phi_{\beta n}\rangle$ is not an eigenstate of h_{α} , $g_{\alpha}(z)|\phi_{\beta n}\rangle$ remains finite for ϵ approaching 0. Hence, what remains after performing the limit $\epsilon \rightarrow 0$ in Eq. ((4.22)), is the solution of the homogeneous equation

$$|\psi_{\beta n}^{(\pm)}\rangle = g_{\alpha}(E \pm i0)\bar{V}_{\alpha}|\psi_{\beta n}^{(\pm)}\rangle. \quad (4.23)$$

It is an additional solution to $|\psi_{\alpha m}^{(\pm)}\rangle$ and can be added to it. In the two-particle case, there exist non-trivial solutions of the homogeneous Lippmann-Schwinger equation too. However, these solutions are found at discrete binding energies of the two-particle system ($E_{bind} < 0$), not in the positive energy region where scattering takes place.

There are further equations beside the Lippmann-Schwinger equation [18], which are satisfied by the scattering state $|\psi_{\alpha m}^{(\pm)}\rangle$, They result from inserting the second resolvent equation of (4.16) for $G(z)$, but now for a different channel than α , e.g. β ,

$$\begin{aligned} |\psi_{\alpha m}^{(+)}\rangle &= \lim_{\epsilon \rightarrow 0} i\epsilon G(E + i\epsilon)|\phi_{\alpha m}\rangle \\ &= \lim_{\epsilon \rightarrow 0} i\epsilon g_{\beta}(E + i\epsilon)|\phi_{\alpha m}\rangle + \lim_{\epsilon \rightarrow 0} i\epsilon g_{\beta}(E + i\epsilon)\bar{V}_{\beta}G(E + i\epsilon)|\phi_{\alpha m}\rangle \\ &= \lim_{\epsilon \rightarrow 0} \frac{i\epsilon}{E + i\epsilon - h_{\beta}}|\phi_{\alpha m}\rangle + g_{\beta}(E + i0)\bar{V}_{\beta}|\psi_{\alpha m}^{(+)}\rangle. \end{aligned} \quad (4.24)$$

The first term vanishes since $|\phi_{\alpha m}\rangle$ is not an eigenstate of h_{β} . Hence, the denominator remains finite while the numerator approaches 0. Finally, in the limit $\epsilon \rightarrow 0$ the product $g_{\beta}|\phi_{\alpha m}\rangle$ vanishes, which is known as the Lippmann identity. A similar equation is obtained by using the γ -resolvent. Glöckle found out that adding two homogeneous equations to the Lippmann-Schwinger equation,

$$\begin{aligned} |\psi_{\alpha m}^{(+)}\rangle &= |\phi_{\alpha m}\rangle + g_{\alpha}(E + i0)\bar{V}_{\alpha}|\psi_{\alpha m}^{(+)}\rangle \\ |\psi_{\alpha m}^{(+)}\rangle &= g_{\beta}(E + i0)\bar{V}_{\beta}|\psi_{\alpha m}^{(+)}\rangle \\ |\psi_{\alpha m}^{(+)}\rangle &= g_{\gamma}(E + i0)\bar{V}_{\gamma}|\psi_{\alpha m}^{(+)}\rangle \end{aligned} \quad (4.25)$$

the scattering solution $|\psi_{\alpha m}^{(+)}\rangle$ becomes unique [19]. These additional equations introduce physical boundary conditions to the Lippmann-Schwinger equation which guarantee that there are no incoming waves in channels β and γ . In the breakup channel the

behavior of $|\psi_{\alpha m}^{(+)}\rangle$ is determined by each of the three equations (4.25). Alternatively one can use the form (4.24) with $\beta = 0$, to describe $|\psi_{\alpha m}^{(+)}\rangle$ in the breakup channel,

$$|\psi_{\alpha m}^{(+)}\rangle = G_0 \bar{V}_0 |\psi_{\alpha m}^{(+)}\rangle = G_0 V |\psi_{\alpha m}^{(+)}\rangle. \quad (4.26)$$

This state again guarantees a purely outgoing wave in the breakup channel [18]. Moreover, the structure of (4.26) gives rise to a decomposition of $|\psi_{\alpha m}^{(+)}\rangle$ into components $|\psi_{\alpha m}^{(+)}\rangle_i$,

$$|\psi_{\alpha m}^{(+)}\rangle = G_0 V |\psi_{\alpha m}^{(+)}\rangle = \sum_{i=1}^3 G_0 V_i |\psi_{\alpha m}^{(+)}\rangle_i, \quad (4.27)$$

which are called *Faddeev components* of the scattering wave function.

However, there are still problems remaining. The integral kernel of Eq. (4.20), $g_\alpha \bar{V}_\alpha$, and the integral kernels of the equations in (4.25) do not have a finite Schmidt norm

$$\|K\|_S = [\text{Tr}(K^\dagger K)]^{1/2} = \left[\iint d^3r d^3r' |K(\vec{r}, \vec{r}')|^2 \right]^{1/2}, \quad (4.28)$$

and they are not compact. Latter is caused by the occurrence of delta functions in the kernel which arise from the fact that the channel resolvent g_α acts in the two-particle subsystem of the three-particle system, and does not affect particle α . This can be expressed by writing down the matrix elements of the resolvent

$$\langle \vec{p}_\alpha \vec{q}_\alpha | g_\alpha(z) | \vec{p}'_\alpha \vec{q}'_\alpha \rangle = \delta(\vec{q}_\alpha - \vec{q}'_\alpha) \langle \vec{p}_\alpha | \tilde{g}_\alpha(z - \frac{q_\alpha^2}{2M_\alpha}) | \vec{p}'_\alpha \rangle. \quad (4.29)$$

Here, \tilde{g}_α is a two-particle operator living in two-particle space, while g_α is a two-particle operator in three-particle space.

Faddeev was the first to realize these problems, which led him to look for new equations, the so-called Faddeev equations.

4.3 Faddeev equations for the T -operator

Similarly to Eq. (2.30) in the two-particle problem one can introduce a three-particle T -operator

$$T(z) = V + VG(z)V \quad (4.30)$$

with the three-particle resolvent

$$G(z) = g_0(z) + g_0(z)T(z)g_0(z). \quad (4.31)$$

Combining them yields two integral equations for the T -operator, i.e.

$$\begin{aligned} T(z) &= V + Vg_0(z)T(z), \\ T(z) &= V + T(z)g_0(z)V. \end{aligned} \quad (4.32)$$

Faddeev suggested to split the T -operator into three components,

$$T_i = v_i + v_i g_0 T, \quad (4.33)$$

where $V = v_1 + v_2 + v_3$ and thus $T = T_1 + T_2 + T_3$. However, the integral kernel remains the same as before and is still non compact. The equations for the three components can be arranged in matrix from

$$\begin{pmatrix} T_1 \\ T_2 \\ T_3 \end{pmatrix} = \begin{pmatrix} v_1 \\ v_2 \\ v_3 \end{pmatrix} + \begin{pmatrix} v_1 & v_1 & v_1 \\ v_2 & v_2 & v_2 \\ v_3 & v_3 & v_3 \end{pmatrix} g_0 \begin{pmatrix} T_1 \\ T_2 \\ T_3 \end{pmatrix}. \quad (4.34)$$

In the following some manipulations to this matrix equation are performed in order to make the integral kernel less singular. The first line of the matrix equation

$$T_1 = v_1 + v_1 g_0 (T_1 + T_2 + T_3) \quad (4.35)$$

can be rewritten as

$$(\mathbb{1} - v_1 g_0) T_1 = v_1 + v_1 g_0 (T_2 + T_3). \quad (4.36)$$

Multiplying this equation by $(\mathbb{1} - v_1 g_0)^{-1}$ from the left leads to

$$T_1 = (\mathbb{1} - v_1 g_0)^{-1} v_1 + (\mathbb{1} - v_1 g_0)^{-1} v_1 g_0 (T_2 + T_3), \quad (4.37)$$

or

$$T_1 = t_1 + t_1 g_0 (T_2 + T_3), \quad (4.38)$$

with the two-particle t -operators

$$t_i = (\mathbb{1} - v_i g_0)^{-1} v_i, \quad (4.39)$$

acting in the three-particle space. The same procedure can be carried out for the second and third line and one ends up with the matrix equation

$$\begin{pmatrix} T_1 \\ T_2 \\ T_3 \end{pmatrix} = \begin{pmatrix} t_1 \\ t_2 \\ t_3 \end{pmatrix} + \begin{pmatrix} 0 & t_1 & t_1 \\ t_2 & 0 & t_2 \\ t_3 & t_3 & 0 \end{pmatrix} g_0 \begin{pmatrix} T_1 \\ T_2 \\ T_3 \end{pmatrix}. \quad (4.40)$$

These are the Faddeev equations for the T -matrix. They can be alternatively written as

$$T_i(z) = t_i(z) + \sum_{j=1}^3 F_{ij}(z) g_0(z) T_j(z) \quad (4.41)$$

with the Faddeev operator

$$F_{ij}(z) = (\mathbb{1} - \delta_{ij}) t_i(z). \quad (4.42)$$

The potentials v_i have been totally replaced by the two-particle operators t_i acting in the three-particle space. Two-particle operators, like t_i that act only in subsystem i , always enter off-shell into three-body scattering amplitudes because of the energy shift $z - q_i^2/2M_i$ in subsystem i . As a consequence, there is more information contained in three-particle scattering data than in pure two-particle data. Additionally, when performing the operator product $t_i g_0 T_j$ one has to integrate over all intermediate states $|\vec{p}'_i\rangle$ and $|\vec{q}'_i\rangle$, where

$$\frac{p_i^2}{2\mu_i} \neq z - \frac{q_i'^2}{2M_i} \neq \frac{p_i'^2}{2\mu_i}. \quad (4.43)$$

The kernel of Eqs. (4.40) and (4.41), $t_i g_0 T_j$, is still not compact and does not have a finite Schmidt norm. This is due to the exclusive action of t_i in subsystem i , which causes δ -functions occurring in the matrix elements,

$$\langle \vec{p}_i \vec{q}_i | t_i(z) | \vec{p}'_i \vec{q}'_i \rangle = \delta(\vec{q}_\alpha - \vec{q}'_\alpha) \langle \vec{p}_i | \tilde{t}_i(z - \frac{q_i^2}{2M_i}) | \vec{p}'_i \rangle, \quad (4.44)$$

with the two-particle operators \tilde{t}_i acting in the two-particle space. The existence of the Schmidt norm [Eq. (4.28)] is a sufficient condition for compactness of the integral kernel. Latter is an important feature of the kernel as it is a necessary condition to enable the Fredholm theory and other methods of integral equation theory to be applied. After a first iteration of Eq. (4.40), not carried out here, there occur operator products such as $t_i g_0 t_j$ with $i \neq j$. Such a product implies an integration over intermediate energy states, where the δ -functions disappear and the particles get linked together. Further

problems and details are treated in [21], however, we can proceed using the form (4.41) of the Faddeev equations for the T -operator. If we continue iterating Eq. (4.40), we get the Neumann series of the Faddeev equations, which is [21],

$$\underline{T}(z) = \sum_{\nu=0}^{\infty} \underline{t}(z) \left(\underline{F}(z) g_0(z) \underline{t}(z) \right)^{\nu}, \quad (4.45)$$

where doubly underlined quantities represent matrices and singly underlined quantities vectors. The Faddeev equations describe the three-particle scattering process as a two-body multiple scattering process, where the individual two-body scattering occurs on-shell or off-shell.

In the next step Faddeev equations for the three-particle resolvent $G_i(z)$ and the scattering wave function $|\psi_{am}^{\pm}\rangle$ will be derived.

4.4 Faddeev equations for the resolvent and scattering states

We start with the resolvent $G(z)$ from Eq. (4.31) and replace the operator T by the sum of its three components T_i (4.32),

$$G(z) = g_0(z) + \sum_{i=1}^3 g_0(z) T_i(z) g_0(z). \quad (4.46)$$

With the definition of components $G_i(z)$,

$$G_i(z) = g_0(z) T_i(z) g_0(z), \quad (4.47)$$

Eq. (4.46) is rewritten as

$$G(z) = g_0(z) + \sum_{i=1}^3 G_i(z). \quad (4.48)$$

Equations that determine $G_i(z)$ can be obtained by inserting the Faddeev equations (4.41) for the T -operator into Eq. (4.47) (omitting the argument z of the resolvents and operators),

$$G_i = g_0 \underline{t}_i g_0 + g_0 \sum_{j=1}^3 F_{ij} g_0 T_j g_0. \quad (4.49)$$

We proceed by including a relation that follows from extending the resolvent equation in two-particle space (operators carrying a tilde are two-particle operators acting in

two-particle space)

$$\tilde{g} = \tilde{g}_0 + \tilde{g}_0 \tilde{t} \tilde{g}_0 \quad (4.50)$$

into three-particle space,

$$g_0 \tilde{t}_i g_0 = g_i - g_0. \quad (4.51)$$

Then,

$$G_i = g_i - g_0 + g_0 \sum_{j=1}^3 F_{ij} g_0 T_j g_0 \quad (4.52)$$

and with Eq. (4.47)

$$G_i = g_i - g_0 + \sum_{j=1}^3 g_0 F_{ij} G_j. \quad (4.53)$$

Let us now find Faddeev equations for the scattering state

$$|\psi_{\alpha m}^{(\pm)}\rangle = \lim_{\epsilon \rightarrow 0} \pm i \epsilon G(E \pm i \epsilon) |\phi_{\alpha m}\rangle \quad (4.54)$$

by inserting the splitting of the resolvent (4.48), which yields

$$|\psi_{\alpha m}^{(\pm)}\rangle = \lim_{\epsilon \rightarrow 0} \pm i \epsilon g_0 (E \pm i \epsilon) |\phi_{\alpha m}\rangle + \lim_{\epsilon \rightarrow 0} \pm i \epsilon \sum_{i=1}^3 G_i(E \pm i \epsilon) |\phi_{\alpha m}\rangle. \quad (4.55)$$

We define

$$|\chi_{i \alpha m}^{(\pm)}\rangle = \lim_{\epsilon \rightarrow 0} \pm i \epsilon g_i (E \pm i \epsilon) |\phi_{\alpha m}\rangle \quad (4.56)$$

and

$$|\psi_{\alpha m}^{(\pm)}\rangle_i = \lim_{\epsilon \rightarrow 0} \pm i \epsilon G_i(E \pm i \epsilon) |\phi_{\alpha m}\rangle, \quad (4.57)$$

with $i = 1, 2, 3$. The state $|\chi_{i \alpha m}^{(\pm)}\rangle$ with $\alpha \neq 0$ can be simplified by performing the limit $\epsilon \rightarrow 0$,

$$|\chi_{i \alpha m}^{(\pm)}\rangle = \lim_{\epsilon \rightarrow 0} \frac{\pm i \epsilon}{E \pm i \epsilon - h_i} |\phi_{\alpha m}\rangle = \delta_{i \alpha} |\phi_{\alpha m}\rangle, \quad i = 0, 1, 2, 3, \quad (4.58)$$

which is true since $|\phi_{\alpha m}\rangle$ is an eigenfunction of h_i if $i = \alpha$. $\alpha \neq 0$ means an incoming state consisting of a bound pair and one particle moving freely. This case will be considered in the following. For $\alpha = 0$, which describes an incoming state consisting of three free particles, we get different results for $|\chi_{i \alpha m}^{(\pm)}\rangle$, which, however, will not concern

us further. As a consequence the scattering state is split into components

$$|\psi_{\alpha m}^{(\pm)}\rangle = |\chi_{0\alpha m}^{(\pm)}\rangle + \sum_{i=1}^3 |\psi_{\alpha m}^{(\pm)}\rangle_i. \quad (4.59)$$

With the Faddeev equations for the resolvent (4.53), these components become

$$|\psi_{\alpha m}^{(\pm)}\rangle_i = \lim_{\epsilon \rightarrow 0} \pm i\epsilon \left[g_i(E \pm i\epsilon) - g_0(E \pm i\epsilon) + \sum_{j=1}^3 g_0(E \pm i\epsilon) F_{ij}(E \pm i\epsilon) G_j(E \pm i\epsilon) \right] |\phi_{\alpha m}\rangle. \quad (4.60)$$

For an incoming state consisting of a bound pair and one particle moving freely one finally obtains

$$|\psi_{\alpha m}^{(\pm)}\rangle_i = \delta_{i\alpha} |\phi_{\alpha m}\rangle + \sum_{j=1}^3 g_0(E \pm i0) F_{ij}(E \pm i0) |\psi_{\alpha m}^{(\pm)}\rangle_j \quad (4.61)$$

and the total scattering wave function is a coherent sum of the three Faddeev components,

$$|\psi_{\alpha m}^{(\pm)}\rangle = \sum_{i=1}^3 |\psi_{\alpha m}^{(\pm)}\rangle_i. \quad (4.62)$$

Eqs. (4.61) and (4.62) are the Faddeev equations for the scattering state.

5 A novel three-body R -matrix formalism

In this main section a novel R -matrix formalism for three-body channels is presented. It provides a full quantum mechanical treatment of three-body processes in the frame of R -matrix theory making use of the Faddeev equations. An important proposal for such a formalism was first given by W. Glöckle in 1974 [10]. It is the only attempt of an R -matrix formalism based on the exact three-body equations until now. However, to our knowledge it has never been numerically implemented and tested.

Dealing with an extension of an R -matrix formalism it is obvious that the asymptotic form of the three-body wave function plays an important role. Therefore it will be topic of the first subsection followed by an outline of the R -matrix procedure and its final equations in the next subsections.

5.1 Faddeev equations and asymptotic wave functions

The Faddeev equation for the scattering wave function (4.61) reads

$$\begin{aligned} |\psi_{\alpha m}^{(\pm)}\rangle_i &= \delta_{i\alpha}|\phi_{\alpha m}\rangle + \sum_{j=1}^3 g_0 F_{ij} |\psi_{\alpha m}^{(\pm)}\rangle_j = \delta_{i\alpha}|\phi_{\alpha m}\rangle + \sum_{j=1}^3 g_0 (\mathbb{1} - \delta_{ij}) t_i |\psi_{\alpha m}^{(\pm)}\rangle_j \\ &= \delta_{i\alpha}|\phi_{\alpha m}\rangle + \sum_{j(\neq i)=1}^3 g_0 t_i |\psi_{\alpha m}^{(\pm)}\rangle_j, \end{aligned} \quad (5.1)$$

with

$$|\psi_{\alpha m}^{(\pm)}\rangle = \sum_{i=1}^3 |\psi_{\alpha m}^{(\pm)}\rangle_i. \quad (5.2)$$

Here the relationship $F_{ij} = (\mathbb{1} - \delta_{ij})t_i$ was used. Starting from the resolvent equation in its two forms,

$$\begin{aligned} g_0(E - h_0 - v_i)g_i &= g_0 = g_i - g_0 v_i g_i \Rightarrow g_i = g_0 + g_0 v_i g_i \Rightarrow g_i = (\mathbb{1} - g_0 v_i)^{-1} g_0 \\ g_i(E - h_0 - v_i)g_0 &= g_0 = g_i - g_i v_i g_0 \Rightarrow g_i = g_0 + g_i v_i g_0 \Rightarrow g_i = g_0 (\mathbb{1} - g_0 v_i)^{-1}, \end{aligned} \quad (5.3)$$

the two-particle t -operators can be expressed by

$$t_i = v_i + v_i g_0 t_i = v_i + t_i g_0 v_i \Rightarrow t_i = (\mathbb{1} - v_i g_0)^{-1} = v_i (\mathbb{1} - g_0 v_i)^{-1}. \quad (5.4)$$

Combining Eq. (5.3) with Eq. (5.4) yields

$$\begin{aligned} g_i &= g_0(\mathbb{1} - v_i g_0)^{-1} \Rightarrow (\mathbb{1} - v_i g_0)^{-1} = g_0^{-1} g_i \Rightarrow t_i = g_0^{-1} g_i v_i \Rightarrow g_0 t_i = g_i v_i \\ g_i &= (\mathbb{1} - g_0 v_i)^{-1} g_0 \Rightarrow g_i g_0^{-1} = (\mathbb{1} - g_0 v_i)^{-1} \Rightarrow t_i = v_i g_i g_0^{-1} \Rightarrow t_i g_0 = v_i g_i \end{aligned} \quad (5.5)$$

Hence, Eq. (5.1) can be rewritten using Eq. (5.5),

$$|\psi_{\alpha m}^{(\pm)}\rangle_i = \delta_{i\alpha} |\phi_{\alpha m}\rangle + g_i v_i \sum_{j(\neq i)=1}^3 |\psi_{\alpha m}^{(\pm)}\rangle_j. \quad (5.6)$$

We use the coordinate space representations of the physical scattering wave functions $|\psi_{\alpha m}^{(+)}\rangle_i$ and suppress the indices α and m

$$\psi_i(\vec{r}_j, \vec{R}_j) \equiv {}_i \langle \vec{r}_j \vec{R}_j | \psi_{\alpha m}^{(+)} \rangle_i. \quad (5.7)$$

The index $i = 1, 2, 3$ and j denote the Faddeev component and a certain set of Jacobi coordinates, respectively. In the following the notation for two-particle Green's functions and two-body potentials ($V_i = V_{jn}$ is the interaction between particle j and n) will change from lowercase to capital letters while leaving their definitions unchanged (see subsection 4.1). In coordinate space representation the Faddeev equations form a set of three coupled integral equations

$$\begin{aligned} \psi_1(\vec{r}_1, \vec{R}_1)_\alpha &= \phi_1(r_1, R_1)_\alpha + \int d^3 r'_1 \int d^3 R'_1 \langle \vec{r}_1 \vec{R}_1 | G_1 | \vec{r}'_1 \vec{R}'_1 \rangle V_{23}(r'_1) [\psi_2(\vec{r}'_2, \vec{R}'_2)_\alpha + \psi_3(\vec{r}'_3, \vec{R}'_3)_\alpha] \\ \psi_2(\vec{r}_2, \vec{R}_2)_\alpha &= \int d^3 r'_2 \int d^3 R'_2 \langle \vec{r}_2 \vec{R}_2 | G_2 | \vec{r}'_2 \vec{R}'_2 \rangle V_{31}(r'_2) [\psi_1(\vec{r}'_1, \vec{R}'_1)_\alpha + \psi_3(\vec{r}'_3, \vec{R}'_3)_\alpha] \\ \psi_3(\vec{r}_3, \vec{R}_3)_\alpha &= \int d^3 r'_3 \int d^3 R'_3 \langle \vec{r}_3 \vec{R}_3 | G_3 | \vec{r}'_3 \vec{R}'_3 \rangle V_{12}(r'_3) [\psi_1(\vec{r}'_1, \vec{R}'_1)_\alpha + \psi_2(\vec{r}'_2, \vec{R}'_2)_\alpha], \end{aligned} \quad (5.8)$$

for channel β

$$\begin{aligned} \psi_1(\vec{r}_1, \vec{R}_1)_\beta &= \int d^3 r'_1 \int d^3 R'_1 \langle \vec{r}_1 \vec{R}_1 | G_1 | \vec{r}'_1 \vec{R}'_1 \rangle V_{23}(r'_1) [\psi_2(\vec{r}'_2, \vec{R}'_2)_\beta + \psi_3(\vec{r}'_3, \vec{R}'_3)_\beta] \\ \psi_2(\vec{r}_2, \vec{R}_2)_\beta &= \phi_2(r_2, R_2)_\beta + \int d^3 r'_2 \int d^3 R'_2 \langle \vec{r}_2 \vec{R}_2 | G_2 | \vec{r}'_2 \vec{R}'_2 \rangle V_{31}(r'_2) [\psi_1(\vec{r}'_1, \vec{R}'_1)_\beta + \psi_3(\vec{r}'_3, \vec{R}'_3)_\beta] \\ \psi_3(\vec{r}_3, \vec{R}_3)_\beta &= \int d^3 r'_3 \int d^3 R'_3 \langle \vec{r}_3 \vec{R}_3 | G_3 | \vec{r}'_3 \vec{R}'_3 \rangle V_{12}(r'_3) [\psi_1(\vec{r}'_1, \vec{R}'_1)_\beta + \psi_2(\vec{r}'_2, \vec{R}'_2)_\beta], \end{aligned} \quad (5.9)$$

and for channel γ

$$\begin{aligned}
\psi_1(\vec{r}_1, \vec{R}_1)_\gamma &= \int d^3 r'_1 \int d^3 R'_1 \langle \vec{r}_1 \vec{R}_1 | G_1 | \vec{r}'_1 \vec{R}'_1 \rangle V_{23}(r'_1) [\psi_2(\vec{r}'_2, \vec{R}'_2)_\gamma + \psi_3(\vec{r}'_3, \vec{R}'_3)_\gamma] \\
\psi_2(\vec{r}_2, \vec{R}_2)_\gamma &= \int d^3 r'_2 \int d^3 R'_2 \langle \vec{r}_2 \vec{R}_2 | G_2 | \vec{r}'_2 \vec{R}'_2 \rangle V_{31}(r'_2) [\psi_1(\vec{r}'_1, \vec{R}'_1)_\gamma + \psi_3(\vec{r}'_3, \vec{R}'_3)_\gamma] \\
\psi_3(\vec{r}_3, \vec{R}_3)_\gamma &= \phi_3(r_3, R_3)_\gamma + \int d^3 r'_3 \int d^3 R'_3 \langle \vec{r}_3 \vec{R}_3 | G_3 | \vec{r}'_3 \vec{R}'_3 \rangle V_{12}(r'_3) [\psi_1(\vec{r}'_1, \vec{R}'_1)_\gamma + \psi_2(\vec{r}'_2, \vec{R}'_2)_\gamma].
\end{aligned} \tag{5.10}$$

All labels correspond to the notations used in Fig. 5 with $V_i(r_i) = V_{jn}(r_i)$. The

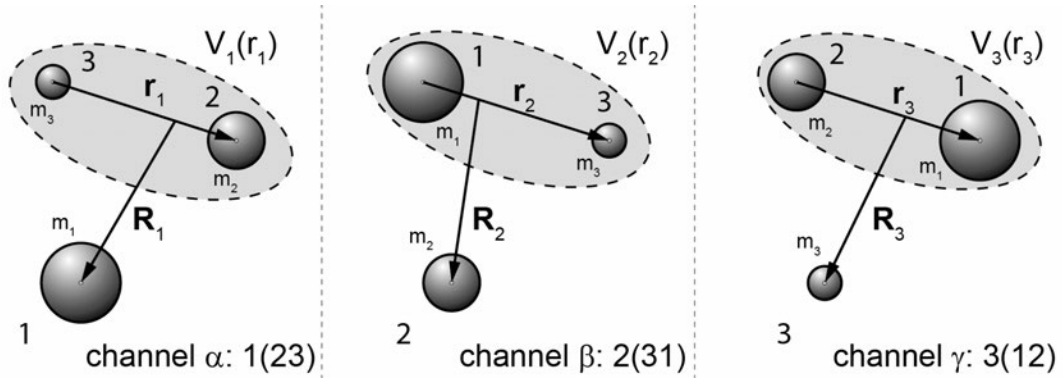


Figure 5: Jacobi coordinates and potentials in a three-body system.

dynamical quantities will be denoted according to the dispersion relation ($\hbar = 1$)

$$E = E_i = -\frac{\kappa_i^2}{2\mu_{jn}} + \frac{Q_i^2}{2\mu_{i(jn)}} = E_b^{(i)} + \frac{Q_i^2}{2\mu_{i(jn)}} = \frac{k_i^2}{2\mu_{jn}} + \frac{Q_{k_i}^2}{2\mu_{i(jn)}} = \frac{q_{K_i}^2}{2\mu_{jn}} + \frac{K_i^2}{2\mu_{i(jn)}}. \tag{5.11}$$

The index i stands for the respective Faddeev component in Eq. (5.8) and will be omitted for the wavenumbers in the following. Eq. (5.11) exhibits the energy-wavenumber relations for all possible channels of the three-body problem. E_b denotes the binding energy of the bound subsystem in the incoming, elastic or rearrangement channel, whereas Q stands for the wavenumber of the projectile or scattered particle. If breakup occurs k denotes the relative wavenumber between the two particles that were bound in the subsystem, but after breakup moving freely and Q_k is the respective wavenumber of the third particle. The wavenumbers k_i and Q_{k_i} are associated with the Jacobi momenta p_i and q_i defined in Eqs. (4.6), (4.7) and (4.8). q_K and K_i have the same physical meaning as k and Q_k and will be needed in the Green's function below to

study an asymptotic limit. The Faddeev equations require different sets of Jacobi coordinates as a function of that set used in a certain subsystem. For $i = 1, 2$ the relation reads ($i \neq j \neq n$ and $i \neq n$)

$$\vec{r}_j = -\frac{m_j}{m_j + m_n} \vec{r}_i - (-1)^j \vec{R}_i, \quad \vec{R}_j = (-1)^j \frac{m_i m_n + m_j m_n + m_n m_n}{(m_i + m_n)(m_j + m_n)} \vec{r}_i - \frac{m_i}{m_i + m_n} \vec{R}_i, \quad (5.12)$$

and for $i = 3$ ($i \neq j \neq n$ and $i \neq n$)

$$\vec{r}_j = -\frac{m_j}{m_j + m_n} \vec{r}_i + (-1)^j \vec{R}_i, \quad \vec{R}_j = -(-1)^j \frac{m_i m_n + m_j m_n + m_n m_n}{(m_i + m_n)(m_j + m_n)} \vec{r}_i - \frac{m_i}{m_i + m_n} \vec{R}_i. \quad (5.13)$$

There are two ways to write down the Faddeev equations either as integral or differential equations. In the following we consider the integral form and restrict ourselves to the s-wave part of the wave functions in Riccati form $u_i(r_i, R_i) = r_i R_i \psi_i(r_i, R_i)$. Then Eq. (5.8) reads (the index "α" will be omitted in the following)

$$\begin{aligned} u_i(r_i, R_i) &= \delta_{i1} u_i^b(r_i) \sin(QR_i) + \int_0^\infty dr'_i \int_0^\infty dR'_i \langle r_i R_i | G_i | r'_i R'_i \rangle V_i(r'_i) \\ &\quad \times \int_{-1}^1 dx' r'_i R'_i \frac{1}{2} \left[\frac{u_j(r'_j, R'_j)}{r'_j R'_j} + \frac{u_k(r'_k, R'_k)}{r'_k R'_k} \right] \\ &= u_i^b(r_i) \sin(QR_i) + \int_0^\infty dr'_i \int_0^\infty dR'_i \langle r_i R_i | G_i | r'_i R'_i \rangle V_i(r'_i) \Lambda_i(r'_i, R'_i) \end{aligned} \quad (5.14)$$

where

$$\Lambda_i(r_i, R_i) = \int_{-1}^1 dx_i \frac{r_i R_i}{2} \sum_{\substack{j=1 \\ j \neq i}}^3 \frac{u_j(r_j, R_j)}{r_j R_j}. \quad (5.15)$$

and x_i is the cosine of the relative angle between \vec{r}_i and \vec{R}_i . Applying $(E - \hat{H}_i)$ on both sides of Eq. (5.14) and using the identity

$$(E - \hat{H}_i) \langle r_i R_i | G_i | r'_i R'_i \rangle = (E - \hat{H}_i) \langle r_i R_i | \frac{1}{E - \hat{H}_i} | r'_i R'_i \rangle = \delta(\vec{r}_i - \vec{r}'_i) \delta(\vec{R}_i - \vec{R}'_i)$$

yields

$$\begin{aligned}
& \left[-\frac{1}{2\mu_{jn}} \frac{d^2}{dr_i^2} - \frac{1}{2\mu_{i(jn)}} \frac{d^2}{dR_i^2} + V_i(r_i) - E \right] u_i(r_i, R_i) \\
&= - \int_0^\infty dr'_i \int_0^\infty dR'_i \delta(\vec{r}_i - \vec{r}'_i) \delta(\vec{R}_i - \vec{R}'_i) V_i(r'_i) \int_{-1}^1 dx'_i \frac{r'_i R'_i}{2} \sum_{\substack{j=1 \\ j \neq i}}^3 \frac{u_j(r'_j, R'_j)}{r'_j R'_j} \\
&= -\frac{1}{2} V_i(r_i) \int_{-1}^1 dx_i r_i R_i \sum_{\substack{j=1 \\ j \neq i}}^3 \frac{u_j(r_j, R_j)}{r_j R_j},
\end{aligned} \tag{5.16}$$

with boundary conditions for outgoing scattered waves. E is the total energy of the system. The Green's function for three-body problems in absence of Coulomb interaction reflects the dispersion relation (5.11) and can be written in two forms [18]

$$\begin{aligned}
\langle r_i R_i | G_i | r'_i R'_i \rangle &= u_i^b(r_i) \left(-2\mu_{i(jn)} e^{iQR_i} \frac{\sin(QR_{i<})}{Q} \right) u_i^b(r'_i) \\
&+ \frac{2}{\pi} \int_0^\infty dk u_k^{(-)}(r_i) \left(-2\mu_{i(jn)} e^{iQ_k R_i} \frac{\sin(Q_k R_{i<})}{Q_k} \right) u_k^{(-)*}(r'_i)
\end{aligned} \tag{5.17a}$$

$$= \frac{2}{\pi} \int_0^\infty dK \sin(KR_i) \left(-\frac{2\mu_{jn}}{qK} u_{qK}^{(+)}(r_{i<}) w_{qK}(r_{i>}) \right) \sin(KR'_i), \tag{5.17b}$$

where $R_{i>} = \max(R_i, R'_i)$, $R_{i<} = \min(R_i, R'_i)$ and $r_{i>} = \max(r_i, r'_i)$, $r_{i<} = \min(r_i, r'_i)$ and i, m, n denote the different particles ($i \neq j \neq n$ and $i \neq n$), respectively. The functions $u_{qK}^{(\pm)}(r)$ and $w_{qK}(r)$ form a complete set of bound- and scattering states and are normalized as

$$u_q^{(\pm)}(r) \simeq e^{\pm i\delta(q)} \sin(qr + \delta(q)) \tag{5.18}$$

and

$$w_q(r) \simeq e^{iqr} \tag{5.19}$$

for $r \rightarrow \infty$. With this Green's functions and the coordinate transformation

$$r_i = \sqrt{\frac{1}{2\mu_{jn}}} \rho \cos \varphi_i, \quad R_i = \sqrt{\frac{1}{2\mu_{i(jn)}}} \rho \sin \varphi_i, \tag{5.20}$$

one obtains after an involved derivation provided detail in [11] the asymptotic form

of the three-body wave function for $R_i \rightarrow \infty$ and r_i fixed and $r_i \rightarrow \infty$ and R_i fixed. These forms are important for the R -matrix procedure. For $R_i \rightarrow \infty$ and r_i fixed we obtain

$$\begin{aligned}
u_i(r_i, R_i) \simeq & u_i^b(r_i) \sin(QR_i) - 2\mu_{i(jn)} u_i^b(r_i) e^{iQR_i} T_i^b - \frac{4}{\pi} \mu_{i(jn)} \int_0^{\sqrt{2\mu_{jn}E}} dk u_k^{(-)}(r_i) e^{iQ_k R_i} T_i(k) \\
& - \sum_{\substack{j=1 \\ j \neq i}}^3 \frac{e^{i\sqrt{2\mu_{j(in)}E} \frac{m_i}{m_i+m_n} R_i / \sin \varphi_j^*}}{R_i^{3/2}} \left(u_i^b(r_i) C_i^b + \frac{2}{\pi} \int_{\sqrt{2\mu_{jn}E}}^{\infty} dk u_k^{(-)}(r_i) C_i(k) \right) \\
& + O\left(\frac{1}{R_i^2}\right)
\end{aligned} \tag{5.21}$$

and for $r_i \rightarrow \infty$ and R_i fixed

$$u_i(r_i, R_i) \simeq -\frac{4\mu_{i(jn)}}{\pi} \int_0^{\sqrt{2\mu_{jn}E}} dk \sin(Q_k R_i) e^{ikr_i} T_i(k) + O\left(\frac{1}{r_i^2}\right). \tag{5.22}$$

The angle φ_j^* is given by

$$\varphi_j^* = \arctan\left(\frac{m_i}{m_i + m_n} \sqrt{\frac{\mu_{j(in)}}{\mu_{ik}}}\right) \tag{5.23}$$

and the numbers C_i^b and $C_i(k)$ are determined by

$$\begin{aligned}
C_i^b = & \sqrt{\frac{2}{\pi}} e^{i\frac{\pi}{4}} 2\mu_{i(jn)} \sqrt{2\mu_{jn}} (2\mu_{j(in)})^{-1/4} \left(\frac{m_i + m_n}{m_i}\right)^{5/2} (\sin \varphi_j^*)^{7/2} E^{1/4} \\
& \times T_i\left(\sqrt{2\mu_{jn}E} \cos \varphi_j^*\right) \frac{2\mu_{i(jn)}}{\mu_{j(in)} \left(E - \frac{2Q^2}{\mu_{j(in)}} \sin^2 \varphi_j^*\right)} \int_0^{\infty} dr u_i^b(r) V_i(r),
\end{aligned} \tag{5.24}$$

and

$$\begin{aligned}
C_i(k) &= \sqrt{\frac{2}{\pi}} e^{i\frac{\pi}{4}} 2\mu_{i(jn)} \sqrt{2\mu_{jn}} (2\mu_{j(in)})^{-1/4} \left(\frac{m_i + m_n}{m_i} \sin \varphi_j^* \right)^{3/2} E^{1/4} T_i \left(\sqrt{2\mu_{jn} E} \cos \varphi_j^* \right) \\
&\quad \times \frac{1}{\frac{1}{\mu_{jn}} k^2 - 2E + 2\frac{\mu_{j(in)}}{\mu_{i(jn)}} E \left(\frac{m_i}{(m_i + m_n) \sin \varphi_j^*} \right)^2} \int_0^\infty dr u_k^{(-)*}(r) V_i(r).
\end{aligned} \tag{5.25}$$

Finally the asymptotic expression of the three-body wave function in the breakup channel where both r_i and R_i tend towards infinity is given by [11]

$$u_i(r_i, R_i) \underset{\rho \rightarrow \infty}{\simeq} (2\mu_{i(jn)})^{3/2} \sqrt{2\mu_{jn}} \sqrt{\frac{2}{\pi}} e^{i\frac{\pi}{4}} E^{1/4} \frac{e^{i\rho\sqrt{E}}}{\rho^{1/2}} \frac{R_i}{\rho} T_i \left(2\mu_{jn} \sqrt{E} \frac{r_i}{\rho} \right), \tag{5.26}$$

with $\rho = \sqrt{2\mu_{jn} r_i^2 + 2\mu_{i(jn)} R_i^2}$.

With the momentum transformation (for details see [11])

$$k = \sqrt{2\mu_{jn} E} \sin \vartheta, \quad Q_k = \sqrt{2\mu_{i(jn)} E} \cos \vartheta \tag{5.27}$$

and the coordinate transformation (5.20) the breakup wave function of the Faddeev component i is calculated according to

$$\begin{aligned}
\psi_i(r_i, R_i) &= \frac{u_i(r_i, R_i)}{r_i R_i} \underset{\rho \rightarrow \infty}{\simeq} 2\mu_{i(jn)} \sqrt{2\mu_{jn}} \sqrt{\frac{2}{\pi}} e^{i\frac{\pi}{4}} E^{1/4} \frac{e^{i\rho\sqrt{E}}}{\rho^{1/2}} \sin \varphi_i \frac{1}{r_i R_i} T_i(k_i) \\
&= 2\mu_{i(jn)} \sqrt{2\mu_{jn}} \sqrt{\frac{2}{\pi}} e^{i\frac{\pi}{4}} E^{1/4} \frac{e^{i\rho\sqrt{E}}}{\rho^{1/2}} \sin \varphi_i \sqrt{2\mu_{i(jn)}} \sqrt{2\mu_{jn}} \frac{1}{\rho \sin \varphi_i} \frac{1}{\rho} \underbrace{\frac{1}{\cos \varphi_i}}_{=\cos(\frac{\pi}{2} - \vartheta_i)} T_i(k_i) \\
&= (2\mu_{i(jn)})^{3/2} 2\mu_{jn} \sqrt{\frac{2}{\pi}} e^{i\frac{\pi}{4}} E^{1/4} \frac{e^{i\rho\sqrt{E}}}{\rho^{5/2}} \frac{T_i(k_i)}{\sin \vartheta_i} \\
&= (2\mu_{i(jn)})^{3/2} 2\mu_{jn} \sqrt{\frac{2}{\pi}} e^{i\frac{\pi}{4}} E^{1/4} \frac{e^{i\rho\sqrt{E}}}{\rho^{5/2}} \frac{\sqrt{2\mu_{jn} E}}{k_i} T_i(k_i) \\
&= (4\mu_{i(jn)} \mu_{jn})^{3/2} \sqrt{\frac{2}{\pi}} e^{i\frac{\pi}{4}} E^{3/4} \frac{e^{i\rho\sqrt{E}}}{\rho^{5/2}} \frac{T_i(k_i)}{k_i}.
\end{aligned} \tag{5.28}$$

Here the saddle point condition $\vartheta_i = \frac{\pi}{2} - \varphi_i$, resulting from the integration along the line of steepest descent carried out in [11] was used.

The total wave function for the breakup channel in the asymptotic region is calculated as a sum over the three Faddeev components, $\psi_i(r_i, R_i)$, according to Eq. (5.2)

$$\Psi_{breakup}^{(+)} = \sum_{i=1}^3 \psi_i(r_i, R_i) \underset{\substack{r_i \rightarrow \infty \\ R_i \rightarrow \infty}}{\simeq} \sqrt{\frac{2}{\pi}} e^{i\frac{\pi}{4}} E^{3/4} \frac{e^{i\rho\sqrt{E}}}{\rho^{5/2}} \sum_{i=1}^3 (4\mu_{i(jn)}\mu_{jn})^{3/2} \frac{T_i(k_i)}{k_i} \quad (5.29)$$

The asymptotic wave function depends on the T -amplitudes. From the derivation of Glöckle and the generalization to different particle masses the form of the T -amplitudes in coordinate representation is given by

$$T_i^b = \int_0^\infty dR \int_0^\infty dr \frac{\sin(QR)}{Q} u_i^b(r) V_i(r) \Lambda(r, R) \quad (5.30)$$

and

$$T_i(k) = \int_0^\infty dR \int_0^\infty dr \frac{\sin(Q_k R)}{Q_k} u_k^{(-)*}(r) V_i(r) \Lambda(r, R) \quad (5.31)$$

with Eq. (5.15),

$$\Lambda_i(r_i, R_i) = \int_{-1}^1 dx_i \frac{r_i R_i}{2} \sum_{\substack{j=1 \\ j \neq i}}^3 \frac{u_j(r_j, R_j)}{r_j R_j}.$$

They must not be confused with the three-body T -operators treated in subsections 4.3 and 4.4.

In the following we show according to [18] that these forms of the transition amplitudes [(5.30) and (5.31)] are equivalent to

$$T_{\beta\alpha} = \langle \phi_\beta | V^\beta | \Psi_\alpha^{(+)} \rangle \quad (5.32)$$

which is the three-body analogue to Eq. (2.28). The channel potential is given by

$$V^\beta = V_\alpha + V_\gamma, \quad \alpha \neq \beta \neq \gamma,$$

where α is the entrance and elastic channel and β and γ are rearrangement channels.

The breakup channel conveniently carries the index 0 with the corresponding potential $V_0 = 0$ and thus $V^0 = V_1 + V_2 + V_3$ where we use the notation $V_\alpha = V_1, V_\beta = V_2$ and $V_\gamma = V_3$.

With the notation $\phi_1 = j_0(QR_1)\varphi_1^b(r_1)$ and $\varphi_1^b(r) = \frac{u_1^b(r)}{r}$ the elastic T -amplitude from Eq. (5.30) reads in abstract vector notation

$$T_b = \langle \phi_1 | V_1 | \psi_2 + \psi_3 \rangle = \langle \phi_1 | V_1 G_0 (V_2 + V_3) | \Psi^{(+)} \rangle = \langle \phi_1 | V_2 + V_3 | \Psi^{(+)} \rangle. \quad (5.33)$$

In the first equality inserted the definition of the Faddeev components,

$$|\psi_i\rangle = G_0 V_i |\Psi^{(+)}\rangle \quad (5.34)$$

and in the second equality we made use of the relation

$$G_0 V_1 |\phi_1\rangle = |\phi_1\rangle. \quad (5.35)$$

To prove Eq. (5.35) we multiply both sides by G_0^{-1} from the left side which leads to

$$\begin{aligned} G_0^{-1} G_0 V_1 |\phi_1\rangle &= G_0^{-1} |\phi_1\rangle \\ V_1 |\phi_1\rangle &= (E - \hat{H}_0) |\phi_1\rangle \\ V_1 |\phi_1\rangle &= (\hat{H}_1 - \hat{H}_0) |\phi_1\rangle \\ V_1 |\phi_1\rangle &= V_1 |\phi_1\rangle. \end{aligned}$$

because $\hat{H}_1 = \hat{H}_0 + V_1$ with the eigenstate $|\phi_1\rangle$, $\hat{H}_1 |\phi_1\rangle = E |\phi_1\rangle$.

The breakup amplitude in channel 1, $T_1(k)$ from Eq. (5.31), in abstract vector notation with $\phi_k = k j_0(kr_1) j_0(Q_k R_1)$ reads

$$T_1(k) = \langle \phi_k^{(-)} | V_1 | \psi_2 + \psi_3 \rangle. \quad (5.36)$$

The scattering state $|\phi_k^{(+)}\rangle$ is a solution of the Lippmann-Schwinger equation

$$|\phi_k^{(+)}\rangle = |\phi_k\rangle + G_0 V_1 |\phi_k^{(+)}\rangle = |\phi_k\rangle + \lim_{\epsilon \rightarrow 0} \frac{1}{E + i\epsilon - \hat{H}_0} V_1 |\phi_k^{(+)}\rangle, \quad (5.37)$$

where $|\phi_k\rangle$ is an eigenstate of \hat{H}_0 , i.e. $\hat{H}_0 |\phi_k\rangle = E_0 |\phi_k\rangle$ and $\hat{H}_1 |\phi_k^{(+)}\rangle = E |\phi_k^{(+)}\rangle$. The scattering state $|\phi_k^{(+)}\rangle$ can also be represented as

$$|\phi_k^{(+)}\rangle = |\phi_k\rangle + G_1 V_1 |\phi_k\rangle, \quad (5.38)$$

and the corresponding vector in dual space

$$\langle \phi_k^{(-)} | = \langle \phi_k | + \langle \phi_k | V_1 G_1. \quad (5.39)$$

Inserting Eq. (5.39) into the expression for the $T_1(k)$ -amplitude, Eq. (5.36), and using relations (5.6) and (5.2) yields

$$\begin{aligned} T_1(k) &= \langle \phi_k | V_1 | \psi_2 + \psi_3 \rangle + \langle \phi_k | V_1 G_1 V_1 | \psi_2 + \psi_3 \rangle = \langle \phi_k | V_1 | \psi_2 + \psi_3 \rangle + \langle \phi_k | V_1 | \psi_1 - \phi_1 \rangle \\ &= \langle \phi_k | V_1 | \psi_1 + \psi_2 + \psi_3 \rangle - \langle \phi_k | V_1 | \phi_1 \rangle = \langle \phi_k | V_1 | \Psi^{(+)} \rangle - \langle \phi_k | V_1 | \phi_1 \rangle. \end{aligned} \quad (5.40)$$

The second term in the last line vanishes on-shell due to strong surface oscillations resulting from partial integration that do not contribute to the cross section [18]. The first term is the breakup T -amplitude in channel 1. The total breakup behavior is obtained by adding up the contributions from all three Faddeev components,

$$T(k) = \langle \phi_k | V_1 + V_2 + V_3 | \Psi^{(+)} \rangle = \langle \phi_k | V^0 | \Psi^{(+)} \rangle \quad (5.41)$$

which corresponds to definition (5.32) of the three body T -amplitudes.

In general the elastic or rearrangement T -amplitudes for the i -th Faddeev component read

$$T_i^b = \langle \phi_i | V_i | \psi_j + \psi_n \rangle \quad (5.42)$$

and for the breakup channel

$$T_i(k) = \langle \phi_k | V_i | \psi_j + \psi_n \rangle, \quad (5.43)$$

which in coordinate representation yield Eqs. (5.30) and (5.31). The indices i, j, n account for three different particles, i.e. $i \neq j \neq n$ and $i \neq n$.

5.2 Derivation of the generalized three-body R -matrix formalism

In this subsection the three-body R -matrix formalism based on Glöckle's ideas, but generalized to different masses according to [11] is presented. The concept of dividing the Jacobi-coordinate space is introduced followed by the determination of the matching radii and finally the path is drawn to a system of equations for the expansion coefficients $c_\mu^{(i)}$ and the T -amplitudes which will be outlined at the end of this subsection.

5.2.1 Division of the Jacobi-coordinate space

The key feature of R -matrix theory is the division of the configuration space into an interior region where strong interactions take place and the complex n -body wave function is substituted by an expansion over a set of basis functions and an exterior region where the asymptotic form of the wave function in terms of the scattering matrix is well known. However, in three-body theory this concept must be modified because, e.g. of the presence of a bound subsystem after scattering or two particles that stay close together after breakup. Both cases imply an interaction of at least two particles also in the asymptotic range. Consequently the concept of a finite interaction volume, a prerequisite of standard R -matrix theory, is not satisfied in three-body problems. In order to transfer the concept of the division of space to three-body systems, Glöckle [10] proposed the introduction of a border in the space of Jacobi-coordinates. Fig. 6 gives a schematic view of the division, where the contours $C_1 = (r_i, A_i), r_i \in [0, a_i]$ and $C_2 = (a_i, R_i), R_i \in [0, A_i]$ confine the "interaction region" D from the exterior region.

It is important to remark that the "inner region" D is not associated with a finite volume in space. However, we have to take care that for each subsystem i the two remaining sets of Jacobi coordinates $\vec{r}_j(\vec{r}_i, \vec{R}_i)$ and $\vec{r}_n(\vec{r}_i, \vec{R}_i)$ are confined to the area D as well. This is the central claim of R -matrix theory. In the r_i direction the potential $V_i(r_i)$ with range r_{0i} is acting, which determines the matching radius a_i . In the dimension R_i , however, there is no such criterion for A_i because due to the definition of the components in the Faddeev equations there is no interaction in R_i . For the moment A_i remains a free parameter and is specified by the requirement that all set of Jacobi coordinates must remain inside D .

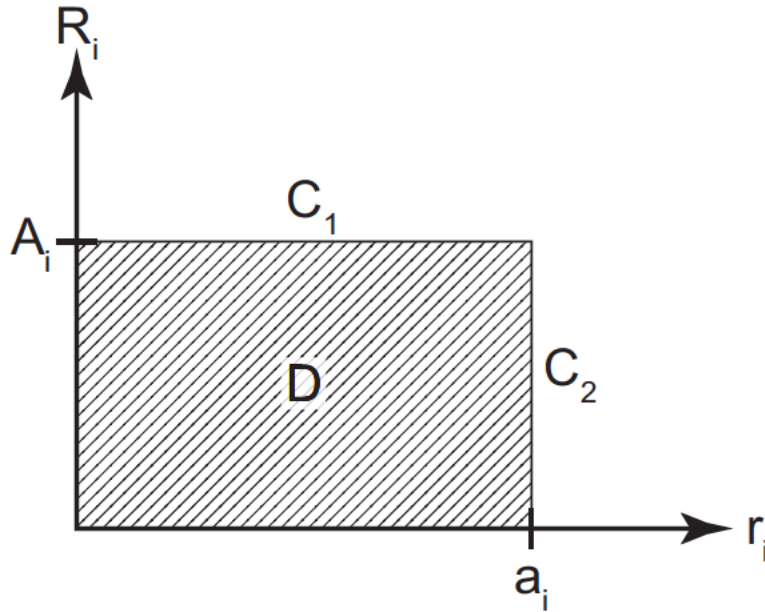


Figure 6: Division of Jacobi coordinate space

An estimation of the magnitudes for the sets of Jacobi coordinates is given by

$$\begin{aligned}
 \text{a) } \vec{r}_j &= -\frac{m_j}{m_j + m_n} \vec{r}_i - (-1)^j \vec{R}_i \xrightarrow{r_j \text{ in } D} \frac{m_j}{m_j + m_n} r_{0i} + A_i \leq a_i \\
 \text{b) } \vec{R}_j &= (-1)^j \frac{m_i m_n + m_j m_n + m_n m_n}{(m_i + m_n)(m_j + m_n)} \vec{r}_i - \frac{m_i}{m_i + m_n} \vec{R}_i \xrightarrow{R_j \text{ in } D} \\
 &\quad \frac{m_i m_n + m_j m_n + m_n m_n}{(m_i + m_n)(m_j + m_n)} r_{0i} + \frac{m_i}{m_i + m_n} A_i \leq A_i
 \end{aligned} \tag{5.44}$$

where we used

$$|\vec{a} \vec{r}_i \pm b \vec{R}_i| = \sqrt{(a r_i)^2 \pm 2ab(\vec{r}_i \cdot \vec{R}_i) + (b R_i)^2} \approx \sqrt{(a r_i)^2 + 2ab r_i R_i + (b R_i)^2} = a r_i + b R_i. \tag{5.45}$$

Expressing A explicitly from relation b) we get

$$\text{b) } A_i \geq \frac{m_i m_n + m_j m_n + m_n m_n}{(m_j + m_n) m_n} r_{0i} = \frac{m_i + m_j + m_n}{(m_j + m_n)} r_{0i} \tag{5.46}$$

Inserting b) in a) gives

$$\text{a) } \frac{m_j}{m_j + m_n} r_{0i} + \frac{m_i + m_j + m_n}{(m_j + m_n)} r_{0i} \leq a_i \Rightarrow a_i \geq \frac{m_i + 2m_j + m_n}{(m_j + m_n)} r_{0i} \tag{5.47}$$

Thus, by choosing the boundary parameters,

$$\begin{aligned} a_i &= \sup_{j \neq i} \left\{ \frac{m_i + 2m_j + m_n}{m_j + m_n} r_{0i} \right\}, \\ A_i &= \frac{m_i + m_j + m_n}{m_j + m_n} r_{0i}, \end{aligned} \quad (5.48)$$

r_j, R_j are confined to D . These are the lower limits for A_i and a_i which can always be enlarged by adding some constant greater than zero.

Proceeding in R -matrix theory the wave function $u_i(r_i, R_i)$ inside the area D is expanded over a complete sets of basis states,

$$u_i(r_i, R_i) = \sum_{\mu} c_{\mu}^{(i)} \varphi_{\mu}^{(i)}(r_i, R_i). \quad (5.49)$$

These states $\varphi_{\mu}^{(i)}(r_i, R_i)$ obey the equation

$$\left[-\frac{1}{2\mu_{jn}} \frac{d^2}{dr_i^2} + V_i(r_i) - \frac{1}{2\mu_{i(jn)}} \frac{d^2}{dR_i^2} - E_{\mu}^{(i)} \right] \varphi_{\mu}^{(i)}(r_i, R_i) = 0, \quad (5.50)$$

with the boundary conditions proposed by Glöckle [10],

$$\varphi_{\mu}^{(i)}(0, R_i) = \varphi_{\mu}^{(i)}(r_i, 0) = \frac{\varphi_{\mu}^{(i)}(r_i, R_i)}{\partial r_i} \Big|_{r_i=a_i} = \frac{\partial \varphi_{\mu}^{(i)}(r_i, R_i)}{\partial R_i} \Big|_{R_i=A_i} = 0, \quad (5.51)$$

which imply the orthonormality relation

$$\iint_D dr dR \varphi_{\mu}^{(i)}(r, R) \varphi_{\mu'}^{(i)}(r, R) = \delta_{\mu\mu'}. \quad (5.52)$$

Thus, the expansion coefficients can be calculated as

$$c_{\mu}^{(i)} = \iint_D dr dR \varphi_{\mu}^{(i)}(r, R) u_i(r, R). \quad (5.53)$$

It is convenient to write the basis functions as product states

$$\varphi_{\mu}^{(i)}(r, R) = X_{\mu_1}(r) Y_{\mu_2}(R), \quad (5.54)$$

where the functions $X_{\mu_1}^{(i)}(r)$ and $Y_{\mu_2}^{(i)}(R)$ are solutions of the equations

$$\left[-\frac{1}{2\mu_{jn}} \frac{d^2}{dr^2} + V_i(r) - \epsilon_{\mu_1}^{(i)} \right] X_{\mu_1}^{(i)}(r) = 0 \quad (5.55)$$

and

$$\left[-\frac{1}{2\mu_{i(jn)}} \frac{d^2}{dR^2} - \epsilon_{\mu_2}^{(i)} \right] Y_{\mu_2}^{(i)}(R) = 0. \quad (5.56)$$

The total energy $E_{\mu}^{(i)} = \epsilon_{\mu_1}^{(i)} + \epsilon_{\mu_2}^{(i)}$ is split into the energy of the two relative motions, $\epsilon_{\mu_1}^{(i)}$ (particle j relative to particle n) and $\epsilon_{\mu_2}^{(i)}$ (particle i relative to particles j and n where $i \neq j \neq n$ and $i \neq n$).

5.2.2 Equations of three-body R -matrix theory

The essential quantities that have to be determined in the three-body problem are the expansion coefficients $c_{\mu}^{(i)}$ for the interior wave function and the elastic, rearrangement and breakup T -amplitudes. In order to get equations for the $c_{\mu}^{(i)}$, Eq. (5.16) is projected onto the basis states $\varphi_{\mu}^{(i)}(r, R)$

$$\begin{aligned} \varphi_{\mu}^{(i)}(r_i, R_i) \left[-\frac{1}{2\mu_{jn}} \frac{d^2}{dr_i^2} + V_i(r_i) - \frac{1}{2\mu_{i(jn)}} \frac{d^2}{dR_i^2} - E \right] u_i(r_i, R_i) = \\ - \varphi_{\mu}^{(i)}(r_i, R_i) V_i(r_i) \int_{-1}^1 dx_i \frac{r_i R_i}{2} \sum_{\substack{j=1 \\ j \neq i}}^3 \frac{u_j(r_j, R_j)}{r_j R_j} \end{aligned} \quad (5.57)$$

and then integrated over the domain D ,

$$\begin{aligned} \iint_D dr dR \varphi_{\mu}^{(i)}(r_i, R_i) \left[-\frac{1}{2\mu_{jn}} \frac{d^2}{dr_i^2} + V_i(r_i) - \frac{1}{2\mu_{i(jn)}} \frac{d^2}{dR_i^2} - E \right] u_i(r_i, R_i) = \\ - \iint_D dr dR \varphi_{\mu}^{(i)}(r_i, R_i) V_i(r_i) \int_{-1}^1 dx_i \frac{r_i R_i}{2} \sum_{\substack{j=1 \\ j \neq i}}^3 \frac{u_j(r_j, R_j)}{r_j R_j}. \end{aligned} \quad (5.58)$$

Integrating the left hand side of Eq. (5.58) by parts and observing the boundary

conditions (5.51) (see Appendix A) yields

$$(E_\mu^{(i)} - E)c_\mu^{(i)} - \frac{1}{2\mu_{i(jn)}} \int_0^{a_i} dr \varphi_\mu^{(i)}(r, A_i) \left. \frac{du_i}{dR} \right|_{R=A_i} - \frac{1}{2\mu_{jn}} \int_0^{A_i} dR \varphi_\mu^{(i)}(a_i, R) \left. \frac{du_i}{dr} \right|_{r=a_i}, \quad (5.59)$$

Inserting the expansion of the wave function the right hand side of Eq. (5.58) one gets

$$\begin{aligned} & - \iint_D dr_i dR_i \varphi_\mu^{(i)}(r_i, R_i) V_i(r_i) \int_{-1}^1 dx_i \frac{r_i R_i}{2} \sum_{\substack{j=1 \\ j \neq i}}^3 \frac{u_j(r_j, R_j)}{r_j R_j} \\ & = - \iint_D dr_i dR_i \varphi_\mu^{(i)}(r_i, R_i) V_i(r_i) \int_{-1}^1 dx_i \frac{r_i R_i}{2} \sum_{\substack{j=1 \\ j \neq i}}^3 \sum_{\mu'} \frac{c_{\mu'}^{(j)} \varphi_{\mu'}^{(j)}(r_j, R_j)}{r_j R_j}. \end{aligned} \quad (5.60)$$

r_j and R_j always remain inside D , which is ensured by the values of the matching radii (5.48). With the matrix element

$$V_{\mu\mu'}^{(ij)} = \iint_D dr_i dR_i \varphi_\mu^{(i)}(r_i, R_i) V_i(r_i) \int_{-1}^1 dx_i r_i R_i \frac{\varphi_{\mu'}^{(j)}(r_j, R_j)}{2r_j R_j}, \quad (5.61)$$

Eq. (5.58) finally becomes

$$\begin{aligned} & (E_\mu^{(i)} - E)c_\mu^{(i)} + \sum_{\mu'} \sum_{\substack{j=1 \\ j \neq i}}^3 V_{\mu\mu'}^{(ij)} c_{\mu'}^{(j)} \\ & = \frac{1}{2\mu_{i(jn)}} \int_0^{a_i} dr \varphi_\mu^{(i)}(r, A_i) \left. \frac{du_i}{dR} \right|_{R=A_i} + \frac{1}{2\mu_{jn}} \int_0^{A_i} dR \varphi_\mu^{(i)}(a_i, R) \left. \frac{du_i}{dr} \right|_{r=a_i}. \end{aligned} \quad (5.62)$$

The wave functions on the borders (5.21) and (5.22) can be plugged into this equation [11] resulting in

$$\begin{aligned}
(E_\mu - E)c_\mu^{(i)} + \sum_{\substack{j=1 \\ j \neq i}}^3 \sum_{\mu'} V_{\mu\mu'}^{(j)} c_{\mu'}^{(j)} &= \frac{1}{2\mu_{i(jn)}} Q M_{\mu b} \cos(Q A_i) - i Q M_{\mu b} e^{i Q A_i} T_i^b \\
&- \frac{2}{\pi} \int_0^{\sqrt{2\mu_{jn}E}} dk i Q_k M_{\mu k}^{(-)} e^{i Q_k A_i} T_i(k) \\
&- \frac{1}{2\mu_{i(jn)}} \sum_{\substack{j=1 \\ j \neq i}}^3 \frac{e^{i\sqrt{2\mu_{j(in)}E} \frac{m_i}{m_i+m_n} A_i / \sin \varphi_j^*}}{A_i^{3/2}} i \sqrt{2\mu_{j(in)}E} \frac{m_i}{m_i+m_n} / \sin \varphi_j^* \\
&\times \left(\sqrt{\frac{2}{\pi}} e^{i\frac{\pi}{4}} 2\mu_{i(jn)} \sqrt{2\mu_{jn}} (2\mu_{j(in)})^{-\frac{1}{4}} \left(\frac{m_i+m_n}{m_i} \right)^{\frac{5}{2}} (\sin \varphi_j^*)^{\frac{7}{2}} E^{\frac{1}{4}} M_{\mu b} T_i \left(\sqrt{2\mu_{jn}E} \cos \varphi_j^* \right)} \right. \\
&\times \frac{2\mu_{i(jn)}}{\mu_{j(in)} \left(E - \frac{2Q^2}{\mu_{j(in)}} \sin^2 \varphi_j^* \right)} \int_0^{r_{0i}} dr u_i^b(r) V_i(r) \\
&+ \left(\frac{2}{\pi} \right)^{\frac{3}{2}} e^{i\frac{\pi}{4}} 2\mu_{i(jn)} \sqrt{2\mu_{jn}} (2\mu_{j(in)})^{-\frac{1}{4}} \left(\frac{m_i+m_n}{m_i} \sin \varphi_j^* \right)^{\frac{3}{2}} E^{\frac{1}{4}} \\
&\times \int_{\sqrt{2\mu_{jn}E}}^{\infty} dk M_{\mu k}^{(-)} T_i \left(\sqrt{2\mu_{jn}E} \cos \varphi_j^* \right) \frac{1}{\frac{1}{\mu_{jn}} k^2 - 2E + 2\frac{\mu_{j(in)}}{\mu_{i(jn)}} E \left(\frac{m_i}{(m_i+m_n) \sin \varphi_j^*} \right)^2} \\
&\times \left. \int_0^{\infty} dr u_k^{(-)*}(r) V_i(r) \right) - \frac{2\mu_{i(jn)}}{\pi \mu_{jn}} \int_0^{\sqrt{2\mu_{jn}E}} dk i k M_{\mu Q_k} e^{i k a_i} T_i(k) \\
&= \frac{1}{2\mu_{i(jn)}} Q M_{\mu b} \cos(Q A_i) - i Q M_{\mu b} e^{i Q A_i} T_i^b - \frac{2}{\pi} \int_0^{\sqrt{2\mu_{jn}E}} dk \left[i Q_k M_{\mu k}^{(-)} e^{i Q_k A_i} + \frac{\mu_{i(jn)}}{\mu_{jn}} i k M_{\mu Q_k} e^{i k a_i} \right] T_i(k) \\
&- \sum_{\substack{j=1 \\ j \neq i}}^3 \frac{i e^{i\sqrt{2\mu_{j(in)}E} \frac{m_i}{m_i+m_n} A_i / \sin \varphi_j^*}}{A_i^{3/2}} T_i \left(\sqrt{2\mu_{jn}E} \cos \varphi_j^* \right) \\
&\times \left(N_b(E) M_{\mu b} \frac{2\mu_{i(jn)}}{\mu_{j(in)} \left(E - \frac{2Q^2}{\mu_{j(in)}} \sin^2 \varphi_j^* \right)} \int_0^{r_{0i}} dr u_i^b(r) V_i(r) \right. \\
&+ \left. \frac{2}{\pi} N_k(E) \int_{\sqrt{2\mu_{jn}E}}^{\infty} M_{\mu k}^{(-)} \frac{1}{\frac{1}{\mu_{jn}} k^2 - 2E + 2\frac{\mu_{j(in)}}{\mu_{i(jn)}} E \left(\frac{m_i}{(m_i+m_n) \sin \varphi_j^*} \right)^2} \int_0^{\infty} dr u_k^{(-)*}(r) V_i(r) \right), \tag{5.63}
\end{aligned}$$

with

$$N_b(E) = \sqrt{\frac{2}{\pi}} e^{i\frac{\pi}{4}} \sqrt{2\mu_{jn}} (2\mu_{j(in)})^{\frac{1}{4}} \left(\frac{m_i + m_n}{m_i} \right)^{\frac{3}{2}} (\sin \varphi_j^*)^{\frac{5}{2}} E^{\frac{3}{4}}, \quad (5.64a)$$

$$N_k(E) = \sqrt{\frac{2}{\pi}} e^{i\frac{\pi}{4}} 2\mu_{i(jn)} \sqrt{2\mu_{jn}} (2\mu_{j(in)})^{\frac{1}{4}} \left(\frac{m_i + m_n}{m_i} \sin \varphi_j^* \right)^{\frac{1}{2}} E^{\frac{3}{4}}. \quad (5.64b)$$

The shortcuts are defined according to

$$\begin{aligned} M_{\mu b} &= \int_0^{a_i} dr \varphi_{\mu}^{(i)}(r, A_i) u_i^b(r), & M_{\mu k}^{(-)} &= \int_0^{a_i} dr \varphi_{\mu}^{(i)}(r, A_i) u_k^{(-)}(r) \\ M_{\mu Q} &= \int_0^{A_i} dR \varphi_{\mu}^{(i)}(a_i, R) \sin(QR), \end{aligned} \quad (5.65)$$

Eq. (5.63) represents a set of $(N_1 + N_2 + N_3)$ equations for the coefficients $c_{\mu}^{(1)}$, $c_{\mu}^{(2)}$ and $c_{\mu}^{(3)}$ and the amplitudes T_i^b and $T(k)$. N_i denotes the number of basis states used in the i -th Faddeev component and therefore $(N_1 + N_2 + N_3)$ is the total number of expansion coefficients $c_{\mu}^{(i)}$. Hence, there is a need of some more equations in order to get a unique solution. At the matching radii it is required that the interior and exterior wave function must equal each other yielding three additional relations. The continuity of the first derivative of the wave function at the matching radii is not explicitly included in this derivation. The consequences and resulting problems are discussed in subsection 7.4.

The leading terms of the wave function (5.21) for $R_i \rightarrow \infty$ and r_i fixed are

$$u_i(r_i, R_i) \simeq u_i^b(r_i) \sin(QR_i) - 2\mu_{i(jn)} u_b^{(i)}(r_i) e^{iQR_i} T_i^b - \frac{4}{\pi} \mu_{i(jn)} \int_0^{\sqrt{2\mu_{jn}E}} dk u_k^{(-)}(r_i) e^{iQ_k R_i} T_i(k) \quad (5.66)$$

Replacing the left hand side by the expansion valid in the interior region and projecting

the equation onto the bound state $u_i^b(r)$ gives

$$\begin{aligned} \int_0^{a_i} dr u_i^b(r) \sum_{\mu} c_{\mu}^{(i)} \varphi_{\mu}^{(i)}(r, A_i) &\simeq \underbrace{\int_0^{a_i} dr |u_i^b(r)|^2}_{=1} \sin(QA_i) - 2\mu_{i(jn)} \underbrace{\int_0^{a_i} dr |u_i^b(r)|^2}_{=1} e^{iQA_i} T_i^b \\ &- \frac{4}{\pi} \mu_{i(jn)} \int_0^{\sqrt{2\mu_{jn}E}} dk \underbrace{\int_0^{a_i} dr u_i^b(r) u_k^{(-)}(r)}_{\approx 0} e^{iQ_k A_i} T_i(k), \end{aligned} \quad (5.67)$$

where the relation $\int_0^{a_i} dr u_i^b(r) u_k^{(-)}(r) \approx 0$ on the line C_1 was used. Latter relation could be proved for the nuclear systems we considered following sections. The normalization of u_i^b ,

$$\int_0^{a_i} dr |u_i^b(r)|^2 = 1 \quad (5.68)$$

is valid only in case if $u_i^b(a_i) \approx 0$. This assumption which Glöckle made in [10] can be problematic for practical calculations and will be discussed in the next subsection.

Finally, T_i^b is given by the coefficients $c_{\mu}^{(i)}$ through

$$\sum_{\mu} M_{\mu b} c_{\mu}^{(i)} \simeq \sin(QA_i) - 2\mu_{i(jn)} e^{iQA_i} T_i^b. \quad (5.69)$$

The integral in Eq. (5.66) can be replaced by the asymptotic expression of the three-body wave function in Eq. (5.26) while the left hand side is again given by an expansion over basis functions. On the contour C_1 Eq. (5.66) reduces to

$$\begin{aligned} \sum_{\mu} c_{\mu}^{(i)} \varphi_{\mu}^{(i)}(r_i, A_i) - u_i^b(r_i) [\sin(QA_i) - 2\mu_{i(jn)} e^{iQA_i} T_i^b] \\ \simeq (2\mu_{i(jn)})^{3/2} \sqrt{2\mu_{jn}} \sqrt{\frac{2}{\pi}} e^{i\frac{\pi}{4}} E^{1/4} \frac{e^{i\rho_A \sqrt{E}}}{\rho_A^{1/2}} \frac{A_i}{\rho_A} T_i \left(2\mu_{jn} \sqrt{E} \frac{r_i}{\rho_A} \right), \end{aligned} \quad (5.70)$$

with $\rho_A = \sqrt{2\mu_{jn} r_i^2 + 2\mu_{i(jn)} A_i^2}$ and $\sin \varphi_i|_{C_1} = \sqrt{2\mu_{i(jn)}} \frac{A_i}{\rho_A}$. The same procedure is

carried out on the line C_2 and provides the fourth equation,

$$\begin{aligned}
& \sum_{\mu} c_{\mu}^{(i)} \varphi_{\mu}^{(i)}(a_i, R_i) \\
& \simeq u_i^b(a_i) [\sin(QR_i) - 2\mu_{i(jn)} e^{iQR_i T_i^b}] + (2\mu_{i(jn)})^{3/2} \sqrt{\frac{2}{\pi}} e^{i\frac{\pi}{4}} E^{1/4} \frac{e^{i\rho_a \sqrt{E}} R_i}{\rho_a^{1/2} \rho_a} T_i \left(2\mu_{jn} \sqrt{E} \frac{a_i}{\rho_a} \right) \\
& \simeq (2\mu_{i(jn)})^{3/2} \sqrt{\frac{2}{\pi}} e^{i\frac{\pi}{4}} E^{1/4} \frac{e^{i\rho_a \sqrt{E}} R_i}{\rho_a^{1/2} \rho_a} T_i \left(2\mu_{jn} \sqrt{E} \frac{a_i}{\rho_a} \right),
\end{aligned} \tag{5.71}$$

with $\rho_a = \sqrt{2\mu_{jn} a_i^2 + 2\mu_{i(jn)} R_i^2}$ and Glöckle's assumption $u_i^b(a_i) \approx 0$.

The set of equations that uniquely determines the expansion coefficients $c_{\mu}^{(i)}$ and the three-body T -amplitudes, T_i^b and $T_i(k)$, reads

$$1) (E_\mu^{(i)} - E) c_\mu^{(i)} + \sum_{\substack{j=1 \\ j \neq i}}^3 \sum_{\mu'} V_{\mu\mu'}^{(j)} c_{\mu'}^{(j)} \quad (5.72a)$$

$$\begin{aligned} &= \frac{1}{2\mu_{i(jn)}} Q M_{\mu b} \cos(QA_i) - iQ M_{\mu b} e^{iQA_i} T_i^b \\ &\quad - \frac{2}{\pi} \int_0^{\sqrt{2\mu_{jn}E}} dk \left[iQ_k M_{\mu k}^{(-)} e^{iQ_k A_i} + \frac{\mu_{i(jn)}}{\mu_{jn}} i k M_{\mu Q_k} e^{i k a_i} \right] T_i(k) \\ &\quad - \sum_{\substack{j=1 \\ j \neq i}}^3 \frac{i e^{i\sqrt{2\mu_{j(in)}E} \frac{m_i}{m_i+m_n} A_i / \sin \varphi_j^*}}{A_i^{3/2}} T_i \left(\sqrt{2\mu_{jn}E} \cos \varphi_j^* \right) \\ &\quad \times \left(N_b(E) M_{\mu b} \frac{2\mu_{i(jn)}}{\mu_{j(in)} \left(E - \frac{2Q^2}{\mu_{j(in)}} \sin^2 \varphi_j^* \right)} \int_0^{r_{0i}} dr u_i^b(r) V_i(r) \right. \\ &\quad \left. + \frac{2}{\pi} N_k(E) \int_{\sqrt{2\mu_{jn}E}}^\infty dk M_{\mu k}^{(-)} \frac{1}{\frac{1}{\mu_{jn}} k^2 - 2E + 2\frac{\mu_{j(in)}}{\mu_{i(jn)}} E \left(\frac{m_i}{(m_i+m_n) \sin \varphi_j^*} \right)^2} \int_0^{r_{0i}} dr u_k^{(-)*}(r) V_i(r) \right) \end{aligned}$$

$$2) \sum_{\mu} M_{\mu b} c_\mu^{(i)} \simeq \sin(QA_i) - 2\mu_{i(jn)} e^{iQA_i} T_i^b \quad (5.72b)$$

$$3) \sum_{\mu} c_\mu^{(i)} \varphi_\mu^{(i)}(r_i, A_i) - u_i^b(r_i) [\sin(QA_i) - 2\mu_{i(jn)} e^{iQA_i} T_i^b] \quad (5.72c)$$

$$\simeq (2\mu_{i(jn)})^{3/2} \sqrt{2\mu_{jn}} \sqrt{\frac{2}{\pi}} e^{i\frac{\pi}{4}} E^{1/4} \frac{e^{i\rho_A \sqrt{E}}}{\rho_A^{1/2}} \frac{A_i}{\rho_A} T_i \left(2\mu_{jn} \sqrt{E} \frac{r_i}{\rho_A} \right)$$

$$4) \sum_{\mu} c_\mu^{(i)} \varphi_\mu^{(i)}(a_i, R_i) \simeq (2\mu_{i(jn)})^{3/2} \sqrt{\frac{2}{\pi}} e^{i\frac{\pi}{4}} E^{1/4} \frac{e^{i\rho_a \sqrt{E}}}{\rho_a^{1/2}} \frac{R_i}{\rho_a} T_i \left(2\mu_{jn} \sqrt{E} \frac{a_i}{\rho_a} \right). \quad (5.72d)$$

This system of equations was first derived by Glöckle for three identical bosons in [10] and is presented here in its generalized form for three different particles elaborated in [11].

5.3 Formulation of a new applicable R -matrix method

In the previous subsection the generalization of the three-body R -matrix formalism to three different masses and different interactions, first presented in [11], was revisited. This generalization was the first important step with regard to applicability of the formalism. The method follows the key idea of the proposal of Glöckle [10], but also bears its shortcomings. Essential modifications are required to obtain an applicable R -matrix formalism for three-body breakup channels. This new R -matrix formalism is subject of this subsection and the updated set of equations suitable for numerical implementation and application is presented at the end of this subsection in Eq. (5.85).

One modification concerns the boundary conditions for the basis functions. In the proposal [10] the following conditions were introduced

$$\varphi_{\mu}^{(i)}(0, R_i) = \varphi_{\mu}^{(i)}(r_i, 0) = \left. \frac{\varphi_{\mu}^{(i)}(r_i, R_i)}{\partial r_i} \right|_{r_i=a_i} = \left. \frac{\partial \varphi_{\mu}^{(i)}(r_i, R_i)}{\partial R_i} \right|_{R_i=A_i} = 0. \quad (5.73)$$

However, from the vanishing first derivatives at the boundaries (see Fig. 6) there results a problem from a practical point of view. The conditions (5.73) imply a discrete energy grid in $E_{\mu}^{(i)}$ which can be problematic for practical calculations because it can occur that the energy step width gets too large and consequently the interior three-body wave function cannot be reproduced properly in certain energy ranges.

This issue gives rise to reduce the boundary conditions (5.73) to

$$\varphi_{\mu}^{(i)}(0, R_i) = \varphi_{\mu}^{(i)}(r_i, 0) = 0. \quad (5.74)$$

Then the orthonormality relation (5.52) is no longer valid, but

$$\int_0^A dR \int_0^a dr \varphi_{\mu}^{(i)}(r, R) \varphi_{\mu'}^{(i)}(r, R) = C_{\mu\mu'}^{(i)}. \quad (5.75)$$

This matrix $C_{\mu\mu'}$ enters Eq. (5.72a) via the integral

$$\int_0^A dR \int_0^a dr (E_{\mu} - E) u_i(r, R) \varphi_{\mu}^{(i)}(r, R) = \sum_{\mu'} C_{\mu\mu'} c_{\mu'} \quad (5.76)$$

since $u_i(r_i, R_i) = \sum_{\mu'} c_{\mu'}^{(i)} \varphi_{\mu'}^{(i)}(r_i, R_i)$ in the interior region.

A further consequence of these boundary conditions shows up when partially integrating the left hand side of Eq. (5.58)

$$\begin{aligned}
(E_\mu^{(i)} - E)c_\mu^{(i)} &- \frac{1}{2\mu_{i(jn)}} \int_0^{a_i} dr \varphi_\mu^{(i)}(r, A_i) \left. \frac{du_i}{dR} \right|_{R=A_i} + \frac{1}{2\mu_{i(jn)}} \int_0^{a_i} dr u_i(r, A_i) \left. \frac{d\varphi_\mu^{(i)}}{dR} \right|_{R=A_i} \\
&- \frac{1}{2\mu_{jn}} \int_0^{A_i} dR \varphi_\mu^{(i)}(a_i, R) \left. \frac{du_i}{dr} \right|_{r=a_i} + \frac{1}{2\mu_{jn}} \int_0^{A_i} dR u_i(a_i, R) \left. \frac{d\varphi_\mu^{(i)}}{dr} \right|_{r=a_i}
\end{aligned} \tag{5.77}$$

The terms containing a first derivative of the basis functions at the boundary lines did not appear in Eq. (5.59) as shown in Appendix A.

Another important modification concerns the bound state wave functions $u_i^b(r)$ in subsystems. In the original proposal [10] it is assumed that $u_i^b(r)$ at $r = a_i$ is negligible. However, in most light nuclear systems the values of $u_i^b(r)$ at $r = a_i$ cannot be ignored for reasonable values of a_i and $u_i^b(a_i)$ must be included in the formulæ. This affects Eq. (5.72a) and the boundary condition in Eq. (5.72d). Latter is derived from Eq. (5.66) using the asymptotic expression (5.26) and the expansion of the wave function in the interior region and now reads

$$\begin{aligned}
&\sum_\mu c_\mu^{(i)} \varphi_\mu^{(i)}(a_i, R_i) \\
&\simeq u_i^b(a_i) e^{iQ(R_i - A_i)} \sum_\mu M_{\mu b} c_\mu^{(i)} + u_i^b(a_i) [\sin(QR_i) - e^{iQ(R_i - A_i)} \sin(QA_i)] \\
&+ (2\mu_{i(jn)})^{3/2} \sqrt{\frac{2}{\pi}} e^{i\frac{\pi}{4}} E^{1/4} \frac{e^{i\rho_a \sqrt{E}} R_i}{\rho_a^{1/2}} \frac{R_i}{\rho_a} T_i \left(2\mu_{jn} \sqrt{E} \frac{a_i}{\rho_a} \right),
\end{aligned} \tag{5.78}$$

with $\rho_a = \sqrt{2\mu_{jn}a_i^2 + 2\mu_{i(jn)}R_i^2}$. The boundary condition (5.72b) which is obtained by projecting $u_i^b(r)$ onto the asymptotic three-body wave function (5.21) gets slightly changed because if $u_i^b(a_i) \neq 0$ then $u_i^b(r)$ is not normalized to 1 in the interval $[0, a_i]$.

Consequently

$$\begin{aligned}
\int_0^{a_i} dr u_i^b(r) \sum_{\mu} c_{\mu}^{(i)} \varphi_{\mu}^{(i)}(r, A_i) &\simeq \underbrace{\int_0^{a_i} dr |u_i^b(r)|^2 \sin(QA_i)}_{=\bar{C}} - 2\mu_{i(jn)} \underbrace{\int_0^{a_i} dr |u_i^b(r)|^2 e^{iQA_i T_i^b}}_{=\bar{C}} \\
&\quad - \frac{4}{\pi} \mu_{i(jn)} \int_0^{\sqrt{2\mu_{jn}E}} dk \underbrace{\int_0^{a_i} dr u_i^b(r) u_k^{(-)}(r) e^{iQ_k A_i T_i(k)}}_{\approx 0},
\end{aligned} \tag{5.79}$$

and Eq. (5.72b) becomes

$$\tilde{C} \sum_{\mu} M_{\mu b} c_{\mu}^{(i)} \simeq \sin(QA_i) - 2\mu_{i(jn)} e^{iQA_i T_i^b}. \tag{5.80}$$

The introduced constants are $1/\bar{C} = \tilde{C}$. The boundary condition (5.72c) is not touched by the introduced modifications.

The extended set of three-body R -matrix equations containing the mentioned modifications is obtained by plugging the asymptotic forms of the three-body wave function (5.21) and (5.22) into the equation

$$\begin{aligned}
(E_{\mu}^{(i)} - E)c_{\mu}^{(i)} + \sum_{\mu'} \sum_{\substack{j=1 \\ j \neq i}}^3 V_{\mu\mu'}^{(ij)} c_{\mu'}^{(j)} &= \\
\frac{1}{2\mu_{i(jn)}} \int_0^{a_i} dr \varphi_{\mu}^{(i)}(r, A_i) \frac{du_i}{dR} \Big|_{R=A_i} - \frac{1}{2\mu_{i(jn)}} \int_0^{a_i} dr u_i(r, A_i) \frac{d\varphi_{\mu}^{(i)}}{dR} \Big|_{R=A_i} &\tag{5.81} \\
+ \frac{1}{2\mu_{jn}} \int_0^{A_i} dR \varphi_{\mu}^{(i)}(a_i, R) \frac{du_i}{dr} \Big|_{r=a_i} - \frac{1}{2\mu_{jn}} \int_0^{A_i} dR u_i(a_i, R) \frac{d\varphi_{\mu}^{(i)}}{dr} \Big|_{r=a_i} &.
\end{aligned}$$

This yields

$$\begin{aligned}
& (E_\mu^{(i)} - E) \sum_{\mu'} C_{\mu\mu'}^{(i)} c_{\mu'}^{(i)} + \sum_{\substack{j=1 \\ j \neq i}}^3 \sum_{\mu'} V_{\mu\mu'}^{(ij)} c_{\mu'}^{(j)} \\
&= \frac{1}{2\mu_{i(jn)}} \left[M_{\mu b} Q \cos(Q A_i) - \tilde{M}_{\mu b} \sin(Q A_i) \right] \\
&+ \frac{1}{2\mu_{jn}} \left[M_{\mu Q} \frac{du_i^b(r)}{dr} \Big|_{r=a_i} - \tilde{M}_{\mu Q} u_i^b(a_i) \right] - (iQ M_{\mu b} - \tilde{M}_{\mu b}) e^{iQ A_i} T_i^b \\
&- \frac{2}{\pi} \int_0^{\sqrt{2\mu_{jn} E}} dk \left[(iQ_k M_{\mu k}^{(-)} - \tilde{M}_{\mu k}^{(-)}) e^{iQ_k A_i} + \frac{\mu_{i(jn)}}{\mu_{jn}} (ik M_{\mu Q_k} - \tilde{M}_{\mu Q_k}) e^{ika_i} \right] T_i(k) \\
&- \sum_{\substack{j=1 \\ j \neq i}}^3 \frac{e^{i\sqrt{2\mu_{j(in)} E} \frac{m_i}{m_i+m_n} A_i / \sin \varphi_j^*}}{A_i^{3/2}} \left(i - \frac{(m_i + m_n) \sin \varphi_j^*}{m_i \sqrt{2\mu_{j(in)} E}} \frac{d\varphi_{\mu 2}^{(i)}(R)}{dR} \Big|_{R=A_i} \frac{1}{\varphi_{\mu 2}^{(i)}(A_i)} \right) \\
&\times T_i \left(\sqrt{2\mu_{jn} E} \cos \varphi_j^* \right) \left(N_b(E) M_{\mu b} \frac{2\mu_{i(jn)}}{\mu_{j(in)} \left(E - \frac{2Q^2}{\mu_{j(in)}} \sin^2 \varphi_j^* \right)} \int_0^{r_{0i}} dr u_i^b(r) V_i(r) \right. \\
&\left. + \frac{2}{\pi} N_k(E) \int_{\sqrt{2\mu_{jn} E}}^\infty dk M_{\mu k}^{(-)} \frac{1}{\frac{1}{\mu_{jn}} k^2 - 2E + 2\frac{\mu_{j(in)}}{\mu_{i(jn)}} E \left(\frac{m_i}{(m_i+m_n) \sin \varphi_j^*} \right)^2} \int_0^{r_{0i}} dr u_k^{(-)*}(r) V_i(r) \right) \\
&\cdot
\end{aligned} \tag{5.82}$$

The shortcuts are

$$\begin{aligned}
M_{\mu b} &= \int_0^{a_i} dr \varphi_\mu^{(i)}(r, A_i) u_i^b(r), & \tilde{M}_{\mu b} &= M_{\mu b} \cdot \left(\frac{d\varphi_{\mu 2}^{(i)}(R)}{dR} \Big|_{R=A_i} \frac{1}{\varphi_{\mu 2}^{(i)}(A_i)} \right) \\
M_{\mu Q} &= \int_0^{A_i} dR \varphi_\mu^{(i)}(a_i, R) \sin(QR), & \tilde{M}_{\mu Q} &= M_{\mu Q} \cdot \left(\frac{d\varphi_{\mu 1}^{(i)}(r)}{dr} \Big|_{r=a_i} \frac{1}{\varphi_{\mu 1}^{(i)}(a_i)} \right) \\
M_{\mu k}^{(-)} &= \int_0^{a_i} dr \varphi_\mu^{(i)}(r, A_i) u_k^{(-)}(r), & \tilde{M}_{\mu k}^{(-)} &= M_{\mu k}^{(-)} \cdot \left(\frac{d\varphi_{\mu 2}^{(i)}(R)}{dR} \Big|_{R=A_i} \frac{1}{\varphi_{\mu 2}^{(i)}(A_i)} \right).
\end{aligned} \tag{5.83}$$

The total system of equations containing all mentioned modifications reads

$$1) (E_\mu^{(i)} - E) \sum_{\mu'} C_{\mu\mu'}^{(i)} c_{\mu'}^{(i)} + \sum_{\substack{j=1 \\ j \neq i}}^3 \sum_{\mu'} V_{\mu\mu'}^{(ij)} c_{\mu'}^{(j)} \quad (5.84a)$$

$$= \frac{1}{2\mu_{i(jn)}} \left[M_{\mu b} Q \cos(QA_i) - \tilde{M}_{\mu b} \sin(QA_i) \right] \\ + \frac{1}{2\mu_{jn}} \left[M_{\mu Q} \frac{du_i^b(r)}{dr} \Big|_{r=a_i} - \tilde{M}_{\mu Q} u_i^b(a_i) \right] - (iQ M_{\mu b} - \tilde{M}_{\mu b}) e^{iQA_i} T_i^b \\ - \frac{2}{\pi} \int_0^{\sqrt{2\mu_{jn}E}} dk \left[(iQ_k M_{\mu k}^{(-)} - \tilde{M}_{\mu k}^{(-)}) e^{iQ_k A_i} + \frac{\mu_{i(jn)}}{\mu_{jn}} (ik M_{\mu Q_k} - \tilde{M}_{\mu Q_k}) e^{ika_i} \right] T_i(k) \\ - \sum_{\substack{j=1 \\ j \neq i}}^3 \frac{e^{i\sqrt{2\mu_{j(in)}E} \frac{m_i}{m_i+m_n} A_i / \sin \varphi_j^*}}{A_i^{3/2}} \left(i - \frac{(m_i + m_n) \sin \varphi_j^*}{m_i \sqrt{2\mu_{j(in)}E}} \frac{d\varphi_{\mu 2}^{(i)}(R)}{dR} \Big|_{R=A_i} \frac{1}{\varphi_{\mu 2}^{(i)}(A_i)} \right)$$

$$\times T_i \left(\sqrt{2\mu_{jn}E} \cos \varphi_j^* \right) \left(N_b(E) M_{\mu b} \frac{2\mu_{i(jn)}}{\mu_{j(in)} \left(E - \frac{2Q^2}{\mu_{j(in)}} \sin^2 \varphi_j^* \right)} \int_0^{r_{0i}} dr u_i^b(r) V_i(r) \right. \\ \left. + \frac{2}{\pi} N_k(E) \int_{\sqrt{2\mu_{jn}E}}^{\infty} dk M_{\mu k}^{(-)} \frac{1}{\frac{1}{\mu_{jn}} k^2 - 2E + 2\frac{\mu_{j(in)}}{\mu_{i(jn)}} E \left(\frac{m_i}{(m_i+m_n) \sin \varphi_j^*} \right)^2} \int_0^{r_{0i}} dr u_k^{(-)*}(r) V_i(r) \right)$$

$$2) \tilde{C} \sum_{\mu} M_{\mu b} c_{\mu}^{(i)} \simeq \sin(QA_i) - 2\mu_{i(jn)} e^{iQA_i} T_i^b \quad (5.84b)$$

$$3) \sum_{\mu} c_{\mu}^{(i)} \varphi_{\mu}^{(i)}(r_i, A_i) - u_i^b(r_i) \sum_{\mu} M_{\mu b} c_{\mu}^{(i)} \quad (5.84c)$$

$$\simeq (2\mu_{i(jn)})^{3/2} \sqrt{2\mu_{jn}} \sqrt{\frac{2}{\pi}} e^{i\frac{\pi}{4}} E^{1/4} \frac{e^{i\rho_A \sqrt{E}}}{\rho_A^{1/2}} \frac{A_i}{\rho_A} T_i \left(2\mu_{jn} \sqrt{E} \frac{r_i}{\rho_A} \right)$$

$$4) \sum_{\mu} c_{\mu}^{(i)} \varphi_{\mu}^{(i)}(a_i, R_i) \quad (5.84d)$$

$$\simeq u_i^b(a_i) e^{iQ(R_i - A_i)} \sum_{\mu} M_{\mu b} c_{\mu}^{(i)} + u_i^b(a_i) [\sin(QR_i) - e^{iQ(R_i - A_i)} \sin(QA_i)]$$

$$+ (2\mu_{i(jn)})^{3/2} \sqrt{\frac{2}{\pi}} e^{i\frac{\pi}{4}} E^{1/4} \frac{e^{i\rho_a \sqrt{E}}}{\rho_a^{1/2}} \frac{R_i}{\rho_a} T_i \left(2\mu_{jn} \sqrt{E} \frac{a_i}{\rho_a} \right),$$

In Eqs. (5.84b)-(5.84d) the T -amplitudes can be expressed explicitly and plugged into

Eq. (5.84a). For the $T_i(k)$ amplitudes it depends on the value of k whether Eq. (5.84c) or (5.84d) is used. This point is discussed in detail in subsection 6.1.

We finally obtain a set of four equations that uniquely determines the three-body problem in the frame of R -matrix theory

$$1) (E_\mu^{(i)} - E) \sum_{\mu'} C_{\mu\mu'}^{(i)} c_{\mu'}^{(i)} + \sum_{\substack{j=1 \\ j \neq i}}^3 \sum_{\mu'} V_{\mu\mu'}^{(ij)} c_{\mu'}^{(j)} \quad (5.85a)$$

$$\begin{aligned} &= \frac{1}{2\mu_{i(jn)}} M_{\mu b} Q \cos(QA_i) - \frac{1}{2\mu_{i(jn)}} M_{\mu b} iQ \sin(QA_i) \\ &+ \frac{1}{2\mu_{jn}} \left[M_{\mu Q} \frac{du_i^b(r)}{dr} \Big|_{r=a_i} - \tilde{M}_{\mu Q} u_i^b(a_i) \right] + \frac{\tilde{C}}{2\mu_{i(jn)}} (iQ M_{\mu b} + \tilde{M}_{\mu b}) \sum_{\mu'} M_{\mu' b} c_{\mu'}^{(i)} \\ &- \frac{2}{\pi} \int_0^{\sqrt{2\mu_{jn}E}} dk \left[(iQ_k M_{\mu k}^{(-)} - \tilde{M}_{\mu k}^{(-)}) e^{iQ_k A_i} + \frac{\mu_{i(jn)}}{\mu_{jn}} (ik M_{\mu Q_k} - \tilde{M}_{\mu Q_k}) e^{ik a_i} \right] T_i(k) \\ &- H_\mu^{(i)}(A_i) \end{aligned}$$

$$2) T_i^b \simeq -\frac{1}{2\mu_{i(jn)}} e^{-iQA_i} \left[\tilde{C} \sum_{\mu} M_{\mu b} c_{\mu}^{(i)} - \sin(QA_i) \right] \quad (5.85b)$$

$$3) T_i \left(2\mu_{jn} \sqrt{E} \frac{r_i}{\rho_A} \right) \quad (5.85c)$$

$$\simeq \left[\sum_{\mu} \varphi_{\mu}^{(i)}(r_i, A_i) - u_i^b(r_i) \sum_{\mu} M_{\mu b} c_{\mu}^{(i)} \right] \left[(2\mu_{i(jn)})^{3/2} \sqrt{2\mu_{jn}} \sqrt{\frac{2}{\pi}} e^{i\frac{\pi}{4}} E^{1/4} \frac{e^{i\rho_A \sqrt{E}}}{\rho_A^{1/2}} \frac{A_i}{\rho_A} \right]^{-1}$$

$$4) T_i \left(2\mu_{jn} \sqrt{E} \frac{a_i}{\rho_a} \right) \quad (5.85d)$$

$$\begin{aligned} &\simeq \left[\sum_{\mu} c_{\mu}^{(i)} \varphi_{\mu}^{(i)}(a_i, R_i) - u_i^b(a_i) e^{iQ(R_i - A_i)} \sum_{\mu} M_{\mu b} c_{\mu}^{(i)} \right. \\ &\left. - u_i^b(a_i) [\sin(QR_i) - e^{iQ(R_i - A_i)} \sin(QA_i)] \right] \left[(2\mu_{i(jn)})^{3/2} \sqrt{\frac{2}{\pi}} e^{i\frac{\pi}{4}} E^{1/4} \frac{e^{i\rho_a \sqrt{E}}}{\rho_a^{1/2}} \frac{R_i}{\rho_a} \right]^{-1} . \end{aligned}$$

with $\rho_a = \sqrt{2\mu_{jn}a_i^2 + 2\mu_{i(jn)}R_i^2}$, $\rho_A = \sqrt{2\mu_{jn}r_i^2 + 2\mu_{i(jn)}A_i^2}$ and the leading asymp-

otic term of order $O\left(\frac{1}{A_i^{3/2}}\right)$,

$$\begin{aligned}
H_\mu^{(i)}(A_i) \equiv & \sum_{\substack{j=1 \\ j \neq i}}^3 \frac{e^{i\sqrt{2\mu_j(in)}E} \frac{m_i}{m_i+m_n} A_i / \sin \varphi_j^*}{A_i^{3/2}} \left(i - \frac{(m_i + m_n) \sin \varphi_j^*}{m_i \sqrt{2\mu_j(in)}E} \frac{d\varphi_{\mu 2}^{(i)}(R)}{dR} \Big|_{R=A_i} \frac{1}{\varphi_{\mu 2}^{(i)}(A_i)} \right) \\
& \times T_i \left(\sqrt{2\mu_{jn}}E \cos \varphi_j^* \right) \left(N_b(E) M_{\mu b} \frac{2\mu_{i(jn)}}{\mu_{j(in)} \left(E - \frac{2Q^2}{\mu_{j(in)}} \sin^2 \varphi_j^* \right)} \int_0^{r_{0i}} dr u_i^b(r) V_i(r) \right. \\
& \left. + \frac{2}{\pi} N_k(E) \int_{\sqrt{2\mu_{jn}}E}^\infty dk M_{\mu k}^{(-)} \frac{1}{\frac{1}{\mu_{jn}} k^2 - 2E + 2\frac{\mu_{j(in)}}{\mu_{i(jn)}} E \left(\frac{m_i}{(m_i+m_n) \sin \varphi_j^*} \right)^2} \int_0^{r_{0i}} dr u_k^{(-)*}(r) V_i(r) \right).
\end{aligned} \tag{5.86}$$

Comparing Eqs.(5.85) with Eqs. (5.72), these extensions result in the additional quantities $\tilde{M}_{\mu b}$, $\tilde{M}_{\mu Q}$, $\tilde{M}_{\mu k}^{(-)}$, $\tilde{M}_{\mu Q k}$ and

$$\sum_{\substack{j=1 \\ j \neq i}}^3 \frac{e^{i\sqrt{2\mu_j(in)}E} \frac{m_i}{m_i+m_n} A_i / \sin \varphi_j^*}{A_i^{3/2}} \frac{(m_i + m_n) \sin \varphi_j^*}{m_i \sqrt{2\mu_j(in)}E} \frac{d\varphi_{\mu 2}^{(i)}(R)}{dR} \Big|_{R=A_i} \frac{1}{\varphi_{\mu 2}^{(i)}(A_i)} \times \dots$$

which is part of the $O\left(\frac{1}{A_i^{3/2}}\right)$ asymptotic term.

We have obtained a system of linear equations (5.85a) for the expansion coefficient $c_\mu^{(i)}$ and the T -amplitudes $T_i(k)$ and T_i^b . There are three additional conditions required [Eqs. (5.85b)-(5.85d)] in order to obtain a unique solution. These conditions were derived in the previous subsection and generalized under the use of the modifications introduced in this subsection.

Recalling the form of the two-body R -matrix in Eq. (2.77) the three-body R -matrix in Eq. (5.85a) exhibits the same structure with everything *inside* the internal region on the left hand side and the terms from *outside* on the right hand side.

The three-body R -matrix equations in the form (5.85) were numerically implemented (Sec. 6) and applied to the neutron+deuteron and the neutron+⁹Be system (Sec. 7).

5.4 Calculation of cross sections

The T -amplitudes determined via solution of the set of linear equations (5.85) provide a direct link to the observables, i.e. the cross sections. The elastic cross section is given in terms of T_1^b [Eq. (5.30)], the rearrangement cross sections in terms of T_2^b and T_3^b [Eq. (5.30)] and the breakup cross section to $T(k)$ [Eq. (5.31)]. Corresponding formulæ for the cross sections in terms of T_i^b and $T_i(k)$ were not available and had to be derived from standard scattering theory (see e.g. [20]). In this subsection we include \hbar explicitly and do not set $\hbar = 1$.

We start with the elastic cross section and consider the elastic T -amplitude, $T_{\vec{Q}'\vec{Q}}$, which is equivalent to Eq. (2.36) in the two-particle case. The only difference is that \vec{k} used for the wavenumber in subsection (2.1) is now replaced by \vec{Q} in the three-body problem. In partial wave expansion $T_{\vec{Q}'\vec{Q}}$ is

$$T_{\vec{Q}'\vec{Q}} = \sum_{l,m} Y_{lm}^*(\hat{Q}') T_l(Q) Y_{lm}(\hat{Q}) = \frac{1}{4\pi} \sum_{\ell=0}^{\infty} (2\ell + 1) T_{\ell}(Q) P_{\ell}(\hat{Q}'\hat{Q}) \quad (5.87)$$

Because in the three-body R -matrix method presented in this thesis we consider s-waves only we also restrict ourselves to $\ell = 0$ (s-waves) here and consider $T_{\vec{Q}'\vec{Q}} = \frac{1}{4\pi} T_0(Q)$ only. The elastic cross section reads in analogy to Eq. (2.42)

$$\begin{aligned} \sigma_{elastic} &= \left(\frac{2\pi}{\hbar}\right)^4 \mu_{1(23)}^2 \int d^2\hat{Q}' |T_{\vec{Q}'\vec{Q}}|^2 = \left(\frac{2\pi}{\hbar}\right)^4 \mu_{1(23)}^2 \int d^2\hat{Q}' \frac{1}{(4\pi)^2} |T_0(Q)|^2 \\ &= \frac{4\pi^3}{\hbar^4} \mu_{1(23)}^2 |T_0(Q)|^2, \end{aligned} \quad (5.88)$$

where $\mu_{1(23)}$ denotes the reduced mass of the projectile and the subsystem in the entrance channel. The on-shell S -matrix $\tilde{S}_{\vec{Q}'\vec{Q}}$ is related to the S -matrix (Eq. (2.24)) via

$$S_{\vec{Q}'\vec{Q}} = \frac{\hbar^2}{Q\mu_{1(23)}} \delta(E_{\vec{Q}'} - E_{\vec{Q}}) \tilde{S}_{\vec{Q}'\vec{Q}} \quad (5.89)$$

with

$$S_{\vec{Q}'\vec{Q}} = \delta(\vec{Q}' - \vec{Q}) - 2\pi i \delta(E_{\vec{Q}'} - E_{\vec{Q}}) T_{\vec{Q}'\vec{Q}} \quad (5.90)$$

and

$$\delta(\vec{Q}' - \vec{Q}) = \frac{\hbar^2}{Q\mu_{1(23)}} \delta(E_{\vec{Q}'} - E_{\vec{Q}}) \delta(\hat{Q}' - \hat{Q}). \quad (5.91)$$

Hence

$$\tilde{S}_{\vec{Q}'\vec{Q}} = \delta(\hat{Q}' - \hat{Q}) - i\mu_{1(23)}Q \frac{2\pi}{\hbar^2} T_{\vec{Q}'\vec{Q}}. \quad (5.92)$$

Glöckle's work [10] is based on the dimensionless on-shell T -amplitude T_i^b . For the optical theorem below the breakup threshold we get for arbitrary masses

$$\text{Im } T_1^b = -2 \frac{\mu_{1(23)}}{m_n} (|T_1^b|^2 + |T_2^b|^2 + |T_3^b|^2). \quad (5.93)$$

where m_n denotes the neutron mass and μ_{23} is the reduced mass of the two particles in the bound subsystem in the entrance channel.

In [20] one finds

$$\text{Im } T_0(Q) = -\mu_{1(23)}Q \frac{\pi}{\hbar^2} |T_0|^2 \quad (5.94)$$

on the energy shell which means $E' = E$. This can be compared with Eq. (5.93) which leads us to the relation

$$T_1^b(Q) = \frac{\pi m_n Q}{2 \hbar^2} T_0(Q) \quad (5.95)$$

for the dimensionless on-shell amplitude T_1^b . The elastic cross section can now be expressed in terms of T_1^b by inserting relation (5.95) into Eq. (5.88)

$$\begin{aligned} \sigma_{elastic} &= \frac{4\pi^3}{\hbar^4} \mu_{1(23)}^2 |T_0(Q)|^2 = \frac{4\pi^3}{\hbar^4} \mu_{1(23)}^2 \left(\frac{\pi}{2}\right)^2 \left(\frac{\hbar^2}{m_n Q}\right)^2 |T_1^b(Q)|^2 \\ &= 16\pi \left(\frac{\mu_{1(23)}}{m_n}\right)^2 \frac{1}{Q^2} |T_1^b(Q)|^2. \end{aligned} \quad (5.96)$$

Analogously the two rearrangement cross sections are determined by

$$\sigma_{rearr}^{(1)} = 16\pi \left(\frac{\mu_{1(23)}}{m_n}\right)^2 \frac{1}{Q^2} |T_2^b(Q)|^2. \quad (5.97)$$

and

$$\sigma_{rearr}^{(2)} = 16\pi \left(\frac{\mu_{1(23)}}{m_n}\right)^2 \frac{1}{Q^2} |T_3^b(Q)|^2. \quad (5.98)$$

Replacing $|T_0|^2$ in Eq. (5.94) by Eq. (5.88) and together with the rearrangement cross sections the optical theorem reads

$$\text{Im } T_{\vec{Q}\vec{Q}} = \frac{1}{4\pi} \text{Im } T_0(Q) = \frac{-\hbar^2}{16\pi^3} \frac{Q}{\mu_{1(23)}} (\sigma_{elastic} + \sigma_{rearr}^{(1)} + \sigma_{rearr}^{(2)}). \quad (5.99)$$

Alternatively starting from the optical theorem in [21]

$$\begin{aligned}
& \langle \phi_{\alpha m} | U_{\alpha\alpha}(E + i0) - U_{\alpha\alpha}(E - i0) | \phi_{\alpha m} \rangle \\
&= -\pi \left[\sum_{\gamma, n} \int dQ_\gamma \delta \left(E - \frac{Q_\gamma^2}{2M_\gamma} - E_{\gamma n}^{bind} \right) |\langle \phi_{\alpha m} | U_{\alpha\gamma}(E + i0) | \phi_{\gamma n} \rangle|^2 \right. \\
&+ \left. \int d^3Q_1 \int d^3k_1 \delta \left(E - \frac{\hbar^2 Q_1^2}{2\mu_{1(23)}} - \frac{\hbar^2 k_1^2}{2\mu_{23}} \right) |\langle \phi_{\alpha m} | U_{\alpha 0}(E + i0) | \vec{Q}_1 \vec{k}_1 \rangle|^2 \right] \quad (5.100) \\
&= -\frac{\hbar^2}{16\pi^3} \frac{Q_1}{\mu_{1(23)}} \left[\sum_{\gamma n} (\sigma_{\gamma n} + \sigma_{breakup}) \right]
\end{aligned}$$

where $U_{\alpha\alpha} = (\Omega^{(-)})^\dagger \Omega^{(+)}$ and $\langle \phi_{\alpha m} | U_{\alpha\alpha}(E + i0) | \phi_{\alpha m} \rangle$ the S -matrix element which represents the overlap of an incoming three-body wave function with quantum numbers αm with an outgoing three-body wave function with the same quantum numbers, i.e. it is the S -matrix element for forward scattering. Considering the relation between the on-shell S - and on-shell T -matrix (2.32), the difference $U_{\alpha\alpha}(E + i0) - U_{\alpha\alpha}(E - i0)$ yields the imaginary part of the T -matrix element, $\text{Im } T_{\vec{Q}\vec{Q}} = \frac{1}{4\pi} \text{Im } T_0$. With this and by using relation for the on-shell T -amplitude (5.95), we could verify the elastic part of the optical theorem by Glöckle (5.93) and the formula for the elastic cross section (5.96).

According to the structure of the Faddeev equations it is obvious that the breakup transition amplitude in Eq. (5.100) is composed of three components

$$\langle \phi_{\alpha m} | U_{\alpha 0}(E + i0) | \vec{Q}_1 \vec{k}_1 \rangle = T_{01} + T_{02} + T_{03}. \quad (5.101)$$

For these components there must be a relation similar to (5.95) between the on-shell amplitudes $T_i(k)$ used by Glöckle and $T_{0i}(k)$

$$T_i(k_i) = C \frac{\pi m_n k_i}{2 \hbar^2} T_{0i}(k_i) \quad (5.102)$$

with an unknown constant C that we were not able to determine definitely from Glöckle's formulæ. Thus we obtain the amplitude of the breakup term in Eq. (5.100)

$$\langle \phi_{\alpha m} | U_{\alpha 0}(E + i0) | \vec{Q}_1 \vec{k}_1 \rangle = C \frac{2 \hbar^2}{\pi m_n} \left[\frac{T_1(k_1)}{k_1} + \frac{T_2(k_2)}{k_2} + \frac{T_3(k_3)}{k_3} \right]. \quad (5.103)$$

Entering this expression into the breakup part of Eq. (5.100) and integrating over Q_1

yields

$$\begin{aligned}
& C^2 32\pi \frac{\hbar^2}{m_n} \frac{\mu_{1(23)}}{m_n} \int_{-1}^1 dx \int_0^{\sqrt{2\mu_{23}E/\hbar^2}} dk'_1 k_1'^2 Q'_{k'_1} \left| \frac{T_1(k'_1)}{k'_1} + \frac{T_2(k'_2)}{k'_2} + \frac{T_3(k'_3)}{k'_3} \right|^2 \\
& = \frac{\hbar^2}{16\pi^3} \frac{Q_1}{\mu_{1(23)}} \sigma_{breakup}.
\end{aligned} \tag{5.104}$$

where x is the cosine of the angle between k'_1 and k'_2 and the angle between k'_1 and k'_3 , respectively. Finally

$$\sigma_{breakup} = 16\pi\beta \left(\frac{\mu_{1(23)}}{m_n} \right)^2 \frac{1}{Q_1} \int_{-1}^1 dx \int_0^{\sqrt{2\mu_{23}E/\hbar^2}} dk'_1 k_1'^2 Q'_{k'_1} \left| \frac{T_1(k'_1)}{k'_1} + \frac{T_2(k'_2)}{k'_2} + \frac{T_3(k'_3)}{k'_3} \right|^2, \tag{5.105}$$

where we set the constant $\beta = 32\pi^3 C^2$. However, we suppose very strongly that β must be equal 1 (which is supported by numerical results (see Sec. 7)). From $\beta = 1$ follows $C = \sqrt{\pi^3/32}$.

Proceeding from (5.99) we can formulate an optical theorem with respect to the amplitude T_1^b

$$T_{\vec{Q}\vec{Q}} = \frac{1}{2\pi^2} \frac{\hbar^2}{m_n Q} T_1^b \tag{5.106}$$

that contains the total cross section which is the sum of the elastic, two rearrangement and the breakup cross sections above the breakup threshold

$$\frac{1}{2\pi^2} \frac{\hbar^2}{m_n Q_1} \text{Im} T_1^b = -\frac{\hbar^2}{16\pi^3} \frac{Q_1}{\mu_{1(23)}} \left[16\pi \left(\frac{\mu_{1(23)}}{m_n} \right)^2 \frac{1}{Q_1^2} (|T_1^b|^2 + |T_2^b|^2 + |T_3^b|^2) + \sigma_{breakup} \right] \tag{5.107}$$

and finally

$$\text{Im} T_1^b = -2 \frac{\mu_{1(23)}}{m_n} (|T_1^b|^2 + |T_2^b|^2 + |T_3^b|^2) - \frac{1}{8\pi} \frac{m_n}{\mu_{1(23)}} Q_1^2 \sigma_{breakup}. \tag{5.108}$$

With Eq. (5.96) one obtains

$$\text{Im} T_1^b = -\frac{1}{8\pi} \frac{m_n}{\mu_{1(23)}} Q_1^2 [\sigma_{elastic} + \sigma_{rearr}^{(1)} + \sigma_{rearr}^{(2)} + \sigma_{breakup}], \tag{5.109}$$

or in terms of the T -amplitudes

$$\begin{aligned} \text{Im } T_1^b &= -2 \frac{\mu_{1(23)}}{m_n} (|T_1^b|^2 + |T_2^b|^2 + |T_3^b|^2) \\ &\quad - 2 \frac{\mu_{1(23)}}{m_n} \beta Q_1 \int_{-1}^1 dx \int_0^{\sqrt{2\mu_{23}E/\hbar^2}} dk'_1 k_1'^2 Q'_{k'_1} \left| \frac{T_1(k'_1)}{k'_1} + \frac{T_2(k'_2(x))}{k'_2(x)} + \frac{T_3(k'_3(x))}{k'_3(x)} \right|^2. \end{aligned} \quad (5.110)$$

The energy dependence of the breakup part in the optical theorem differs from Glöckle's formula in [10]. Instead of $\frac{1}{Q_1}$ in [10] we got Q_1 .

The observables for the three-body problem can be summarized

$$\sigma_{elastic} = 16\pi \left(\frac{\mu_{1(23)}}{m_n} \right)^2 \frac{1}{Q_1^2} |T_1^b(Q_1)|^2, \quad (5.111a)$$

$$\sigma_{rearr}^{(1)} = 16\pi \left(\frac{\mu_{1(23)}}{m_n} \right)^2 \frac{1}{Q_1^2} |T_2^b(Q)|^2, \quad (5.111b)$$

$$\sigma_{rearr}^{(2)} = 16\pi \left(\frac{\mu_{1(23)}}{m_n} \right)^2 \frac{1}{Q_1^2} |T_3^b(Q)|^2, \quad (5.111c)$$

$$\sigma_{breakup} = \left(\frac{\mu_{1(23)}}{m_n} \right)^2 \frac{16\pi\beta}{Q_1} \int_{-1}^1 dx \int_0^{\sqrt{2\mu_{23}E/\hbar^2}} dk'_1 k_1'^2 Q'_{k'_1} \left| \frac{T_1(k'_1)}{k'_1} + \frac{T_2(k'_2)}{k'_2} + \frac{T_3(k'_3)}{k'_3} \right|^2. \quad (5.111d)$$

Optical theorem :

$$\begin{aligned} \text{Im } T_1^b &= -2 \frac{\mu_{1(23)}}{m_n} (|T_1^b(Q_1)|^2 + |T_2^b(Q_1)|^2 + |T_3^b(Q_1)|^2) \\ &\quad - 2 \frac{\mu_{1(23)}}{m_n} Q_1 \int_{-1}^1 dx \int_0^{\sqrt{2\mu_{23}E/\hbar^2}} dk'_1 k_1'^2 Q'_{k'_1} \left| \frac{T_1(k'_1)}{k'_1} + \frac{T_2(k'_2(x))}{k'_2(x)} + \frac{T_3(k'_3(x))}{k'_3(x)} \right|^2. \end{aligned} \quad (5.112)$$

6 Numerical implementation

This section focuses on a strategy of solving the system of equations (5.85) numerically. Entering the expressions for the $T_i(k)$ amplitude, Eqs. (5.85c) and (5.85d), into Eq. (5.85a) yields a uniquely solvable set of linear equations for the coefficients $c_\mu^{(i)}$. With the coefficients $c_\mu^{(i)}$ and the amplitudes T_i^b and $T_i(k)$ the wave functions and the cross sections can be determined via (5.111).

6.1 Setting up a system of linear equations for $c_\mu^{(i)}$

The system of linear equations (5.85a) reads

$$\begin{aligned}
 & (E_\mu^{(i)} - E) \sum_{\mu'} C_{\mu\mu'}^{(i)} c_{\mu'}^{(i)} + \sum_{\substack{j=1 \\ j \neq i}}^3 \sum_{\mu'} V_{\mu\mu'}^{(ij)} c_{\mu'}^{(j)} \\
 &= \frac{1}{2\mu_{i(jn)}} M_{\mu b} Q \cos(QA_i) - \frac{1}{2\mu_{i(jn)}} M_{\mu b} i Q \sin(QA_i) \\
 &+ \frac{1}{2\mu_{jn}} \left[M_{\mu Q} \frac{du_i^b(r)}{dr} \Big|_{r=a_i} - \tilde{M}_{\mu Q} u_i^b(a_i) \right] + \frac{\tilde{C}}{2\mu_{i(jn)}} (iQM_{\mu b} + \tilde{M}_{\mu b}) \sum_{\mu'} M_{\mu' b} c_{\mu'}^{(i)} \quad (6.1) \\
 &- \frac{2}{\pi} \int_0^{\sqrt{2\mu_{jn}E}} dk \left[(iQ_k M_{\mu k}^{(-)} - \tilde{M}_{\mu k}^{(-)}) e^{iQ_k A_i} + \frac{\mu_{i(jn)}}{\mu_{jn}} (ik M_{\mu Q_k} - \tilde{M}_{\mu Q_k}) e^{ik a_i} \right] T_i(k) \\
 &- H_i(A_i).
 \end{aligned}$$

with $H_i(A_i)$ defined in Eq. (5.86).

Regarding the $T_i(k)$ -amplitude we introduce the component notation for Eq. (5.85c)

$$\begin{aligned}
 & T_{3,\mu}^{(i)} \left(2\mu_{jn} \sqrt{E} \frac{r_i}{\rho_A} \right) \\
 & \simeq \left[(2\mu_{i(jn)})^{3/2} \sqrt{2\mu_{jn}} \sqrt{\frac{2}{\pi}} e^{i\frac{\pi}{4}} E^{1/4} \frac{e^{i\rho_A \sqrt{E}}}{\rho_A^{1/2}} \frac{A_i}{\rho_A} \right]^{-1} [\varphi_\mu^{(i)}(r_i, A_i) - u_i^b(r_i) M_{\mu b}]. \quad (6.2)
 \end{aligned}$$

and for Eq. (5.85d),

$$\begin{aligned}
& T_{4,\mu}^{(i)} \left(2\mu_{jn} \sqrt{E} \frac{a_i}{\rho_a} \right) \\
& \simeq \left[(2\mu_{i(jn)})^{3/2} \sqrt{\frac{2}{\pi}} e^{i\frac{\pi}{4}} E^{1/4} \frac{e^{i\rho_a \sqrt{E}} R_i}{\rho_a^{1/2} \rho_a} \right]^{-1} \left[\varphi_{\mu}^{(i)}(a_i, R_i) - u_i^b(a_i) e^{iQ(R_i - A_i)} M_{\mu b} \right] \\
& T_{4,inh}^{(i)} \left(2\mu_{jn} \sqrt{E} \frac{a_i}{\rho_a} \right) \\
& \simeq -u_i^b(a_i) [\sin(QR_i) - e^{iQ(R_i - A_i)} \sin(QA_i)] \left[(2\mu_{i(jn)})^{3/2} \sqrt{\frac{2}{\pi}} e^{i\frac{\pi}{4}} E^{1/4} \frac{e^{i\rho_a \sqrt{E}} R_i}{\rho_a^{1/2} \rho_a} \right]^{-1}
\end{aligned} \tag{6.3}$$

Eq. (5.85d) is split into a part depending on μ , $T_{4,\mu}^{(i)}$, and one independent of μ , $T_{4,inh}^{(i)}$. Latter is a result of the finite value of $u_i^b(r)$ at the matching radius a_i .

In both Eqs. (6.2) and (6.3) the argument of $T_{3,\mu}^{(i)}$ and $T_{4,\mu}^{(i)}$ is the wavenumber k which is parametrized in two different ways by the spatial coordinates r_i and R_i . A graphical representation of the relationships is given in Fig. 7. In this plot the functions are normalized to $a_i = A_i = 1$ and also $\mu_{jn} = \mu_{i(jn)} = 1$. In order to cover the full

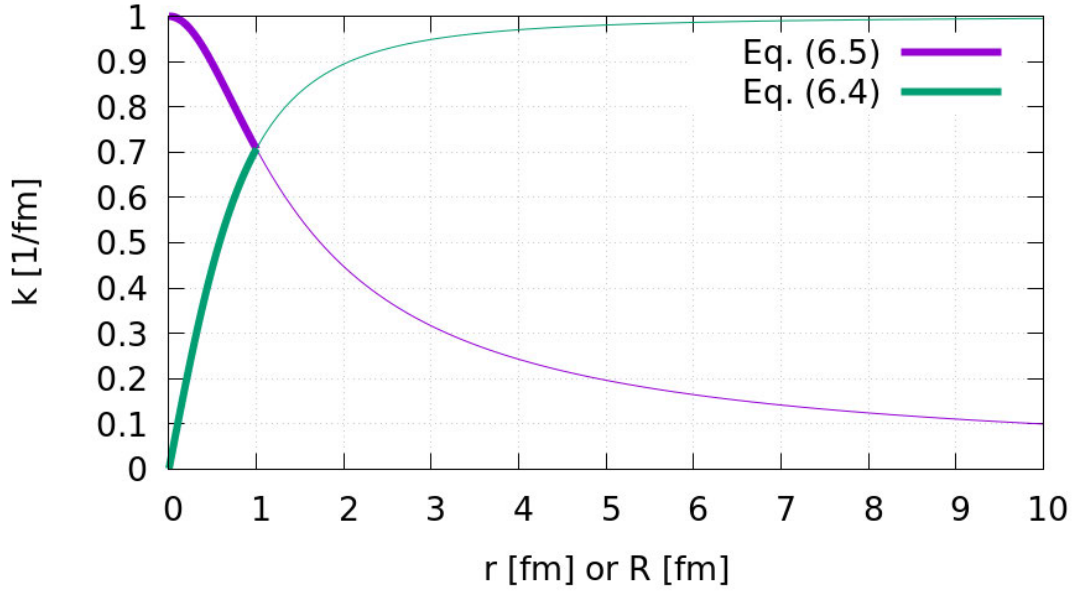


Figure 7: Functional dependence of k on r and R in Eqs. (6.2) and (6.3).

k range the parametrization at the intersection point which is located at $r = a_i$ and

$R = A_i$ must be changed from Eq. (6.2) to (6.3). Hence the components $T_\mu^{(i)}(k)$ of $T_i(k)$ are given by

$$T_\mu^{(i)}(k) = \begin{cases} T_{3,\mu}^{(i)} & \text{for } 0 \leq k < 2\mu_{jn}\sqrt{E} \frac{a_i}{\sqrt{2\mu_{jn}a_i^2 + 2\mu_{i(jn)}A_i^2}} \\ T_{4,\mu}^{(i)} + T_{4,inh}^{(i)} & \text{for } 2\mu_{jn}\sqrt{E} \frac{a_i}{\sqrt{2\mu_{jn}a_i^2 + 2\mu_{i(jn)}A_i^2}} \leq k \leq k_{max} \end{cases} \quad (6.4)$$

with $k_{max} = \sqrt{\mu_{jn}E}$. $T_i(k)$ is obtained from $T_\mu^{(i)}(k)$ by

$$T_i(k) = \sum_{\mu} T_\mu^{(i)}(k). \quad (6.6)$$

Plugging $T_\mu^{(i)}(k)$ according to conditions (6.4) and (6.5) into Eq. (6.1) yields a system of linear equations for the expansion coefficients $c_\mu^{(i)}$,

$$\begin{aligned} & (E_\mu^{(i)} - E) \sum_{\mu'} C_{\mu\mu'}^{(i)} c_{\mu'}^{(i)} + \sum_{\substack{j=1 \\ j \neq i}}^3 \sum_{\mu'} V_{\mu\mu'}^{(ij)} c_{\mu'}^{(j)} \\ &= \frac{1}{2\mu_{i(jn)}} M_{\mu b} Q \cos(QA_i) - \frac{1}{2\mu_{i(jn)}} M_{\mu b} iQ \sin(QA_i) \\ &+ \frac{1}{2\mu_{jn}} \left[M_{\mu Q} \frac{du_i^b(r)}{dr} \Big|_{r=a_i} - \tilde{M}_{\mu Q} u_i^b(a_i) \right] + \frac{\tilde{C}}{2\mu_{i(jn)}} (iQ M_{\mu b} + \tilde{M}_{\mu b}) \sum_{\mu'} M_{\mu' b} c_{\mu'}^{(i)} \\ &- \frac{2}{\pi} \int_0^{\sqrt{2\mu_{jn}E}} dk \left[(iQ_k M_{\mu k}^{(-)} - \tilde{M}_{\mu k}^{(-)}) e^{iQ_k A_i} + \frac{\mu_{i(jn)}}{\mu_{jn}} (ik M_{\mu Q_k} - \tilde{M}_{\mu Q_k}) e^{ika_i} \right] \sum_{\mu'} c_{\mu'}^{(i)} T_{\mu'}^{(i)}(k) \\ &- \sum_{\mu'} c_{\mu'}^{(i)} \tilde{H}_{\mu\mu'}^{(i)}(A_i). \end{aligned} \quad (6.7)$$

with

$$\begin{aligned}
\tilde{H}_{\mu\mu'}^{(i)}(A_i) = & \sum_{\substack{j=1 \\ j \neq i}}^3 \frac{e^{i\sqrt{2\mu_{j(in)}E} \frac{m_i}{m_i+m_n} A_i / \sin \varphi_j^*}}{A_i^{3/2}} \left(i - \frac{(m_i + m_n) \sin \varphi_j^*}{m_i \sqrt{2\mu_{j(in)}E}} \frac{d\varphi_{\mu 2}^{(i)}(R)}{dR} \Big|_{R=A_i} \frac{1}{\varphi_{\mu 2}^{(i)}(A_i)} \right) \\
& \times T_{\mu'}^i \left(\sqrt{2\mu_{jn}E} \cos \varphi_j^* \right) \left(N_b(E) M_{\mu b} \frac{2\mu_{i(jn)}}{\mu_{j(in)} \left(E - \frac{2Q^2}{\mu_{j(in)}} \sin^2 \varphi_j^* \right)} \int_0^{r_{0i}} dr u_i^b(r) V_i(r) \right. \\
& \left. + \frac{2}{\pi} N_k(E) \int_{\sqrt{2\mu_{jn}E}}^{\infty} dk M_{\mu k}^{(-)} \frac{1}{\frac{1}{\mu_{jn}} k^2 - 2E + 2\frac{\mu_{j(in)}}{\mu_{i(jn)}} E \left(\frac{m_i}{(m_i+m_n) \sin \varphi_j^*} \right)^2} \int_0^{r_{0i}} dr u_k^{(-)*}(r) V_i(r) \right).
\end{aligned} \tag{6.8}$$

The potential elements are [Eq. (5.61)]

$$V_{\mu\mu'}^{(ij)} = \iint_D dr_i dR_i \varphi_{\mu}^{(i)}(r_i, R_i) V_i(r_i) \int_{-1}^1 dx_i r_i R_i \frac{\varphi_{\mu'}^{(j)}(r_j, R_j)}{2r_j R_j}.$$

The system of linear equations (6.7) can be written in matrix notation

$$\underline{\underline{A}} \times \underline{c} = \underline{b} \tag{6.9}$$

with

$$\underline{\underline{A}} = \begin{pmatrix} N'_1 & N'_2 & N'_3 \\ \boxed{D_1} & \boxed{V_{12}} & \boxed{V_{13}} \\ \boxed{V_{21}} & \boxed{D_2} & \boxed{V_{23}} \\ \boxed{V_{31}} & \boxed{V_{32}} & \boxed{D_3} \end{pmatrix} \begin{matrix} N_1 \\ N_2 \\ N_3 \end{matrix} \quad \text{and} \quad \underline{c} = \begin{pmatrix} \boxed{c_{\mu}^{(1)}} \\ \boxed{c_{\mu}^{(2)}} \\ \boxed{c_{\mu}^{(3)}} \end{pmatrix} \begin{matrix} N'_1 \\ N'_2 \\ N'_3 \end{matrix} \quad \text{and} \quad \underline{b} = \begin{pmatrix} \boxed{b_{\mu}^{(1)}} \\ \boxed{b_{\mu}^{(2)}} \\ \boxed{b_{\mu}^{(3)}} \end{pmatrix} \begin{matrix} N_1 \\ N_2 \\ N_3 \end{matrix}$$

where N_i denotes the number of basis states for the i -th Faddeev component.

The matrix $\underline{\underline{A}}$ is the coefficient matrix for the vector of solutions $c_{\mu}^{(i)}$ and is of dimension $(N_1 + N_2 + N_3) \times (N'_1 + N'_2 + N'_3)$. The vector \underline{c} contains the coefficients $c_{\mu}^{(i)}$ for each subsystem which are the solutions of the system.

The elements used in matrix $\underline{\underline{A}}$ are $V_{ij} = V_{\mu\mu'}^{(ij)}$ from Eq.(5.61) and

$$\begin{aligned}
D_i \equiv D_{\mu\mu'}^{(i)} &= (E_{\mu}^{(i)} - E)C_{\mu\mu'}^{(i)} - \frac{\tilde{C}}{2\mu_{i(jn)}}(iQ M_{\mu b} + \tilde{M}_{\mu b})M_{\mu' b} \\
&+ \frac{2}{\pi} \int_0^{\sqrt{2\mu_{jn}E}} dk \left[(iQ_k M_{\mu k}^{(-)} - \tilde{M}_{\mu k}^{(-)})e^{iQ_k A_i} + \frac{\mu_{i(jn)}}{\mu_{jn}}(ik M_{\mu Q_k} - \tilde{M}_{\mu Q_k})e^{ika_i} \right] T_{\mu'}^{(i)}(k) \\
&- H_{\mu\mu'}^{(i)}(A_i).
\end{aligned} \tag{6.10}$$

Finally the vector of inhomogeneities \underline{b} is made up of the components

$$\begin{aligned}
b_{\mu}^{(i)} &= \frac{1}{2\mu_{i(jn)}} M_{\mu b} Q \cos(Q A_i) - \frac{1}{2\mu_{i(jn)}} M_{\mu b} iQ \sin(Q A_i) \\
&+ \frac{1}{2\mu_{jn}} \left[M_{\mu Q} \frac{du_i^b(r)}{dr} \Big|_{r=a_i} - \tilde{M}_{\mu Q} u_i^b(a_i) \right] \\
&- u_i^b(a_i) [\sin(Q R_i) - e^{iQ(R_i - A_i)} \sin(Q A_i)] \left[(2\mu_{i(jn)})^{3/2} \sqrt{\frac{2}{\pi}} e^{i\frac{\pi}{4}} E^{1/4} \frac{e^{i\rho_a \sqrt{E}}}{\rho_a^{1/2}} \frac{R_i}{\rho_a} \right]^{-1},
\end{aligned} \tag{6.11}$$

where the last term comes from $T_{4,inh}^{(i)}$ in Eq. (6.3).

For the numerical solution of the system of linear equations the LAPACK routine ZGESV is used. It computes the solution to a system of complex linear equations $\underline{\underline{A}} \times \underline{x} = \underline{b}$, where $\underline{\underline{A}}$ is an $n \times n$ matrix and \underline{x} and \underline{b} are n -dimensional vectors. For integration the QUADPACK routine "qags" was used which is a quadrature routine that applies the Gauss-Kronrod 21-point integration rule adaptively until an estimate of the integral over (a, b) is achieved within the desired absolute and relative error limits.

6.2 Stability of the algorithm

Before applying the theory to realistic nuclear systems it is important to probe the stability of the numerically implemented algorithm. This was done by considering a hypothetical system of three identical spinless bosons with equal masses and a potential of Woods-Saxon type,

$$V(r) = \frac{v_0}{1 + \exp[(r - a)/b]}, \quad (6.12)$$

with $v_0 = -50$ MeV, $a = 1.25$ fm and $b = 0.1$ fm.

A first calculation led to an extremely spiky unphysical breakup cross section which was a hint that the system of linear equations was ill-conditioned. Checking the eigenvalues of the coefficient matrix $\underline{\underline{A}}$ revealed some leading values and the remaining ones being very small. Table 1 lists the first 12 eigenvalues.

i	λ_i
1	$-8048.04 - 5395.58 i$
2	$262.08 + 213.62 i$
3	$8.42 - 16.52 i$
4	$1.07 + 1.11 i$
5	$-0.58 - 3.73 \cdot 10^{-2} i$
6	$0.15 + 7.02 \cdot 10^{-4} i$
7	$-6.82 \cdot 10^{-3} - 2.42 \cdot 10^{-3} i$
8	$-2.69 \cdot 10^{-3} + 1.20 \cdot 10^{-3} i$
9	$-2.25 \cdot 10^{-4} - 3.64 \cdot 10^{-5} i$
10	$1.23 \cdot 10^{-4} - 1.34 \cdot 10^{-6} i$
11	$-1.05 \cdot 10^{-5} - 4.46 \cdot 10^{-6} i$
12	$7.85 \cdot 10^{-6} - 5.65 \cdot 10^{-9} i$

Table 1: The first twelve eigenvalues of the matrix $\underline{\underline{A}}$.

The small eigenvalues cause highly fluctuating solutions (e.g. solution c_8 in Fig. 8) and consequently lead to unphysical fluctuations in the cross section. A possibility to cure that ill-conditioned system is to apply a regularization procedure

$$\underline{\underline{A'}} = \underline{\underline{A}} + \eta \underline{\underline{I}} \quad (6.13)$$

where $\underline{\underline{I}}$ is the identity matrix.

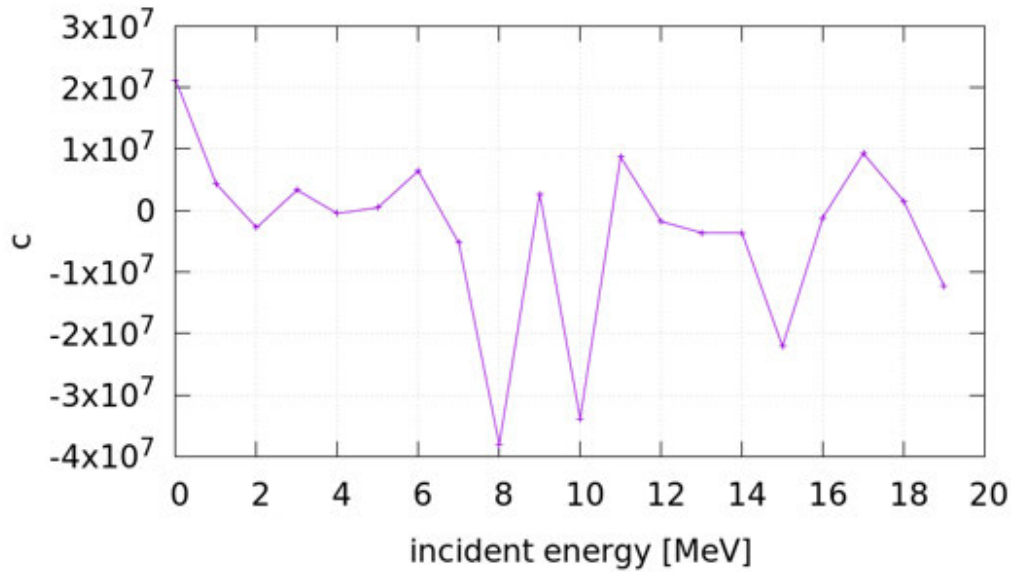


Figure 8: Solution c_8 as a function of the incident energy without regularization.

The solutions for the coefficients $c_\mu^{(i)}$ associated with the new matrix \underline{A}' as a function of the incident energy exhibit a much smoother behavior (solution c_8 in Fig. 9) than before. Consequently also the fluctuations are removed in the cross sections (Fig. 10).

In a highly dynamical eigenvalue spectrum like in Tab. 1 the eigenvectors associated with very small eigenvalues tend to point out exactly every inaccuracy (e.g. rounding errors, algorithm errors,...) resulting in unphysical fluctuations. The regularization suppresses these contributions of the eigenvectors associated with small eigenvalues and confines the system to the essential components. The number of contributing eigenvectors can be controlled by the regularization parameter η . Latter must be chosen such that the components with small eigenvalues are suppressed while the those governing the physical behavior must be retained. The figures should illustrate the influence and impact of regularization in the presented method. Albeit the considered schematic example is not directly related to any real nuclear system the impact and observed properties of the system and its regularization will remain similar also for real systems.

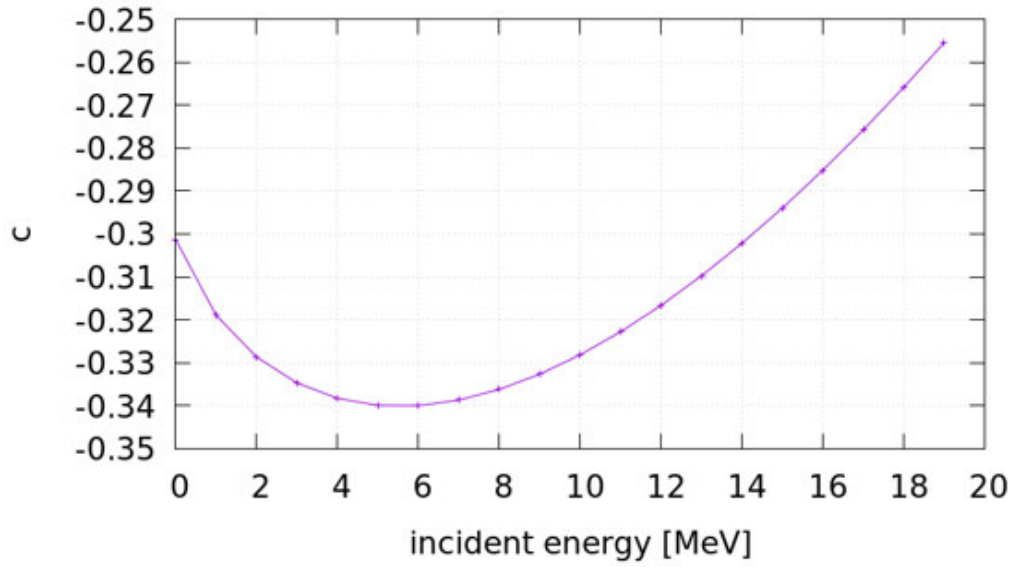


Figure 9: Solution c_8 as a function of the incident energy with regularization $\eta = 0.1$.

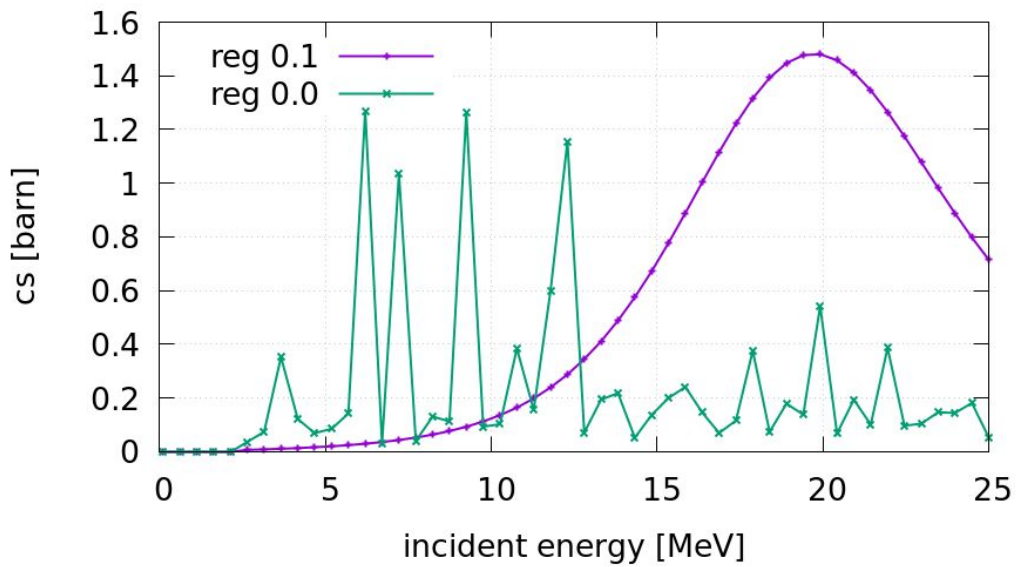


Figure 10: Breakup cross section with regularization $\eta = 0.1$.

7 Results

7.1 The neutron+deuteron system

The deuteron (from greek $\delta\epsilon\upsilon\tau\epsilon\rho\omicron\nu$ 'the second one') is the simplest existing nuclear bound system. The bound state is a coupled 3S_1 - 3D_1 state with a binding energy of 2.225 MeV. Measurements show that the quadrupole moment of the deuteron is not vanishing and hence there must be a certain admixture of a 3D_1 -state in the total bound state. Depending on the nucleon-nucleon potential used, it is about 3-6%. Consequently, the force acting between the neutron and the proton is not only a central one, but has a tensor component. The latter will not be considered in the following because the developed R -matrix formalism is limited to s-waves.

The available experimental data for the breakup and the elastic cross section are taken from the EXFOR library [1] and are displayed in Figs. 11 and 12.

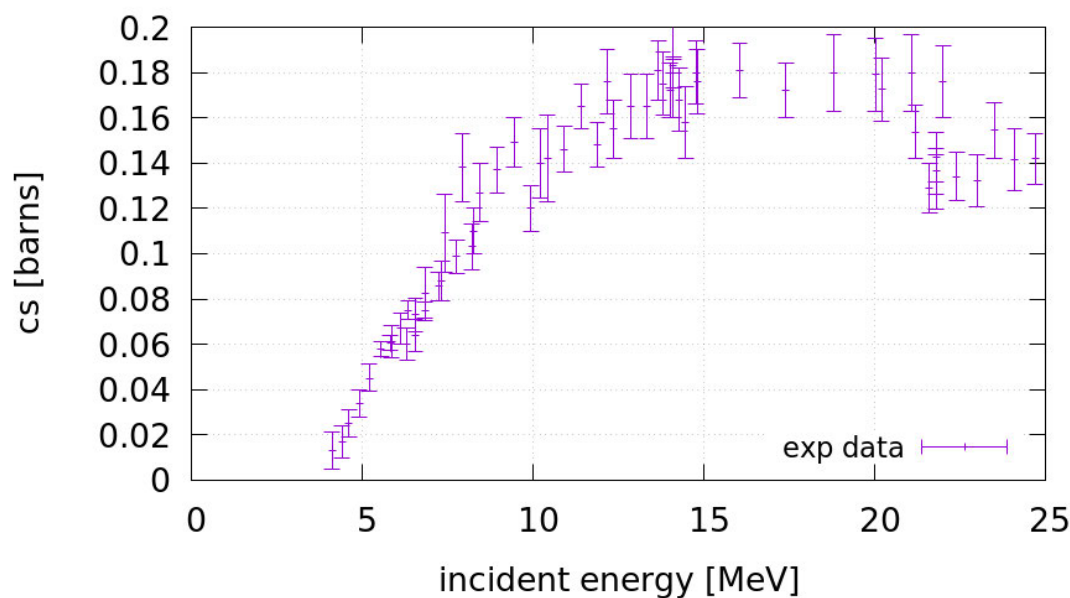


Figure 11: Experimental data for the breakup cross section. The references of the experimental data are given in Appendix B.1

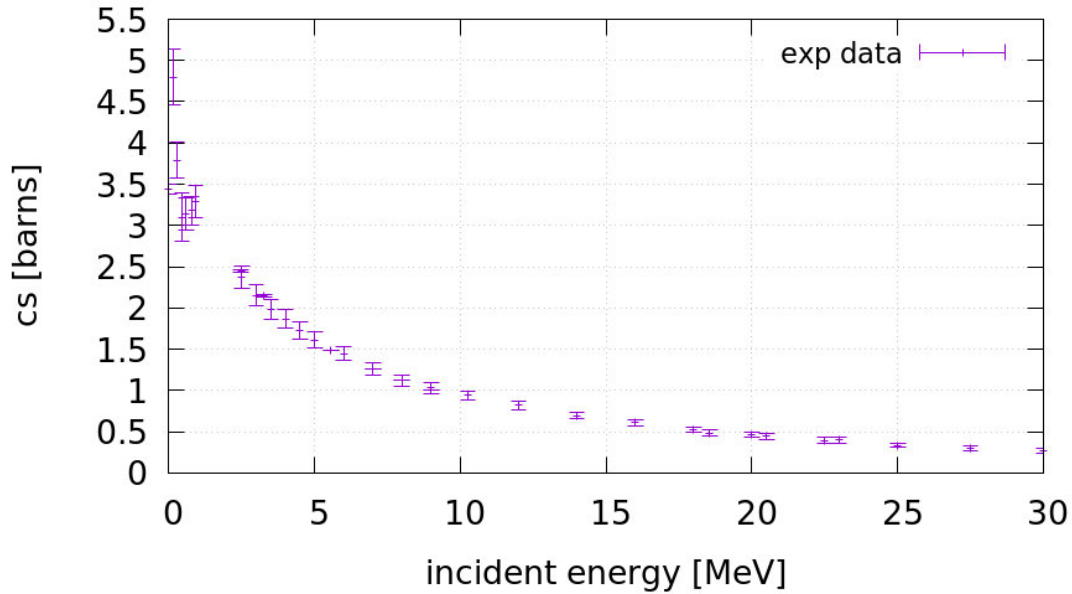


Figure 12: Experimental data for the angle-integrated elastic cross section. The references of the experimental data are given in Appendix B.2.

The interaction between the neutron and proton in the deuteron is ideally modeled by a Reid soft core potential of the form

$$V(r) = -10.463 \frac{e^{-\mu_1 r}}{\mu_1 r} - v_{01} \cdot 1650.6 \frac{e^{-4\mu_1 r}}{\mu_1 r} + v_{02} \cdot 6484.2 \frac{e^{-7\mu_1 r}}{\mu_1 r} \quad (7.1)$$

with $\mu_1 = \left(\frac{\hbar c}{m_\pi c^2}\right)^{-1}$ where m_π is the mass of the force carrier, the pion mass. v_{01} and v_{02} are determined such that the derived neutron-proton (3S_1 state) phase shift coincides with the Nijmegen multi-energy analysis data [22] and that the bound state at $E_b = -2.225\text{MeV}$ is reproduced. This is fulfilled by setting

$$v_{01} = 1.000, \quad v_{02} = 0.830. \quad (7.2)$$

The potential for the neutron-neutron interaction is determined analogously. The Reid soft core form is fitted to the neutron-neutron (1S_0 state) phase shift data from Nijmegen multi-energy analysis [22] with the constraint that there must not exist any bound state. The obtained parameters are

$$v_{01} = 0.733, \quad v_{02} = 0.657. \quad (7.3)$$

Both the neutron-proton and the neutron-neutron potential are displayed in Fig. 13 and the derived phase shifts in Fig. 14. The bound state wave function that results from this potential is shown in Fig. 15 with a binding energy $E_b = -2.2249\text{MeV}$.

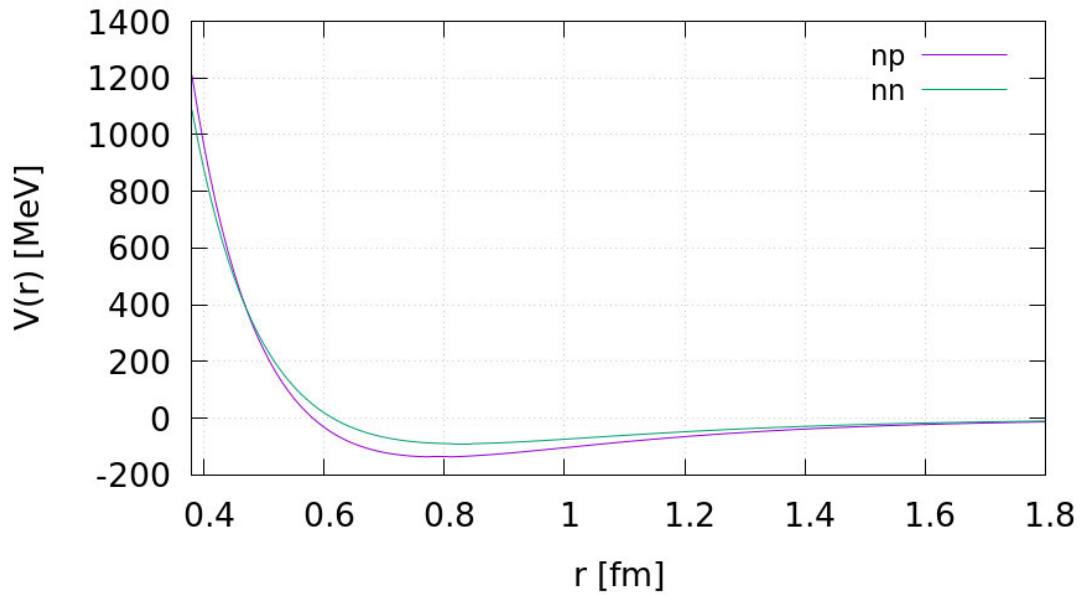


Figure 13: Neutron-proton and neutron-neutron potentials.

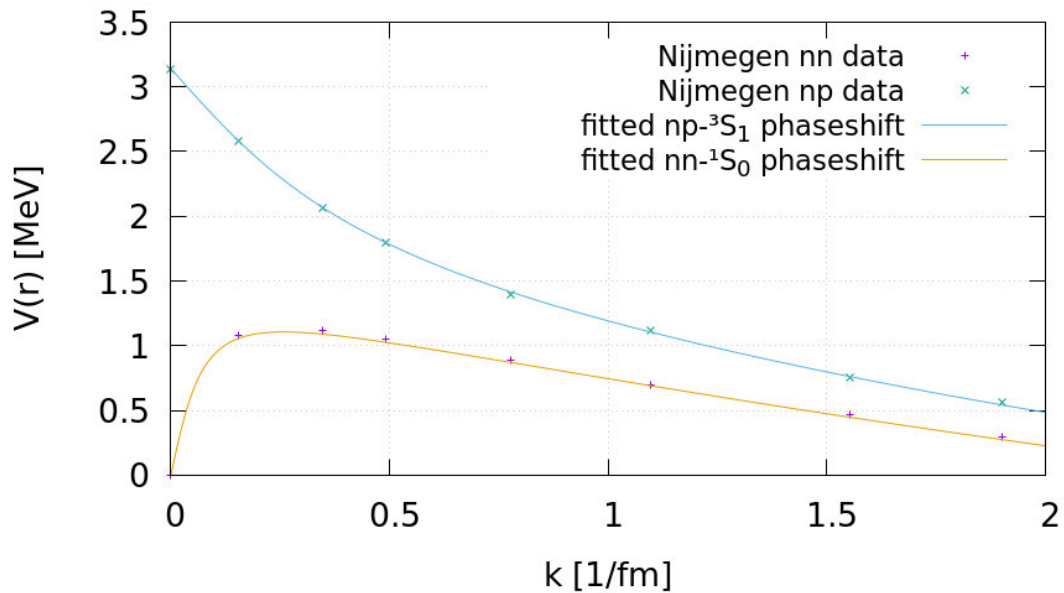


Figure 14: Fitted phase shift curves compared to Nijmegen multi-energy analysis data [22].

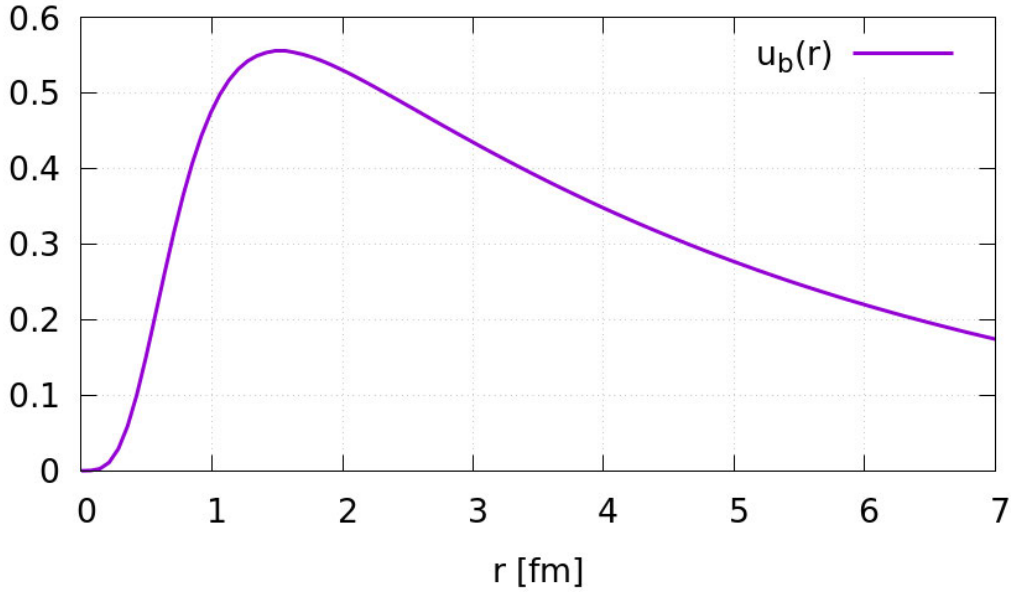


Figure 15: Bound state wave function $u_i^b(r)$ of the deuteron.

The bound state wave function is normalized by $\int_0^\infty dr |u_i^b(r)|^2 = 1$.

7.2 Application of the novel formalism on the neutron+deuteron system

The novel three-body R -matrix theory was first applied to the neutron+deuteron system where the breakup (Fig. 11) and the angle-integrated elastic cross section (Fig. 12) were calculated. The breakup of the deuteron represents the most simple and genuine nuclear three-body system without any further nuclear structure to be considered. Hence it is obvious to use this system as a first check of the new formalism. The only approximation is the use of an effective central potential instead of the realistic interaction with a tensor component since we restrict ourselves to s-waves.

7.2.1 Pauli principle and consequences

In the neutron+deuteron system there are two indistinguishable neutrons. Therefore, the wave function

$$u_1 = (\psi_a |s_a\rangle)_1 \otimes (\psi_b |s_b\rangle)_2 \otimes (\psi_c |s_c\rangle)_3 \quad (7.4)$$

must be antisymmetric with respect to an interchange of the two neutrons. If we assume that the two neutrons are in a spin-0 state, the application of the antisymmetrization

operator yields

$$\begin{aligned} \frac{\sqrt{2}}{2!}[1 - P_{12}]u_1 &= [(\psi_a |s_a\rangle)_1 \otimes (\psi_b |s_b\rangle)_2 - (\psi_b |s_b\rangle)_1 \otimes (\psi_a |s_a\rangle)_2] \otimes (\psi_c |s_c\rangle)_3 \\ &= \frac{1}{\sqrt{2}}(\psi_a \psi_b \psi_c) [|s_a\rangle_1 |s_b\rangle_2 - |s_b\rangle_1 |s_a\rangle_2] |s_c\rangle_3. \end{aligned} \quad (7.5)$$

Since the permutation affects only the spin part, the spatial functions of the two Faddeev components where the position of the neutrons are changed are identical. As a consequence the number of Faddeev components in Eq. (5.8) is reduced from three to two because now subsystem 1 and 2 where one neutron is bound to the proton and the other one free, respectively, are identical. Hence also the system of linear equations (6.9) is reduced in its dimension,

$$\underline{\underline{A}} = \begin{pmatrix} \mu_1 & \mu_3 \\ \boxed{D_1} & \boxed{V_{13}} \\ \boxed{V_{31}} & \boxed{D_3} \end{pmatrix} \begin{matrix} \mu'_1 \\ \mu'_3 \end{matrix} \quad \text{and} \quad \underline{c} = \begin{pmatrix} \boxed{c_\mu^{(1)}} \\ \boxed{c_\mu^{(3)}} \end{pmatrix} \begin{matrix} \mu_1 \\ \mu_3 \end{matrix} \quad \text{and} \quad \underline{b} = \begin{pmatrix} \boxed{b_\mu^{(1)}} \\ \boxed{b_\mu^{(3)}} \end{pmatrix} \begin{matrix} \mu_1 \\ \mu_3 \end{matrix}$$

As a consequence of the non-distinguishableness of the two neutrons and the fact that a bound state between two neutrons does not exist, the neutron+deuteron system does not exhibit any rearrangement channels.

7.2.2 Basis states

Beside the potentials and the resulting phase shifts and the bound state wave function, presented in the previous subsection, an appropriate set of basis functions is required within the R -matrix formalism. As already mentioned in subsection 5.2 the basis functions depend on the two Jacobi-coordinates r_i , R_i and are assumed to be factorized in the variables r_i and R_i (see subsection 5.2.1). The basis functions $\varphi_\mu^{(i)}(r, R)$ according to Eq. (5.54) are product states

$$\varphi_\mu^{(i)}(r, R) = X_{\mu_1}(r)Y_{\mu_2}(R).$$

These functions $X_{\mu_1}(r)$ and $Y_{\mu_2}(R)$ for both the neutron-proton (np) and the neutron-neutron (nn) subsystem are eigenfunctions of the Schrödinger equations for the respective subsystems [Eqs.(5.55) and (5.56)] and their energy-eigenvalues ϵ_{μ_1} and ϵ_{μ_2} .

For the np -subsystem the number of $X(r)$ -states was chosen to be 12 scattering states with equidistant energy steps between 0.1 and 5.5083 MeV for the eigenenergies

ϵ_{μ_1} plus the neutron-proton bound state, so in total 13 states (Table 2). For the function $Y(R)$, which describes the free motion of the third particle, three states were chosen with three equidistant eigenenergies ϵ_{μ_2} 0.1 MeV, 1.909 MeV and 3.718 MeV (Table 2). The functions $X(r)$ and $Y(R)$ for the np -system are shown in Fig. 16. The total eigenenergies $E_{\mu}^{(1)} = \epsilon_{\mu_1}^{(1)} + \epsilon_{\mu_2}^{(1)}$ of the basis states $\varphi_{\mu}^{(1)}(r, R)$ of the np -subsystem are summarized in Table 3.

μ_1/μ_2	$\epsilon_{\mu_1}^{(1)}$ [MeV]	$\epsilon_{\mu_2}^{(1)}$ [MeV]
1	-2.225	0.100
2	0.100	1.909
3	0.592	3.718
\vdots	\vdots	
13	5.5083	

Table 2: Eigenenergies $\epsilon_{\mu_1}^{(1)}$ and $\epsilon_{\mu_2}^{(1)}$ for the np -subsystem.

μ	$E_{\mu}^{(1)}$ [MeV]
1	-2.125
2	-0.316
3	1.493
4	0.200
5	2.009
6	3.818
7	0.692
\vdots	\vdots
30	9.2263

Table 3: Eigenenergies $E_{\mu}^{(1)}$ of the basis states for the np -subsystem.

For the nn -subsystem the number of basis functions $X(r)$ is also 12 and the energy eigenvalues $\epsilon_{\mu_1}^{(3)}$ are equidistantly distributed between 0.1 and 5.5083 MeV (Table 4). The $Y(R)$ -states are the same as for the np -subsystem (Table 4). $X(r)$ and $Y(R)$ for the nn -system are shown in Fig. 17. Again the basis functions $\varphi_{\mu}^{(3)}(r, R)$ are product states with the energy-eigenvalues $E_{\mu}^{(3)} = \epsilon_{\mu_1}^{(3)} + \epsilon_{\mu_2}^{(3)}$ given in natural order in Table 5.

μ_1/μ_2	$\epsilon_{\mu_1}^{(3)}$ [MeV]	$\epsilon_{\mu_2}^{(3)}$ [MeV]
1	0.100	0.100
2	0.592	1.909
3	1.083	3.718
\vdots	\vdots	
12	5.5083	

Table 4: Eigenenergies $\epsilon_{\mu_1}^{(3)}$ and $\epsilon_{\mu_2}^{(3)}$ for the nn -subsystem.

μ	$E_{\mu}^{(3)}$ [MeV]
1	0.200
2	2.009
3	3.818
4	0.692
5	2.501
6	4.310
7	1.183
\vdots	\vdots
30	9.2263

Table 5: Eigenenergies $E_{\mu}^{(3)}$ of the basis states for the nn -subsystem.

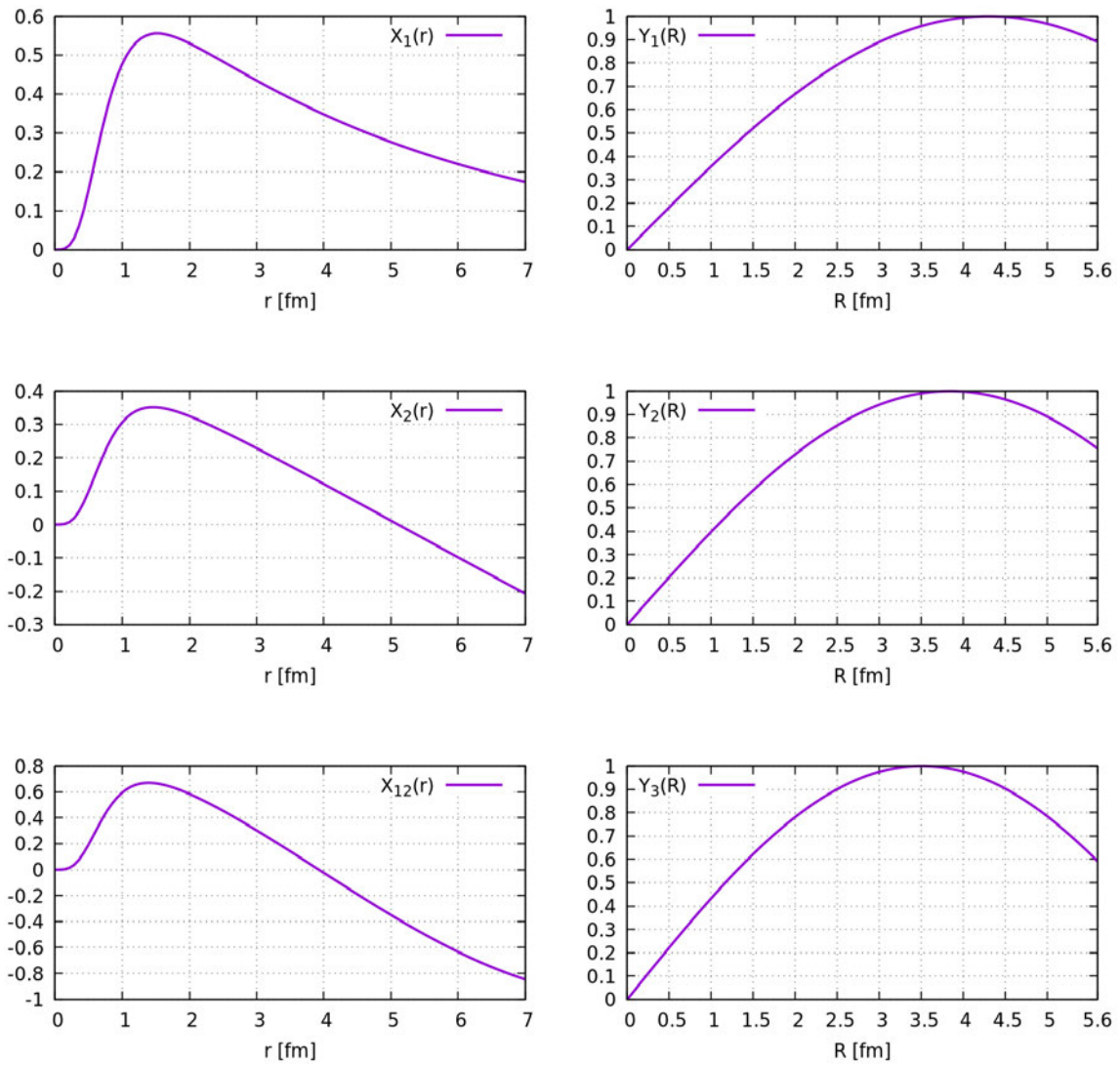


Figure 16: Basis functions for the np subsystem.

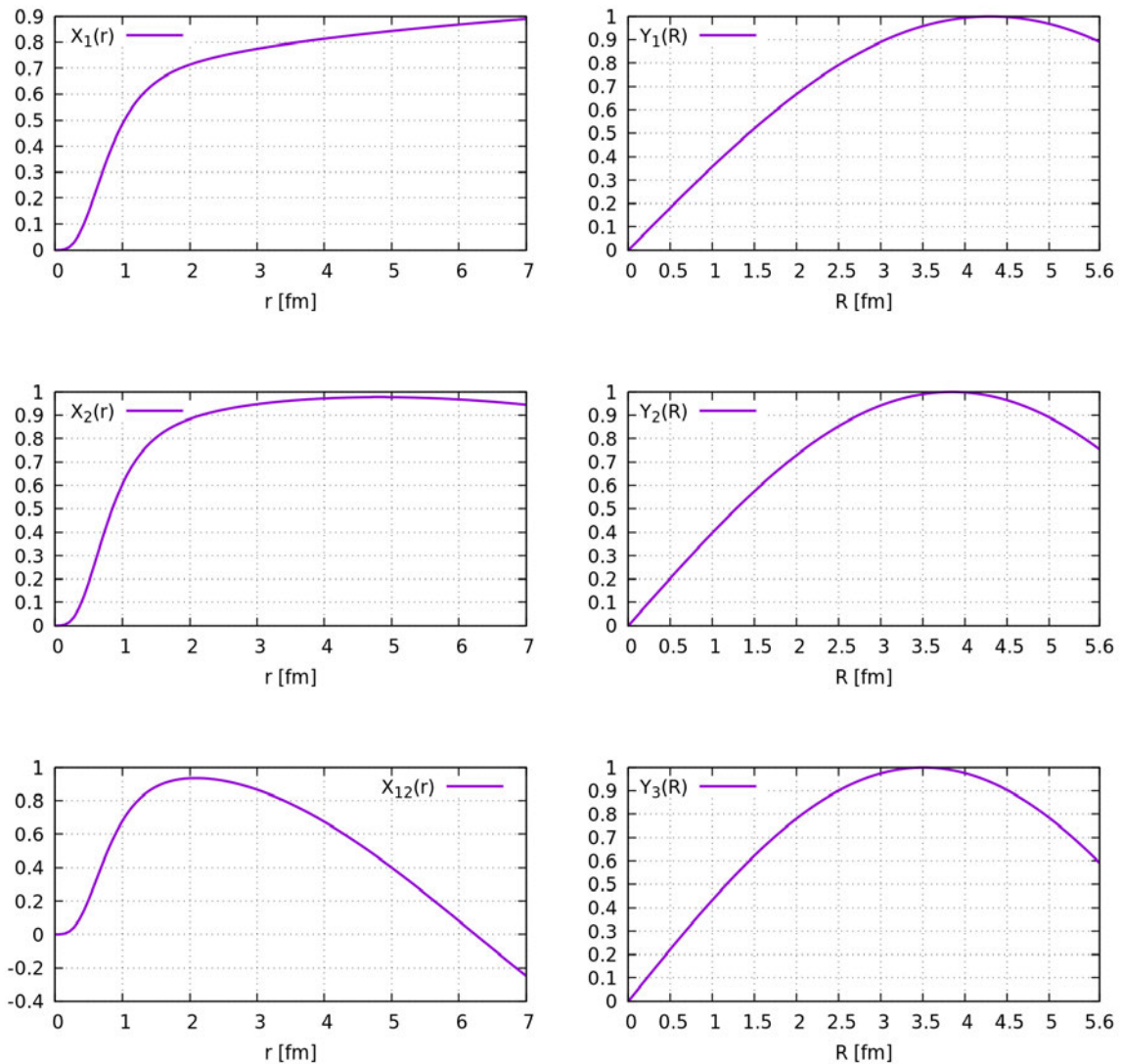


Figure 17: Basis functions for the nn subsystem.

7.3 Results for the neutron+deuteron system

The numerical implementation and application on the neutron+deuteron system was carried out successfully. To our knowledge it was actually the first application of a three-body R -matrix formalism to a real system. The results are very promising and will be presented in this subsection. The observables calculated were the total elastic and the breakup cross section according to (5.111). The results were compared with the experimental data from the EXFOR library [1].

The the minimum values for the matching radii are calculated according to Eq.

(5.48) and yield for the potential (7.1) with a range $r_0 \sim 2$ fm,

$$a_i = 4 \text{ fm and } A_i = 3 \text{ fm} . \quad (7.6)$$

The number of basis functions in both subsystems was set to be 30 with the properties described above.

The breakup and elastic cross sections obtained are displayed in Figs. 18 and 19 for different values of the regularization parameter η . The regularization parameter η was introduced in order to remove unphysical fluctuations. The first calculation was carried through with matching radii

$$a_i = 7 \text{ fm and } A_i = 5.6 \text{ fm} . \quad (7.7)$$

Both cross sections show a distinct convergence with respect to η . In Figs. 20 and 21 the breakup cross section is plotted as a function of the regularization parameter η for the two incident energy points 8.01 MeV and 11.15 MeV . For both incident energies a plateau is reached starting at $\eta = 22$. For this value of η the experimental data are very well reproduced (Fig. 22). However, while the breakup cross section at an incident energy of 8 MeV is stable for values of $\eta \geq 22$, the cross section drops significantly at an incident energy of 11.7 MeV for η greater than 35. In the energy range below 8-9 MeV we observed that the calculated cross section data remain stable for $\eta \geq 22$ while in the energy region above 9 MeV there is a certain range for η between 22 and about 35 where convergence is obtained. The result for $\eta = 40$ is displayed in Fig. 23. The reason for this behavior of the cross section might be the fact that in the higher energy region more basis states are needed to reproduce the three-body wave function properly . The parameter η removes fluctuations, i.e. it cuts off the basis states with very small eigenvalues which cause these fluctuations. If the number of basis functions contributing to the result is reduced too drastically by the regularization, one observes the drop in the cross section which occurs for higher energies at lower values of η .

Simultaneously convergence is reached for the elastic cross section beginning with $\eta = 22$ (Fig.19). However, there is a significant drop for energies greater than 8 MeV in the converged curve (Fig. 24).

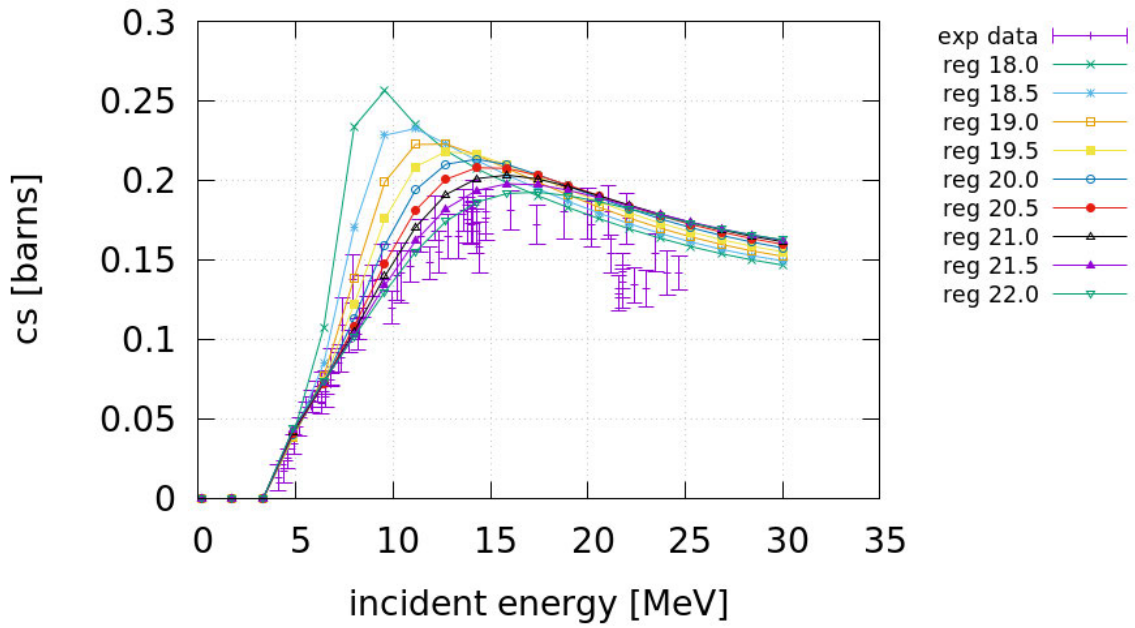


Figure 18: Breakup cross section for $a_i = 7$ fm and $A_i = 5.6$ fm for different values of η .

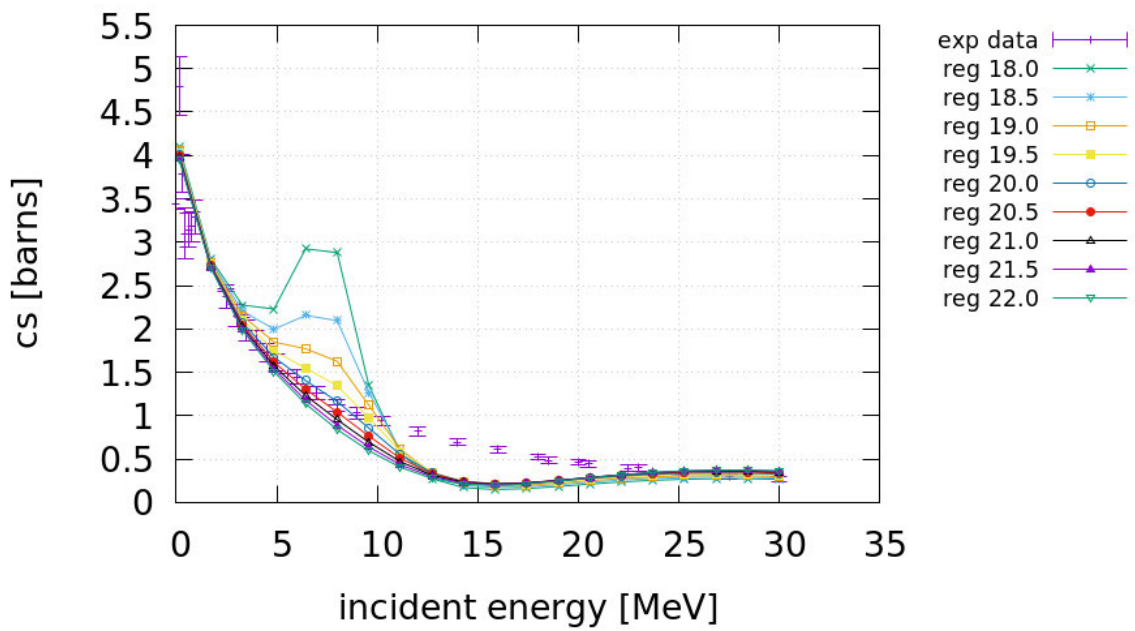


Figure 19: Elastic cross section for $a_i = 7$ fm and $A_i = 5.6$ fm for different values of η .

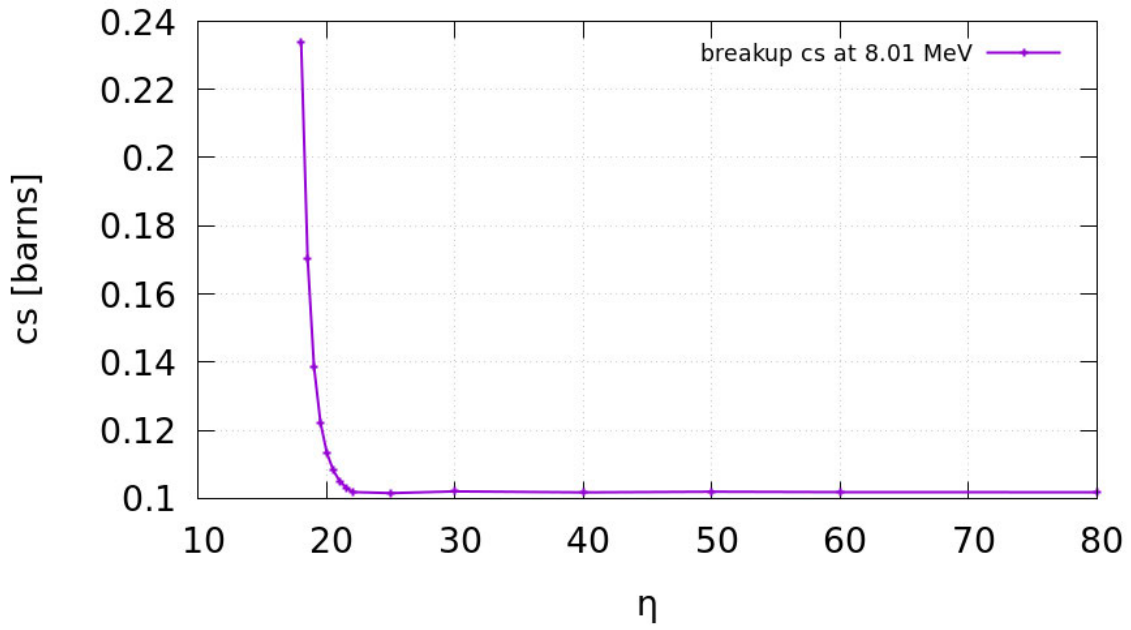


Figure 20: Breakup cross section at 8.01 MeV as a function of the regularization parameter η .

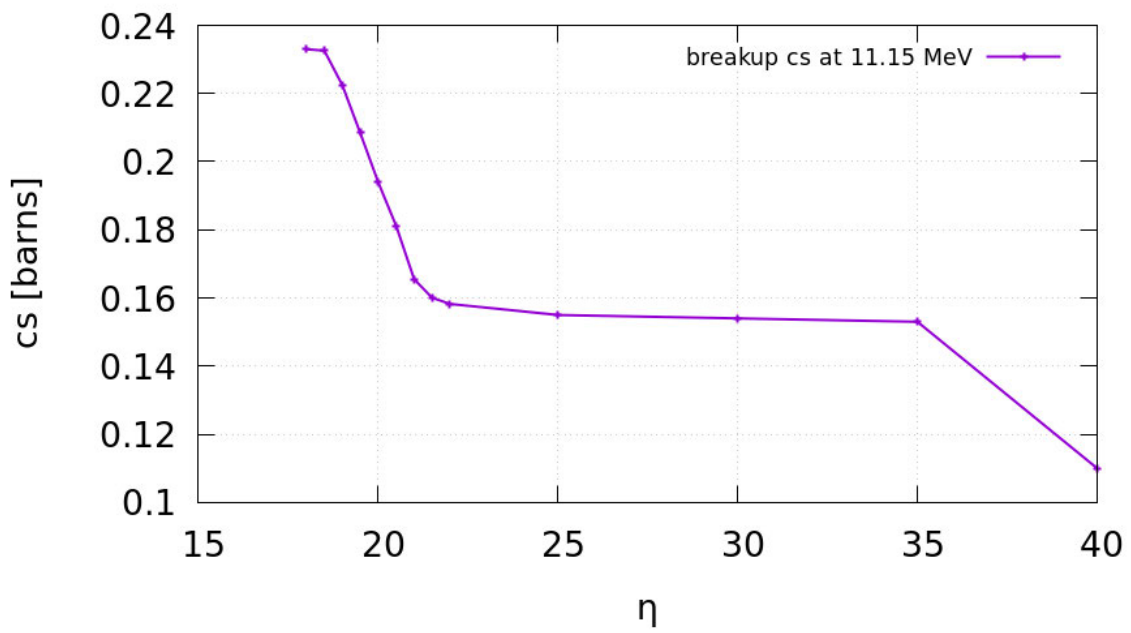


Figure 21: Breakup cross section at 11.15 MeV as a function of the regularization parameter η .

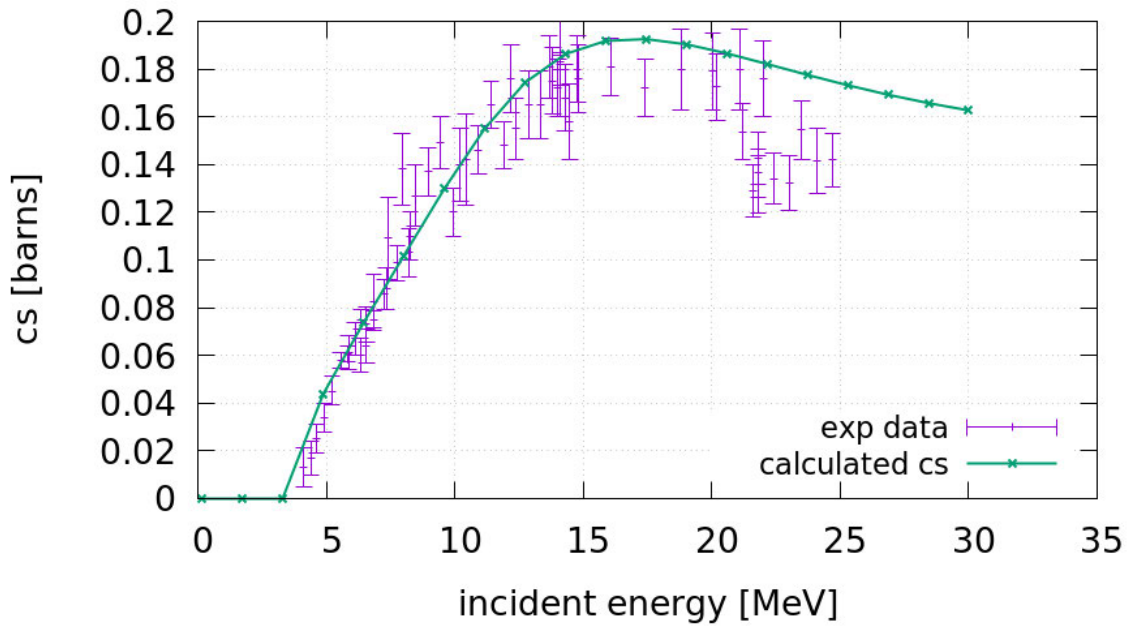


Figure 22: Breakup cross section for $a_i = 7$ fm and $A_i = 5.6$ fm and with $\eta = 22$.

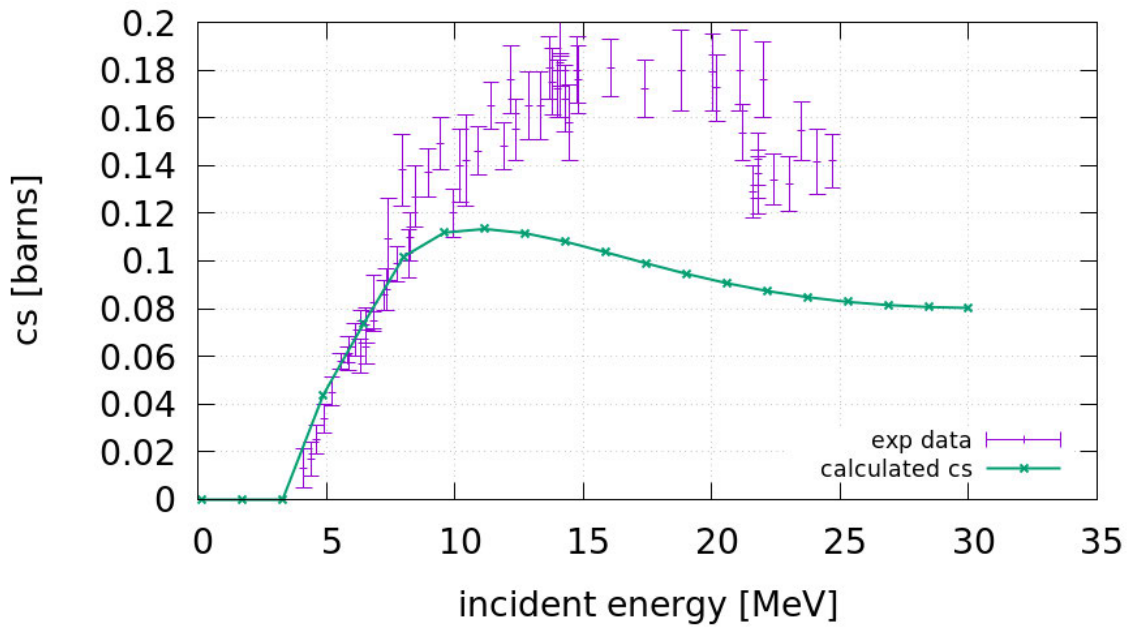


Figure 23: Elastic cross section for $a_i = 7$ fm and $A_i = 5.6$ fm with $\eta = 40$.

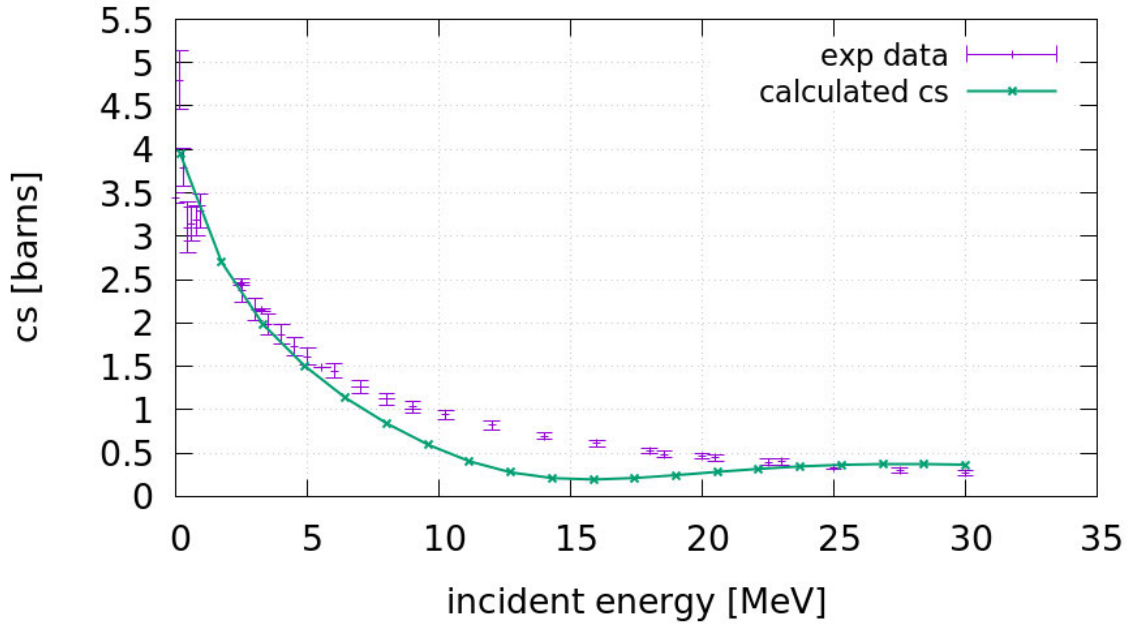


Figure 24: Elastic cross section for $a_i = 7$ fm and $A_i = 5.6$ fm and with $\eta = 22$.

7.4 The problem of the continuity of flux

The underestimation of the elastic neutron+deuteron cross section beyond 8 MeV appears to be a problem of the algorithm because even drastic changes of the basis functions do not lead to significant changes of the breakup and elastic cross sections. Therefore, the basics of the algorithm and its derivation were revisited. In the current derivation of the R -matrix formalism for three-body channels all, but one basic conditions of R -matrix theory for two-body problems were properly transferred to three-body channels. The only condition which is missing in the new formalism is the constraint of a continuous first derivative of the three-body wave function at the border of the domain D (Fig. 6). The evaluation of the three-body wave function in terms of the coefficients $c_\mu^{(i)}$ in the interior and via T_i^b and $T_i(k)$ in the exterior region [Eqs. (5.21), (5.22) and (5.29)] clearly indicates discontinuities in the first derivative of the total three-body wave function

$$u(r, R) = \sum_{i=1}^3 u_i(r, R) \quad (7.8)$$

beyond 8 MeV (Fig. 25), while the situation at lower energies is in general much better (Fig. 26). The discontinuities in the first derivative of the wave function are associated

with discontinuities in the particle flux and represent a severe problem. In order to cure this problem one can introduce the constraint of a continuous first derivative into the algorithm. However, this would lead to an overdetermined system. Taking into account that the asymptotic three-body wave function is of limited accuracy at the matching radius the actual improvement of such an extension is questionable. Therefore a different procedure which remains within the developed formalism was searched. Considering the Faddeev equations one basic concept is the division of the wave function in three components each associated with a system, where one particle is a free spectator and the remaining two are interacting in the subsystem. Because the spectator is free there exists no natural bound of A_i whereas a_i is determined by the range of the potential in the subsystem. Hence, cross sections change with respect to the value of A_i while a_i if greater than a minimum value of 4 fm (Eq. (7.6)) has practically no impact on the observables. Therefore we can use A_i as an additional parameter which can be adjusted in order to optimize the continuity of the first derivative of the three-body wave function. A_i must be chosen in different incident energy regions in such a way that continuity in the first derivative is given in some areas of r . Continuity on the full r -range cannot be reached. These areas of r can be determined by considering the parametrization of k in terms the coordinates r and R [see Eqs. (6.2) and (6.3)]

$$k = 2\mu_{jn}\sqrt{E}\frac{r_i}{\rho} \quad (7.9)$$

with $\rho = \sqrt{2\mu_{jn}r_i^2 + 2\mu_{i(jn)}A_i^2}$ and k denotes the wavenumber between the two particles in the subsystem. A criterion could be that the wave function depending on R should be continuous for such values of r yielding energies in the vicinity of considered energy point.

With this criterion it was found that the ideal value for A_i in the energy region below 8 MeV is $A_i = 5.6$ fm yielding the cross sections Fig. 22 and Fig. 24.

Above 8 MeV $A_i = 3$ fm yielding the cross sections in Figs. 27 and 28. In this energy range the value $A_i = 3$ leads to a significant improvement of the continuity of the first derivative of the wave function in Fig. 29 compared to the energy region below 8 MeV (Fig. 30).

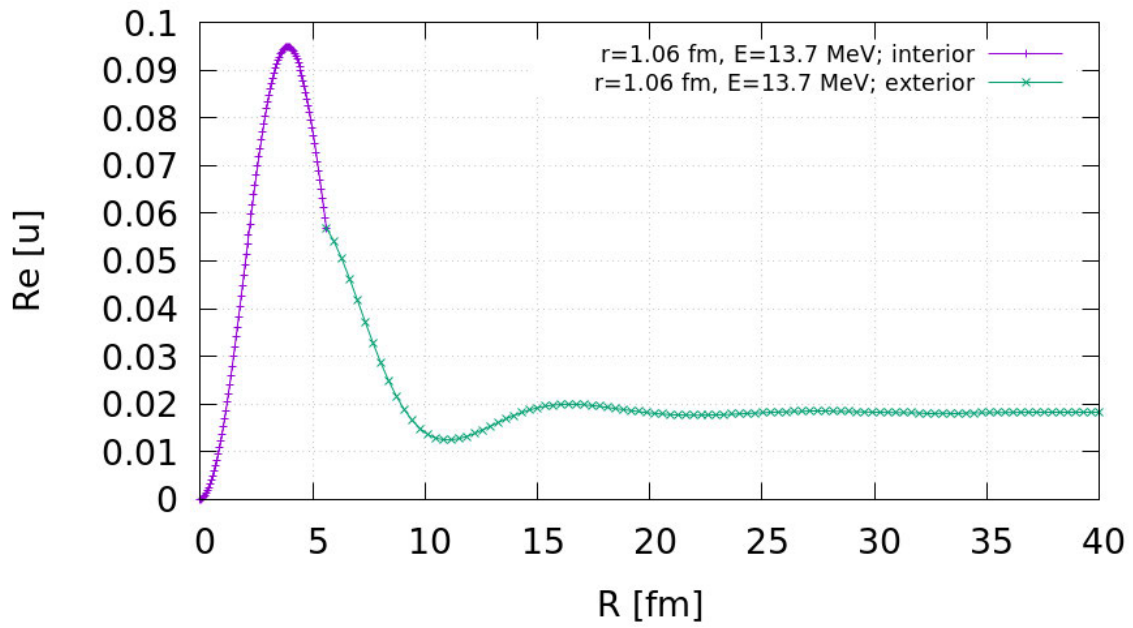


Figure 25: Real part of the wave function $u(r, R)$ for a fixed value of r in the interior (purple) and exterior (green) region.

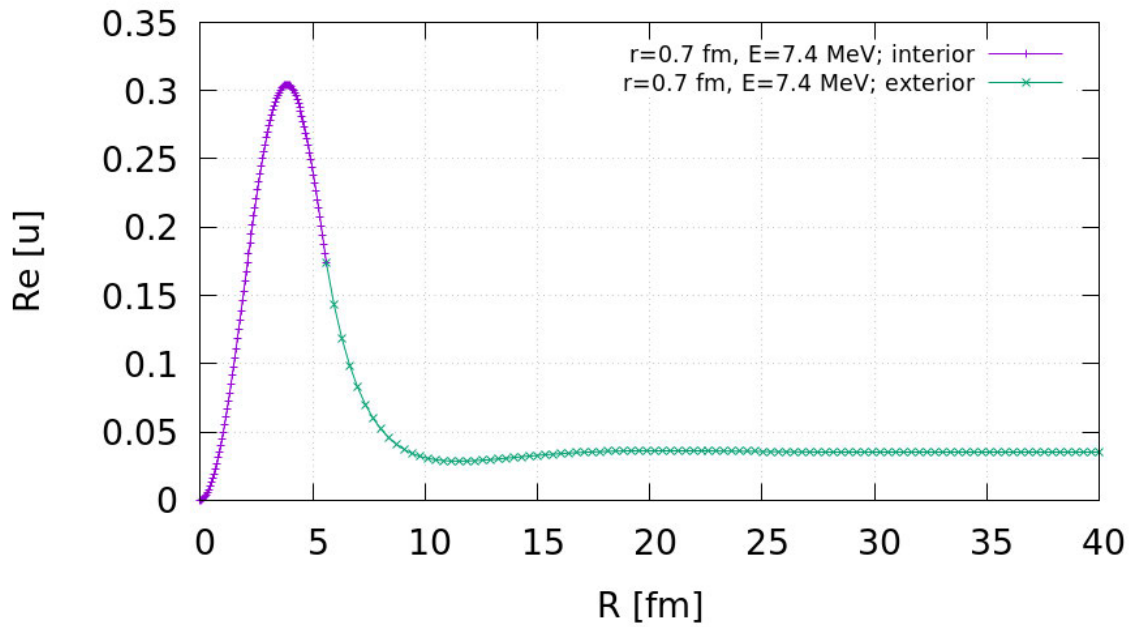


Figure 26: Real part of the wave function $u(r, R)$ for a fixed value of r in the interior (purple) and exterior (green) region.

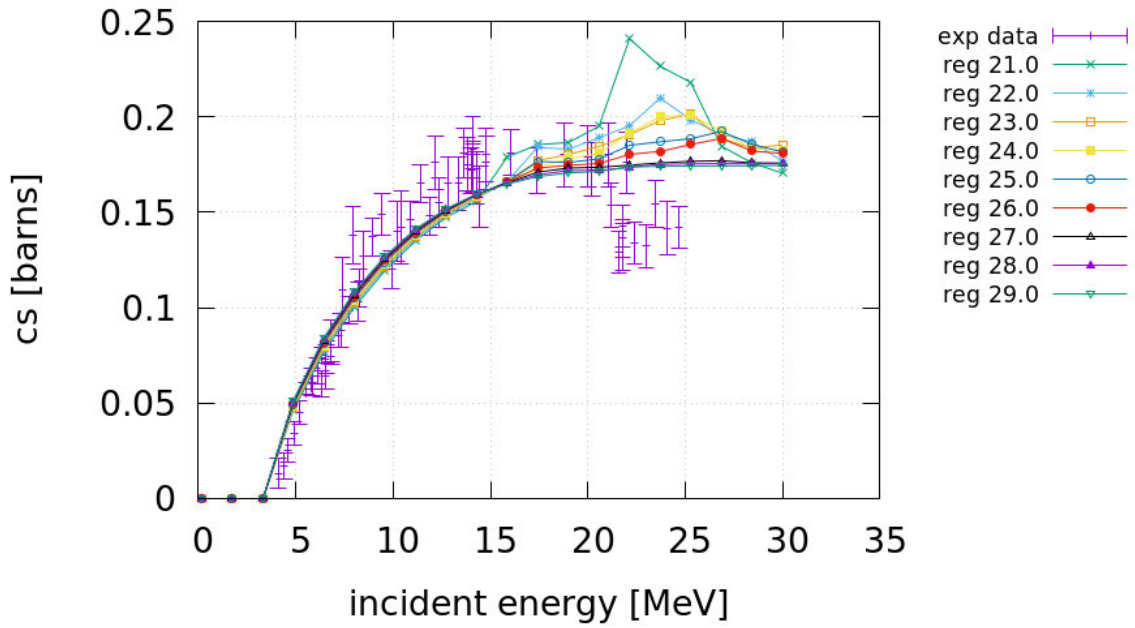


Figure 27: Breakup cross section for $a_i = 5$ fm and $A_i = 3.3$ fm for different values of η .

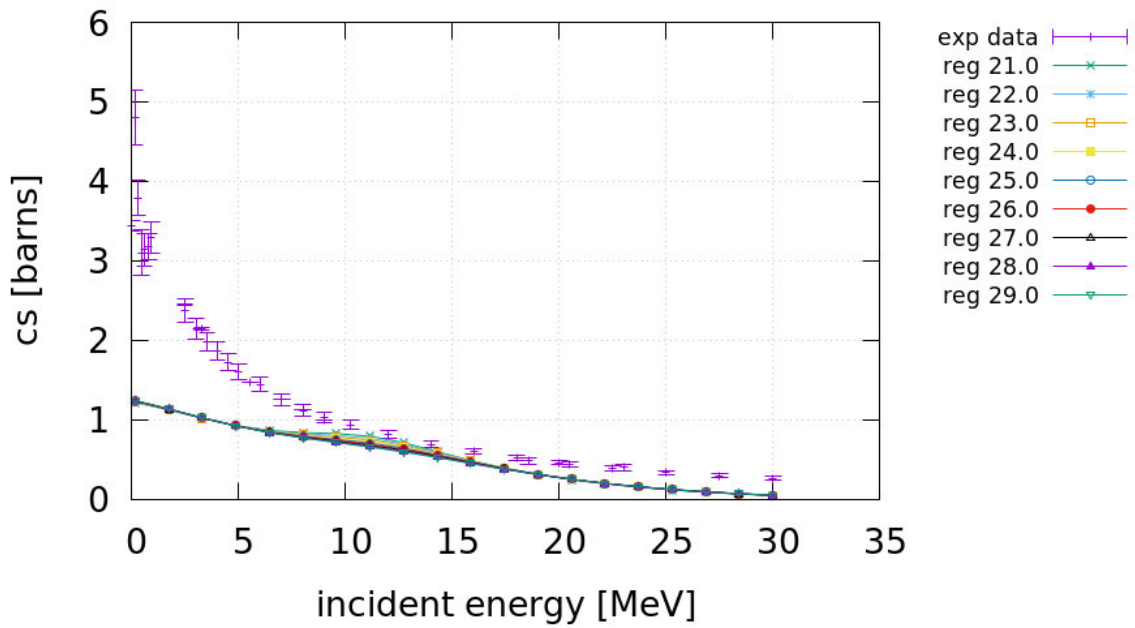


Figure 28: Elastic cross section for $a_i = 5$ fm and $A_i = 3.3$ fm for different values of η .

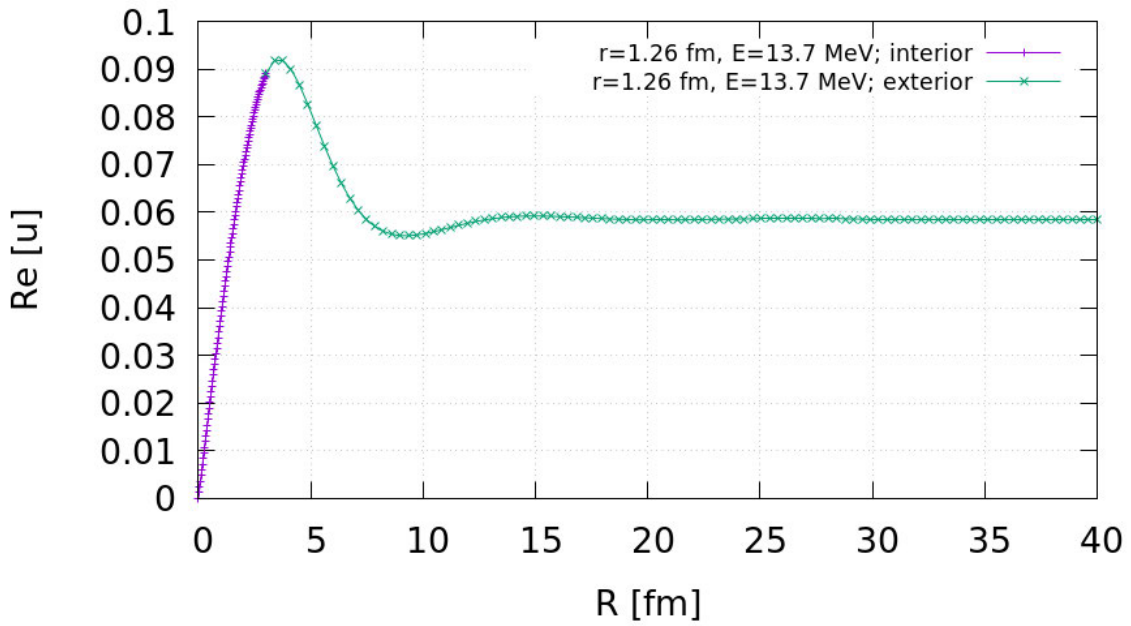


Figure 29: Real part of the wave function $u(r, R)$ for a fixed value of r in the interior (purple) and exterior (green) region.

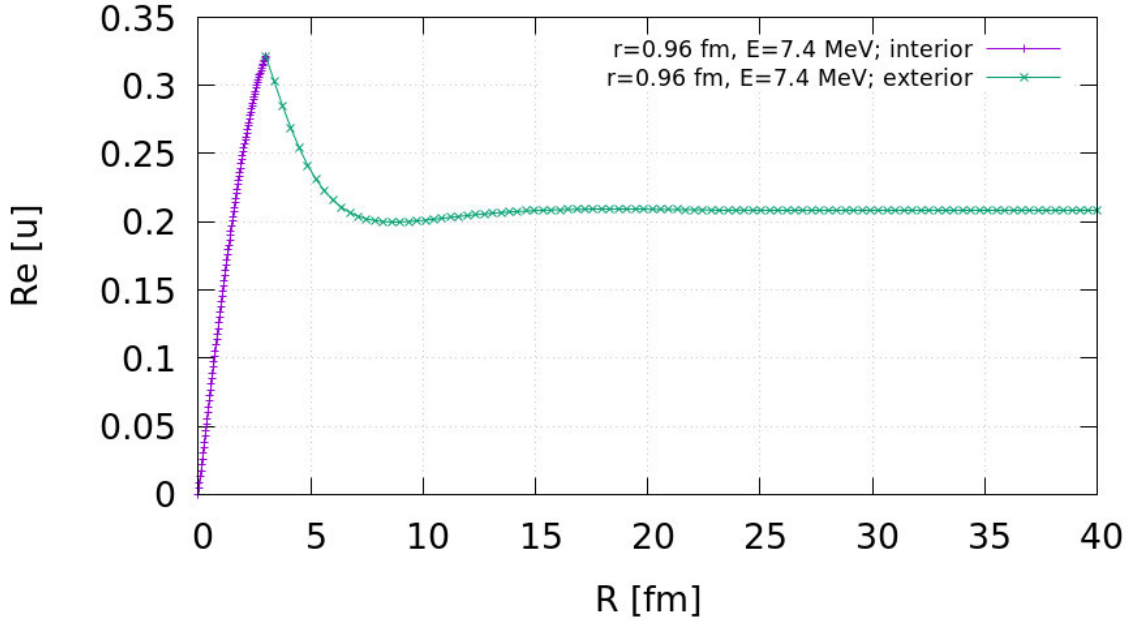


Figure 30: Real part of the wave function $u(r, R)$ for a fixed value of r in the interior (purple) and exterior (green) region.

Hence, by using the argument of continuity of the first derivative of the three-body wave function at the matching radius A_i we obtain a set of ideal matching radii depending on the energy range

$$A_i = \begin{cases} 5.6 \text{ fm} & \text{for } 0 \text{ MeV} < E \leq 8 \text{ MeV} \\ 3.0 \text{ fm} & \text{for } 8 \text{ MeV} < E < 30 \text{ MeV} \end{cases}$$

and

$$a_i = \begin{cases} 7.0 \text{ fm} & \text{for } 0 \text{ MeV} < E \leq 8 \text{ MeV} \\ 5.0 \text{ fm} & \text{for } 8 \text{ MeV} < E < 30 \text{ MeV} \end{cases}$$

Hence, the cross sections giving the best description over the total energy range are shown in Figs. 31 and 32. They are composed of two parts with different values for the matching radii which are merged smoothly at 8 MeV.

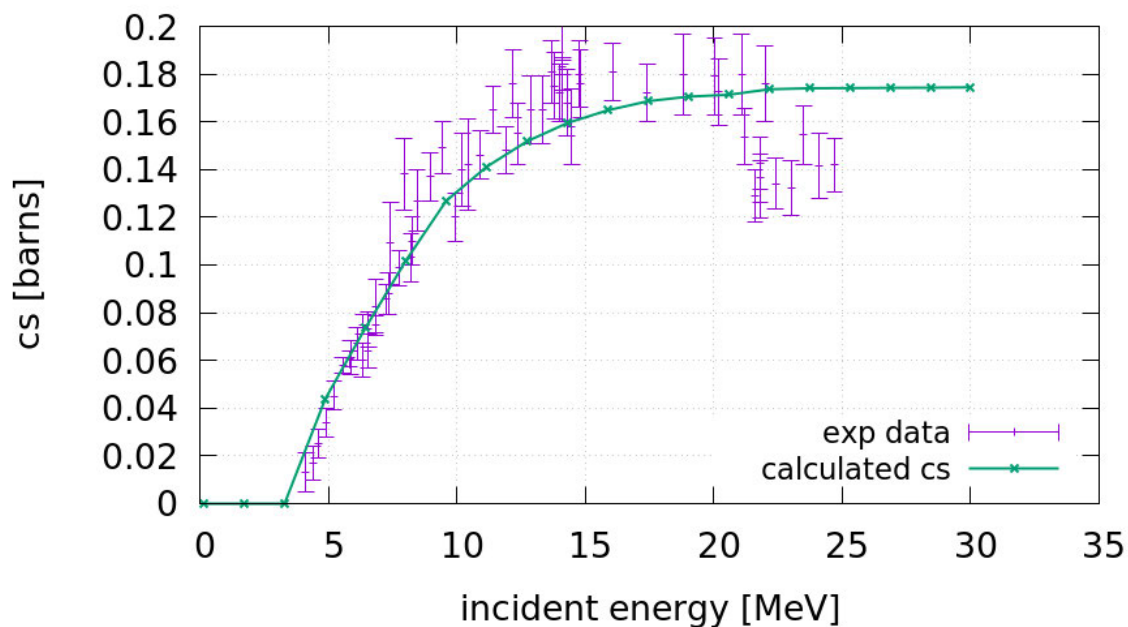


Figure 31: Breakup cross section for the total energy range.

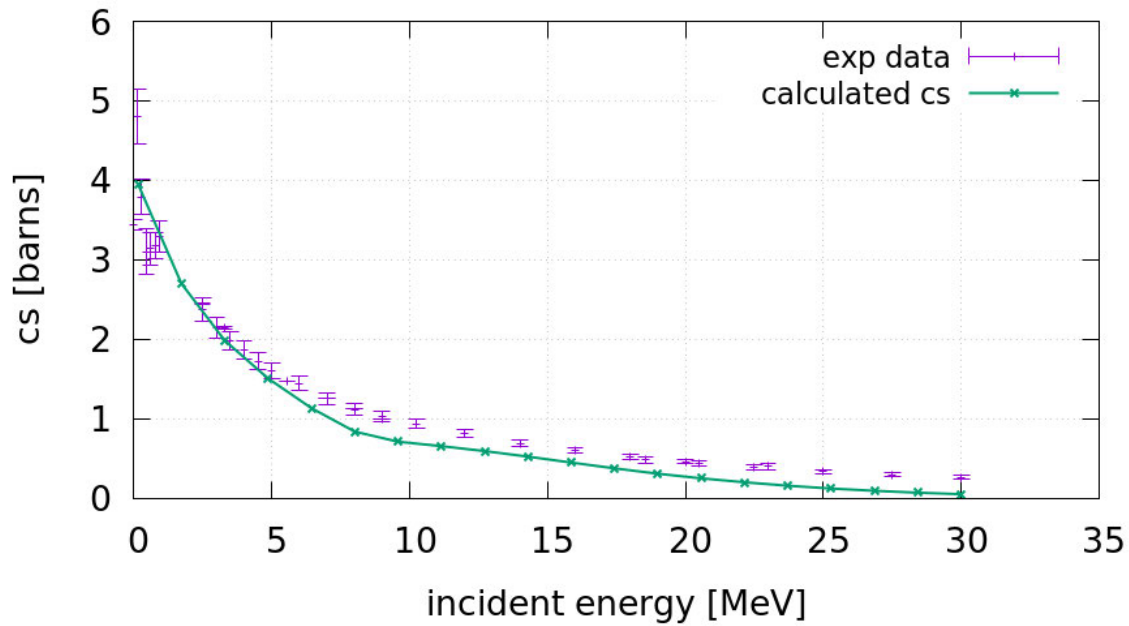


Figure 32: Elastic cross section for the total energy range.

As mentioned above the continuity of the first derivative of the wave function is directly related with the continuity of the particle flux. The conservation of flux is directly related with the unitarity of the S -matrix and leads to the optical theorem (5.112). We insert the T -amplitudes T_1^b and $T_i(k)$ (rearrangement T -amplitudes do not exist in the neutron+deuteron system) obtained from our calculations and compare the left and right hand side of the optical theorem (5.112) in Fig. 33 (the step at 8 MeV results from the change of the matching radii).

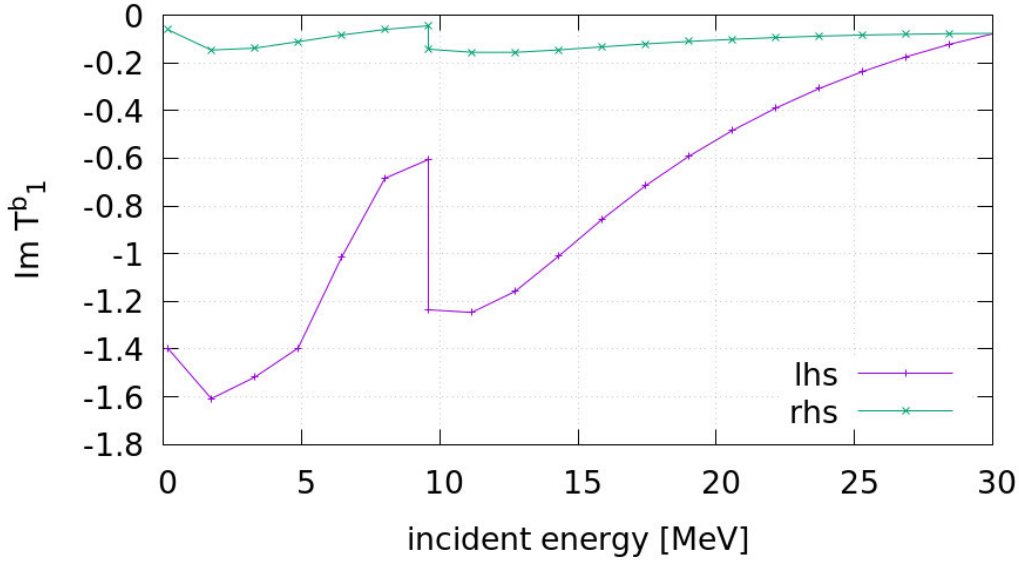


Figure 33: Left and right hand side of the optical theorem, Eq. (5.112).

It is obvious from Fig. 33 that the calculated quantities do not fulfill the optical theorem. However, the evaluated cross sections agree fairly well with the experimental data from which follows that the absolute value of T_1^b must be correct. We compared $\text{Im } T_1^b$ obtained from the three-body R -matrix calculations with $\text{Im } T_1^b$ calculated from the optical theorem (5.109),

$$\text{Im } T_1^b = -\frac{1}{8\pi} \frac{m_n}{\mu_{1(23)}} Q_1^2 [\sigma_{elastic} + \sigma_{breakup}].$$

where we use the experimental values for the cross sections. For both cases we determine the complex phase angles according to

$$\text{Im } T_1^b = |T_1^b| \sin \varphi, \quad (7.10)$$

The angle φ_{calc} , which is the one for the calculated quantity $\text{Im } T_1^b$ and φ_{exp} which comes from the experimental data are plotted in Fig. 34. One can interpret the difference $\Delta = \varphi_{calc} - \varphi_{exp}$ (Fig. 35) as phase shift error of the calculation. This phase shift Δ may result from the asymptotic wave function which will exhibit a different phase compared to the asymptotic form used in our derivation. This different phase in the asymptotic form of the wave function results in a phase shift in the calculated T_1^b

amplitudes

$$\text{Im } T_1^b = |T_1^b| \sin(\varphi_{exp} + \Delta). \quad (7.11)$$

Therefore this difference Δ can be considered as the error of the algorithm.

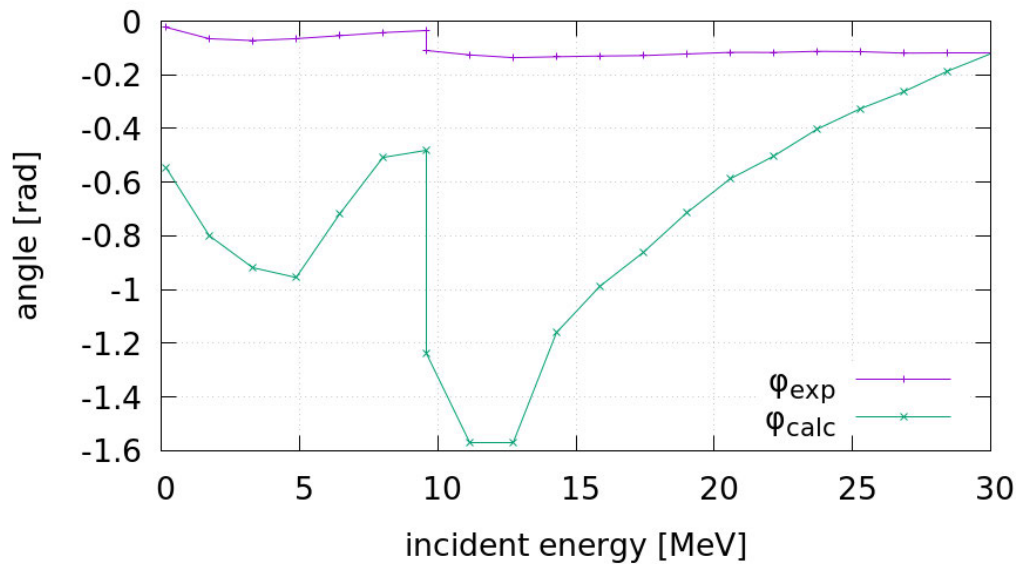


Figure 34: Angles φ_{exp} and φ_{calc} .

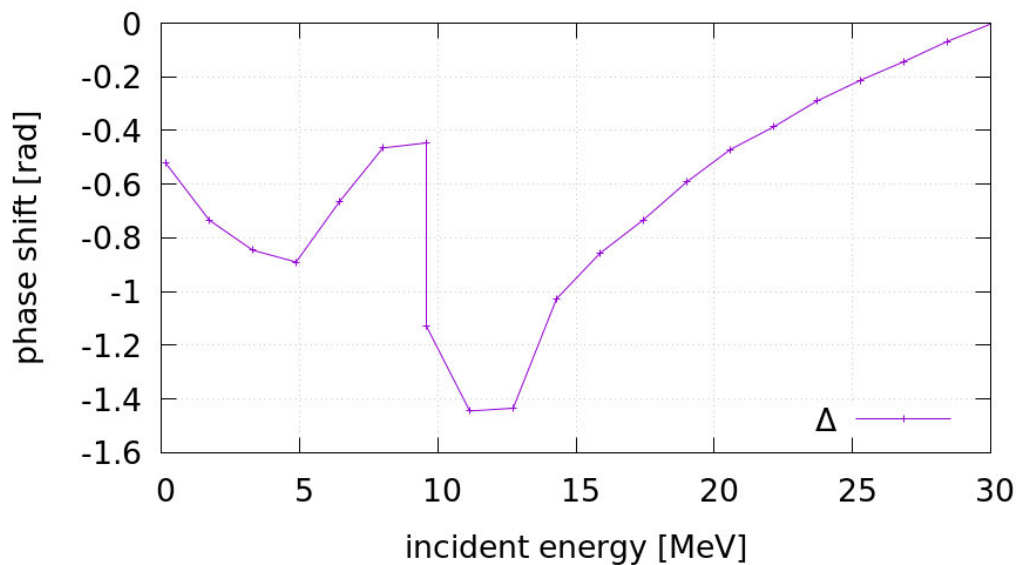


Figure 35: Phase shift Δ for the calculated complex T_1^b amplitude.

The excellent agreement between the experimental cross section data and the calculated ones confirms that our assumption concerning the normalization of the breakup cross section ((5.111d)) was correct and the open parameter $\beta = 1$. This is also confirmed by the optical theorem which is exactly fulfilled with $\beta \approx 1$ up to about 15 MeV (Fig. 36).

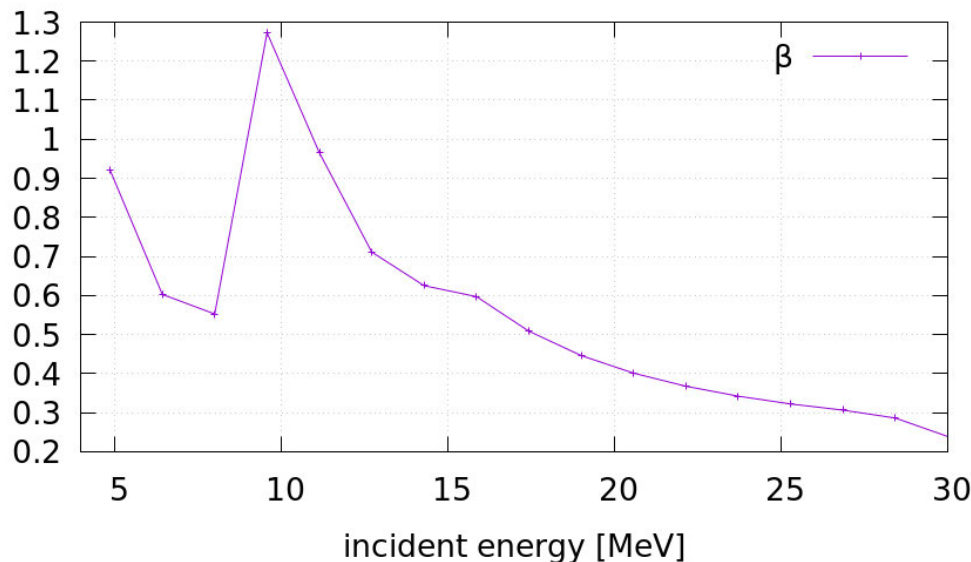


Figure 36: The factor β calculated for the case that the optical theorem is exactly fulfilled.

Limits of the model

There are two main limitations of the presented novel three-body R -matrix model. First there is the asymptotic form of the three-body wave function which does not match the interior wave function properly at the values of the matching radii that were used. However, if one increases the radii the number of basis states must be increased drastically and therefore the stability of the algorithm gets worse and the computation time increases significantly. These asymptotic problems are also supposed to be the reason for the phase difference with respect to experimental data that occurs in $\text{Im } T_1^b$. Secondly we have included s-waves only. As a consequence the results are reasonable only at low energies up to about 10 MeV. At higher energies it is expected that p-waves and higher partial waves contribute significantly.

7.5 The neutron+⁹Be system

Beryllium plays an important role in fusion and fission devices. It is an important ingredient of plasma facing components and a neutron multiplier for tritium breeding. The neutron (n) multiplying reaction is $n+{}^9\text{Be}\rightarrow n+n+({}^8\text{Be})^*\rightarrow n+n+{}^4\text{He}+{}^4\text{He}$ and occurs at relatively low incident energies (Tab. 6).

reaction	Q -value [MeV]
${}^9\text{Be}(n,n){}^9\text{Be}$	0.0000
${}^9\text{Be}(n,\alpha){}^6\text{He}$	-0.5971
${}^9\text{Be}(n,2n\alpha){}^4\text{He}$	-1.6636
${}^9\text{Be}(n,n\alpha){}^5\text{He}$	-2.3073
${}^9\text{Be}(n,t){}^7\text{Li}$	-10.4373
${}^9\text{Be}(n,p){}^9\text{Li}$	-12.8248
${}^9\text{Be}(n,t\alpha)t$	-12.9049
${}^9\text{Be}(n,d){}^8\text{Li}$	-14.6615
${}^9\text{Be}(n,t){}^8\text{Li}$	-14.6615
${}^9\text{Be}(n,nd){}^7\text{Li}$	-16.6932
${}^9\text{Be}(n,np){}^8\text{Li}$	-16.8861
${}^9\text{Be}(n,nt){}^6\text{Li}$	-17.6871
${}^9\text{Be}(n,n\alpha){}^6\text{Li}$	-19.2874
${}^9\text{Be}(n,pt){}^6\text{He}$	-20.4108
${}^9\text{Be}(n,{}^3\text{He})({}^7\text{He})$	-21.5845
${}^9\text{Be}(n,p\alpha){}^5\text{H}$	-23.1857

Table 6: Reaction channels in the $n+{}^9\text{Be}$ system with the associated Q -values.

We are interested to evaluate this four-body breakup reaction because it dominates the reaction cross section at low energies. The exact threshold for this reaction is at 1.664 MeV and at 5 MeV it has a share of about 20% on the total cross section. Hence this channel can no longer be handled approximatively. The two alpha particles form a resonance state (${}^8\text{Be}$) at 92 keV which has a lifetime of about $8.19\cdot 10^{-17}$ s thus four magnitudes longer than nuclear reaction times. Because of that we can treat this four-body breakup reaction as an effective three-body problem. The available evaluations in ENDF/B-VIII.0 [2], JENDL-4.0 [4] and JEFF-3.1/A [3] are shown in Fig. 37, but all of them are based exclusively on analyses of experimental data.

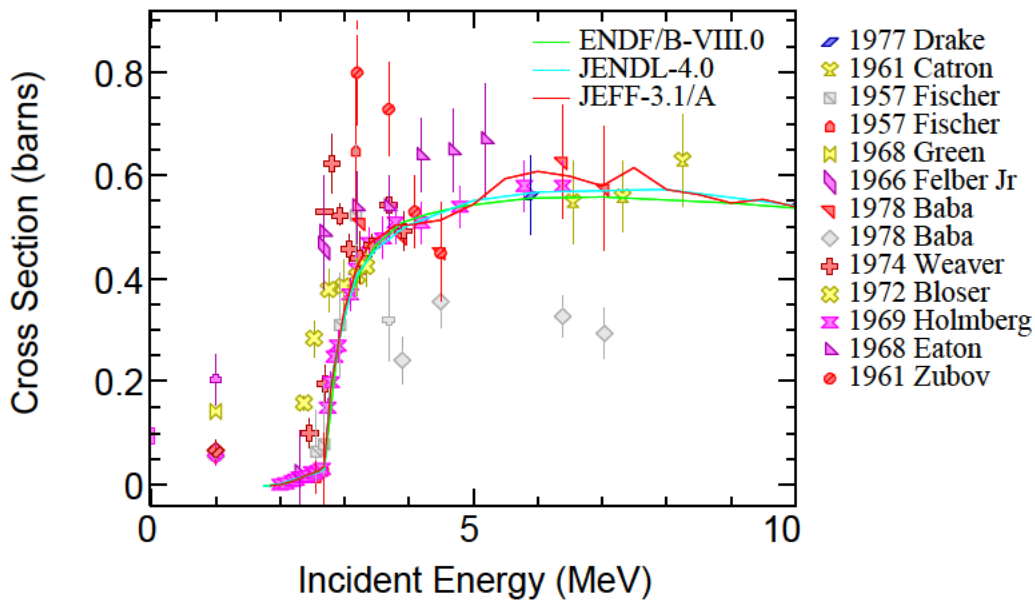


Figure 37: Neutron+⁹Be breakup: Experimental data from EXFOR [1] and evaluated curves from [2], [23] and [4].

In this subsection we present an application of the three-body R -matrix formalism to the $n+^9\text{Be}$ system in order to determine the breakup cross section. The Faddeev-based three-body R -matrix requires a separation of the total three-body system according to the three Faddeev-components (Fig. 38).

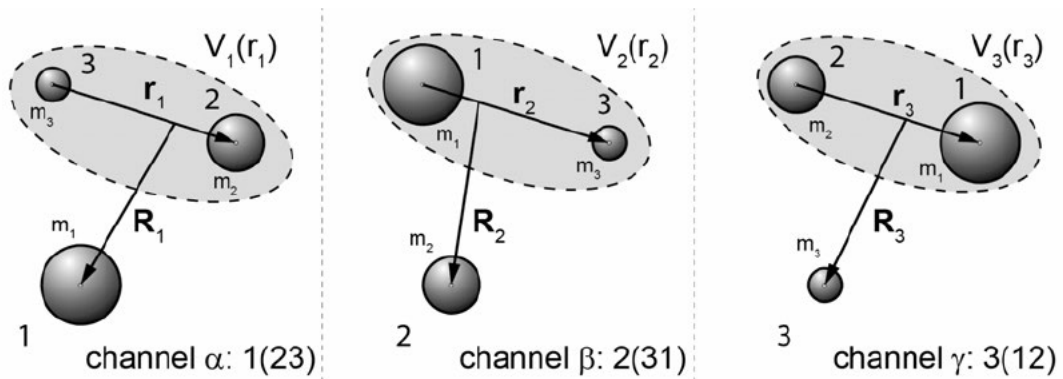


Figure 38: Illustration of the three Faddeev-components in a three-body system.

If particles 2 and 3 are assumed to be two neutrons and particle 3 the resonance state (⁸Be) then subsystems two and three are identical. In this subsystem the neutron

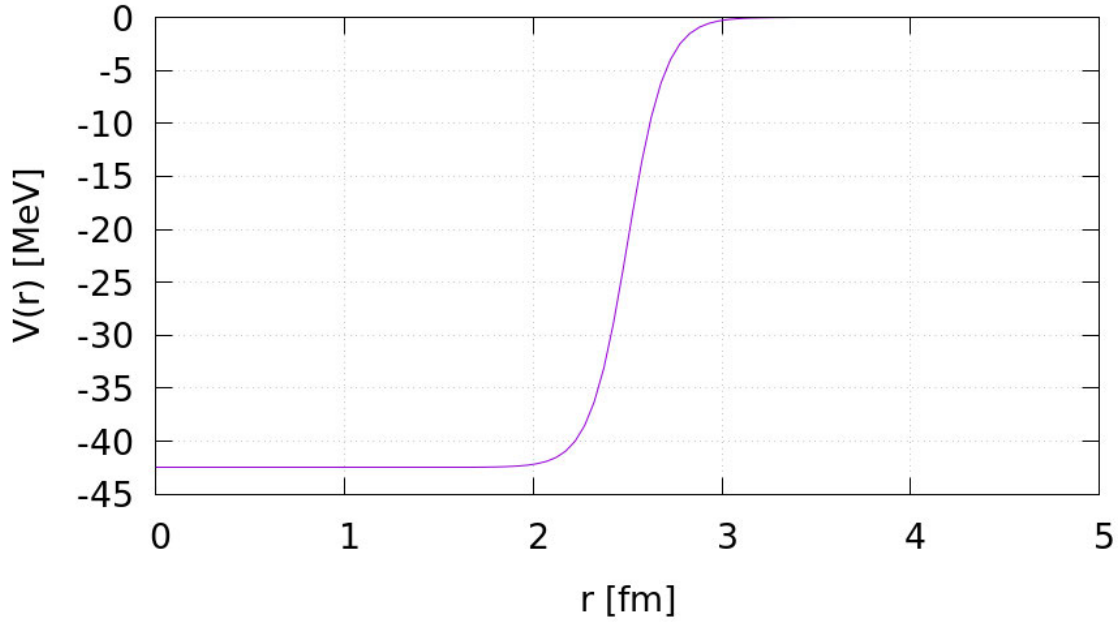


Figure 39: Neutron+⁸Be potential of Woods-Saxon form.

is bound to (⁸Be) in an angular momentum state $\ell = 1$ via a potential that is assumed to be of Woods-Saxon form

$$V(r) = \frac{v_0}{1 + \exp((r - a)/b)} \quad (7.12)$$

with $a = 1.25\sqrt[3]{A} = 1.25\sqrt[3]{8} = 2.5$ fm and $b = 0.1$ fm (Fig. 39). The potential depth $v_0 = -42.4519$ MeV is chosen such that there exists a bound state (shown in Fig. 40) at -1.664 MeV which corresponds to the neutron-separation energy.

In the first subsystem - in analogy to the neutron+deuteron system - the two neutrons interact via the Reid soft-core potential in Eq. (7.1) with the parameters (7.3). From the range of the potential one can determine the matching radii a_i and A_i according to Eq. (5.48). In the case of the Woods-Saxon potential in Eq. (7.12) with a range of about 3 fm reasonable values are

$$a_i = 16 \text{ fm and } A_i = 13.5 \text{ fm} . \quad (7.13)$$

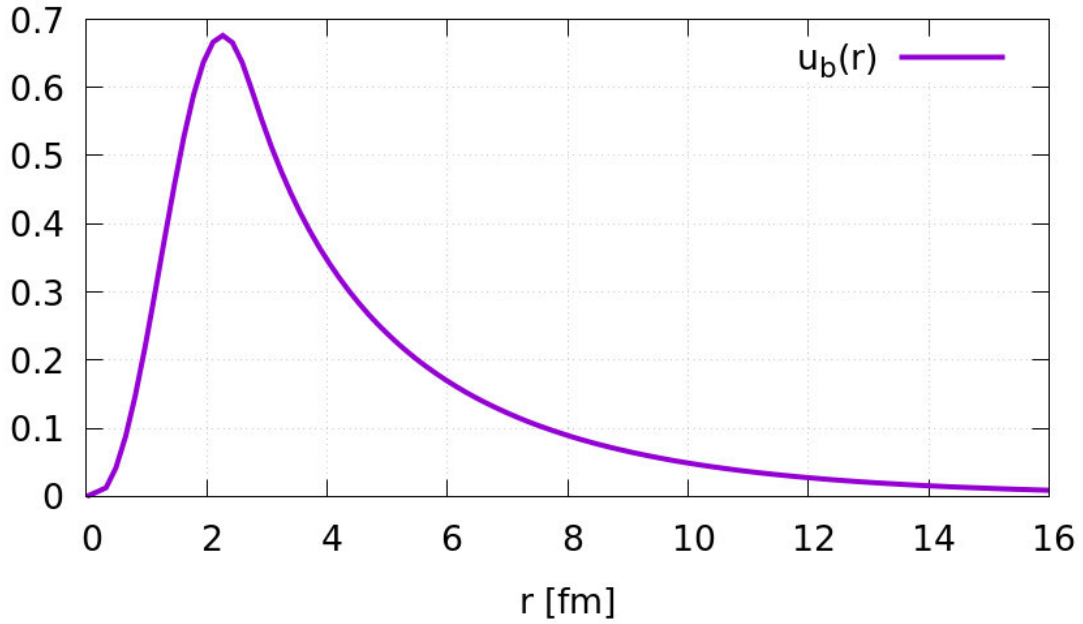


Figure 40: Bound wave function of the $n+{}^8\text{Be}$ subsystem.

7.5.1 Basis states

Because the two neutrons are indistinguishable the total wave function must be anti-symmetric with the consequences described in Sec.7.2.1. The numerical implementation is completely analogue to the neutron+deuteron system in section 6 although we now have an $\ell = 1$ state in subsystem 2 and the theory was elaborated only for s-waves. Because p-waves are not included in the formalism we did some kind of approximation. We stuck to the formalism restricted to s-waves, but took basis states for subsystem 2 with angular momentum $\ell = 1$ in order to describe the neutron density correctly. The set of basis states $X(r)$ [Eq. (5.55)] is composed of the bound state wave function and 14 scattering states with equidistant eigenenergies $\epsilon_{\mu 1}^{(2)}$ between 0.1 and 6 MeV (Table 7). The set of basis states $Y(R)$ [Eq. (5.56)] consist of 15 states with eigenenergies $\epsilon_{\mu 2}^{(2)}$ equidistantly partitioned between 0.1 and 6 MeV (Table 7). The total basis comprises 225 states $\varphi_{\mu}^{(2)}(r, R) = X_{\mu 1}(r) \cdot Y_{\mu 2}(R)$ and energy eigenvalues $E_{\mu}^{(2)} = \epsilon_{\mu 1}^{(2)} + \epsilon_{\mu 2}^{(2)}$. A selection of basis states for subsystem 2 is displayed in Fig. 41. A selection of the energy eigenvalues is given in Tables 7 and 8.

μ_1/μ_2	$\epsilon_{\mu_1}^{(1)}$ [MeV]	$\epsilon_{\mu_2}^{(1)}$ [MeV]
1	-1.664	0.100
2	0.100	0.521
3	0.554	0.942
\vdots	\vdots	\vdots
15	6.000	6.000

Table 7: Eigenenergies $\epsilon_{\mu_1}^{(2)}$ and $\epsilon_{\mu_2}^{(2)}$ for the $n+^8\text{Be}$ -subsystem.

μ	$E_{\mu}^{(2)}$ [MeV]
1	-1.564
2	-1.143
3	-0.722
4	-0.301
5	0.120
6	0.541
7	0.962
\vdots	\vdots
225	12.000

Table 8: Eigenenergies $E_{\mu}^{(2)}$ of the basis states $\varphi_{\mu}^{(2)}(r, R)$ for the $n+^8\text{Be}$ -subsystem.

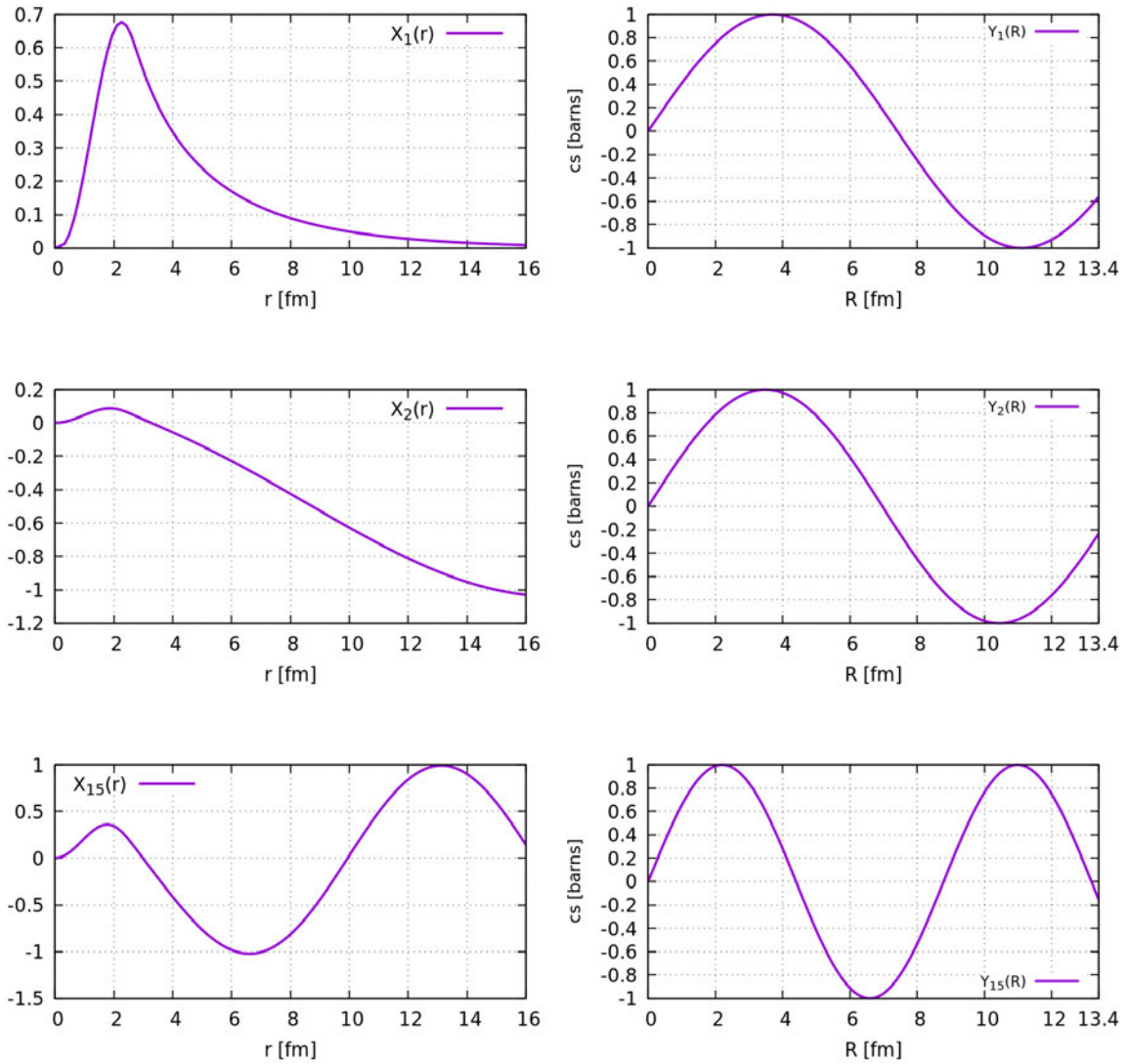


Figure 41: Basis functions for the neutron+ ^8Be subsystem.

The basis states of the nn -subsystem are chosen quite similarly to those in the neutron+deuteron section. Their number is now 225 with the eigenenergies $\epsilon_{\mu 1}^{(1)}$ of the $X_{\mu 1}(r)$ states and $\epsilon_{\mu 2}^{(1)}$ of the $Y_{\mu 2}(R)$ states listed in Table 9 and the total basis states energies are given in Table 10. A selection of the basis states $\varphi_{\mu}^{(1)}(r, R)$ is displayed in Fig. 42.

μ_1/μ_2	$\epsilon_{\mu_1}^{(1)}$ [MeV]	$\epsilon_{\mu_2}^{(1)}$ [MeV]
1	0.100	0.100
2	0.521	0.521
3	0.942	0.942
\vdots	\vdots	
12	6.000	6.000

Table 9: Eigenenergies $\epsilon_{\mu_1}^{(1)}$ and $\epsilon_{\mu_2}^{(1)}$ for the nn -subsystem.

μ	$E_{\mu}^{(1)}$ [MeV]
1	0.200
2	0.621
3	1.042
4	1.463
5	1.884
6	2.305
7	2.726
\vdots	\vdots
30	12.000

Table 10: Eigenenergies $E_{\mu}^{(1)}$ of the basis states $\varphi_{\mu}^{(1)}(r, R)$ for the nn -subsystem.

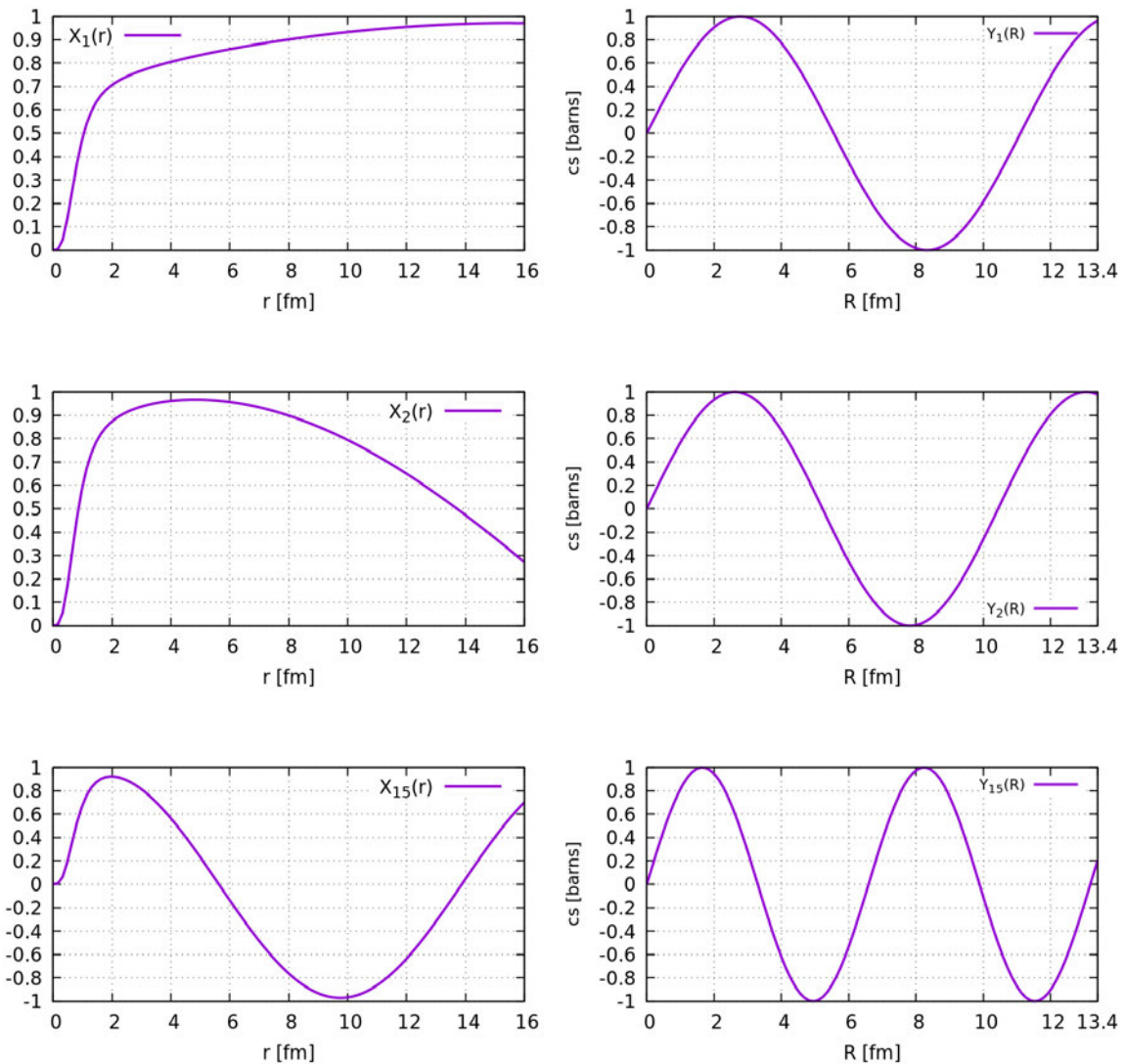


Figure 42: Basis functions for the nn subsystem.

7.6 Results for the neutron+ ^9Be system

The application of the R -matrix formalism requires an additional approximation because of the p -state in ^9Be . In order to simulate the radial neutron density distribution we use $\ell = 1$ basis wave functions in this subsystem, but keep the remaining formalism unchanged. The application of the formalism yields the breakup cross section and the angle-integrated elastic cross section. However, the latter cannot be compared to the experiment because the assumed three-body structure does not contain two-body channels such as $^6\text{He} + \alpha$ which opens already at 0.5971 MeV in the center of mass

system (see Tab. 6). In principle the three-body model would allow the description of inelastic $n+{}^9\text{Be}^*$ channels to an excited single-particle state. Because of the approximations involved we calculate only the breakup cross section and the elastic cross section. These cross sections are calculated by Eqs. (5.111d) and (5.111a). Like in the neutron+deuteron system there exist no rearrangement channels in the neutron+ ${}^9\text{Be}$ system. The obtained results for the breakup cross section are displayed in Fig. 43 for different values of the regularization parameter η (Eq. 6.13). Convergence with respect to η is reached at a value of about 1.6. For this regularization value the final breakup curve is shown in Fig. 44 together with the available experimental data from the EXFOR library [1]. Up to 4 MeV the calculated cross sections are in excellent agreement with measured data. At energies greater than 4 MeV the algorithm fails independent of the choice of basis functions. We suppose that the coarse approximation to deal with quasi s-states breaks down and a detailed treatment of higher partial waves would be required.

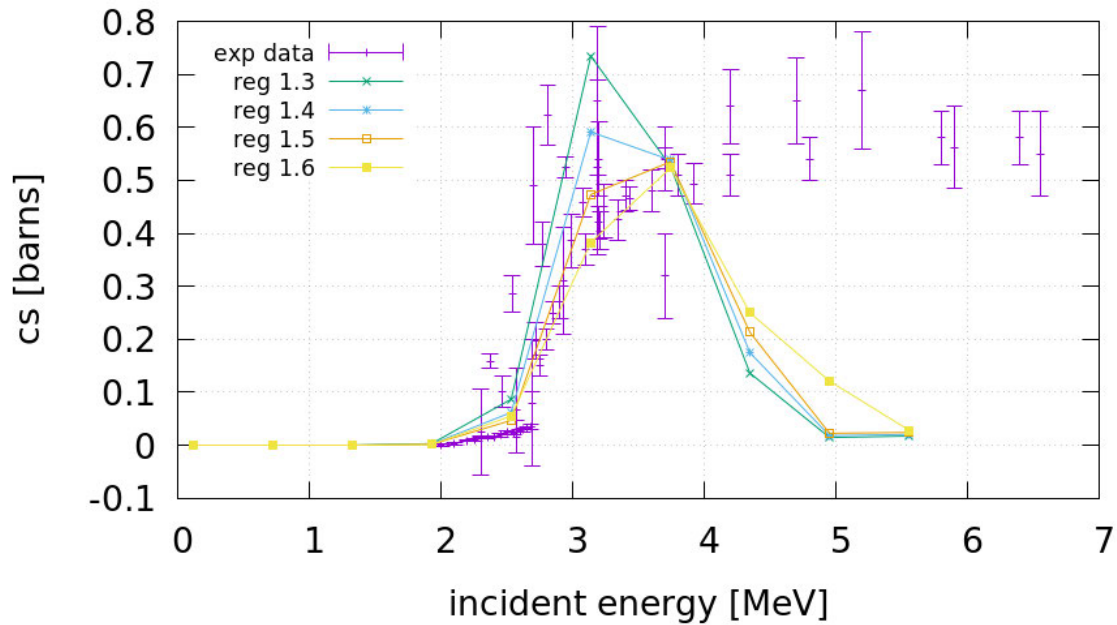


Figure 43: Breakup cross section for different values of η .

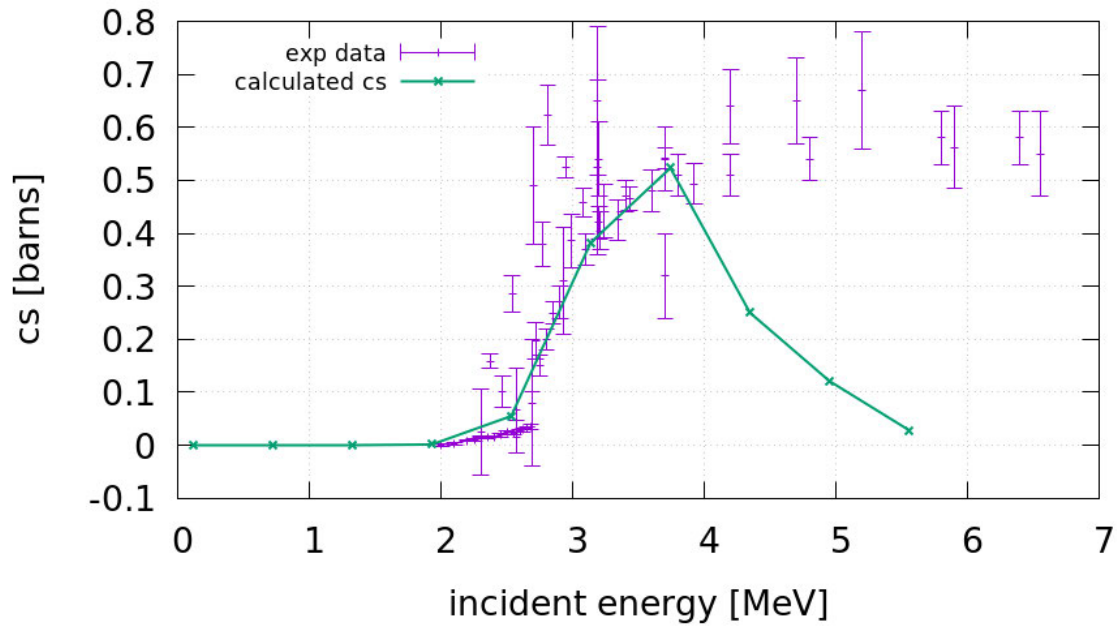


Figure 44: Breakup cross section for $\eta = 1.6$.

The calculated elastic angle-integrated cross section is presented in Fig. 45 and compared to EXFOR data [1]. It is also in fair agreement with the experiments between 2 and 4 MeV. The peak below 3 MeV is not well reproduced, but the results show a correct indication of the resonance associated with the breakup channel. Below 1 MeV our results differ significantly from the experimental data. However, as mentioned above the structures below 1 MeV in the elastic cross section result from the appearance of the ${}^9\text{Be}(n,\alpha){}^6\text{He}$ reaction channel which is not included in the three-body model and therefore cannot be reproduced in our calculation. Similarly to the neutron+deuteron system A_i is not fixed because there exists no potential in R . However, one can use A_i to restore continuity of the first derivative of the wave function at the matching radius A_i which is not inherently requested in the formalism. To justify the choice of the value for $A_i = 13.5$ fm the first derivative of the R -dependent part of the wave function should be continuous at $R = A_i$ for values of r that correspond to a k -value (Eq. (7.9)) or energy in the vicinity of the considered incident energy point. This is shown in Figs. 46 and 47 for the energy point 3.75 MeV.

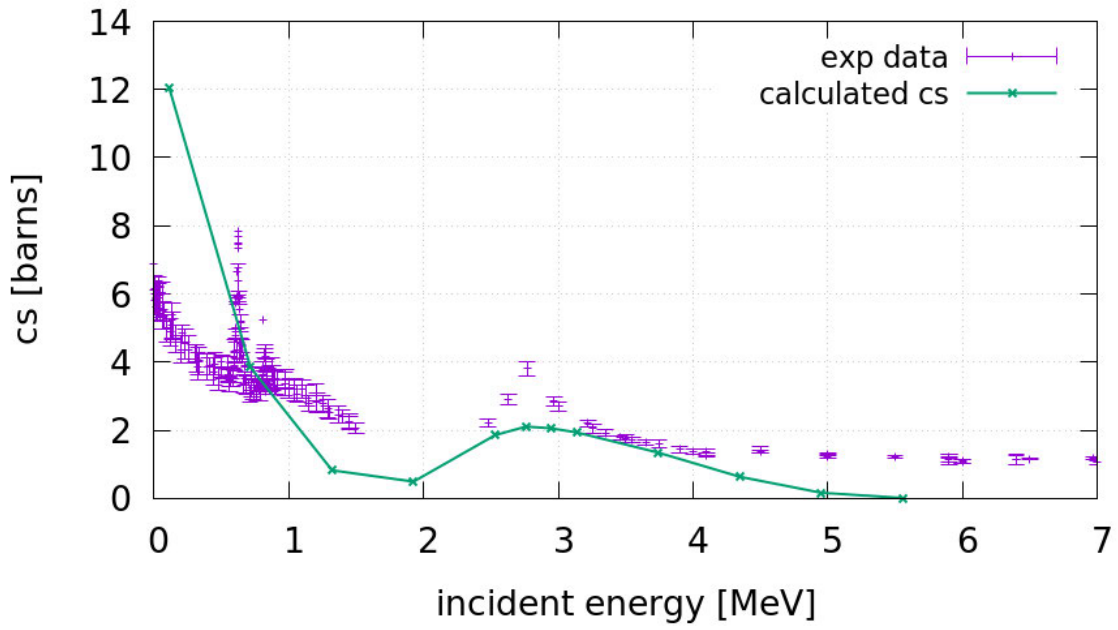


Figure 45: Elastic cross section for $\eta = 1.6$.

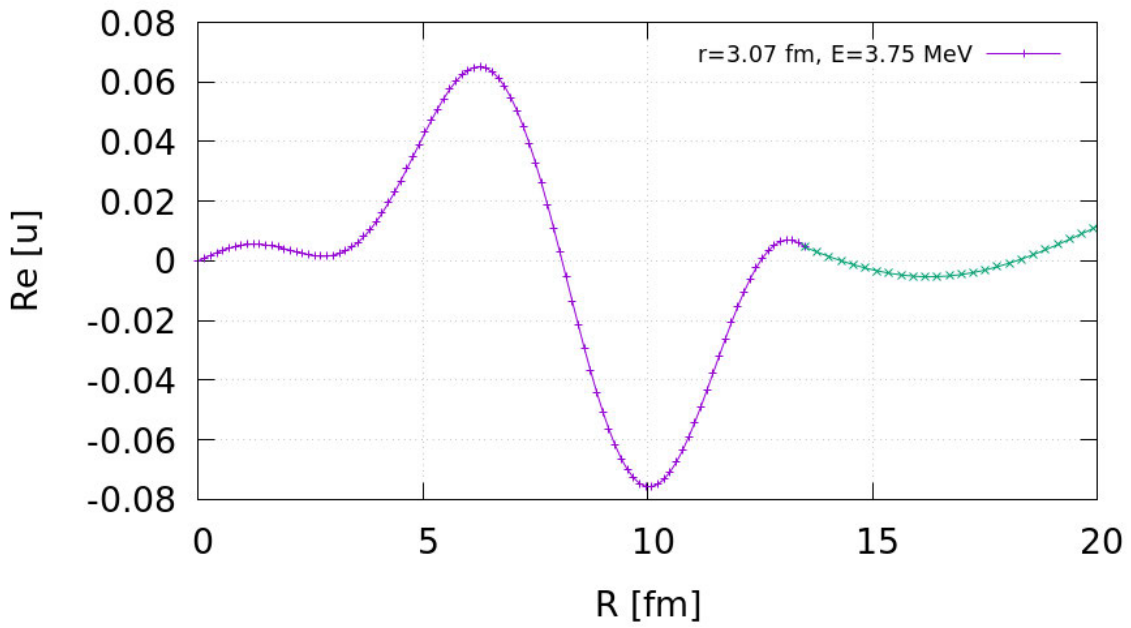


Figure 46: Real part of the wave function $u(r, R)$ for a fixed value of r in the interior (purple) and exterior (green) region.

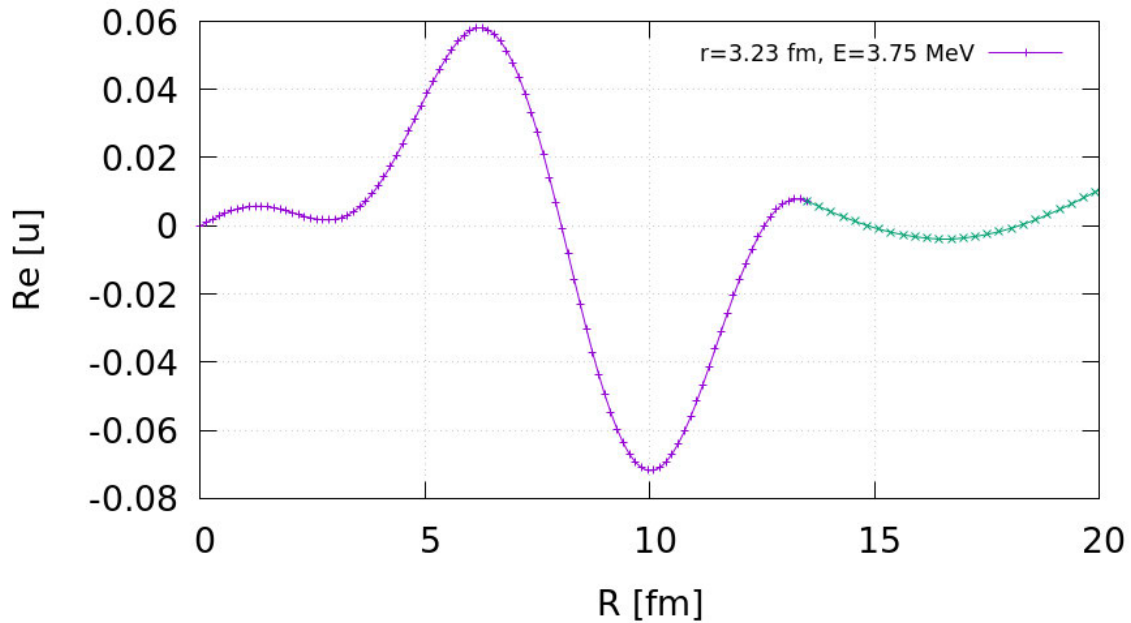


Figure 47: Real part of the wave function $u(r, R)$ for a fixed value of r in the interior (purple) and exterior (green) region.

Finally we also considered the optical theorem (5.110) for the $n+{}^9\text{Be}$ system which accounts for flux conservation. Fig. 48 reveals an excellent agreement of the optical theorem for energies greater than 1.3 MeV. One reason for the better agreement compared to the n +deuteron system might be the larger matching radii that we had to use in this system. Thus the asymptotic form of the three-body wave function seems more appropriate at the matching radii. Below 1.3 MeV the results are not reliable at all which was already visible in the elastic cross section data (Fig. 45).

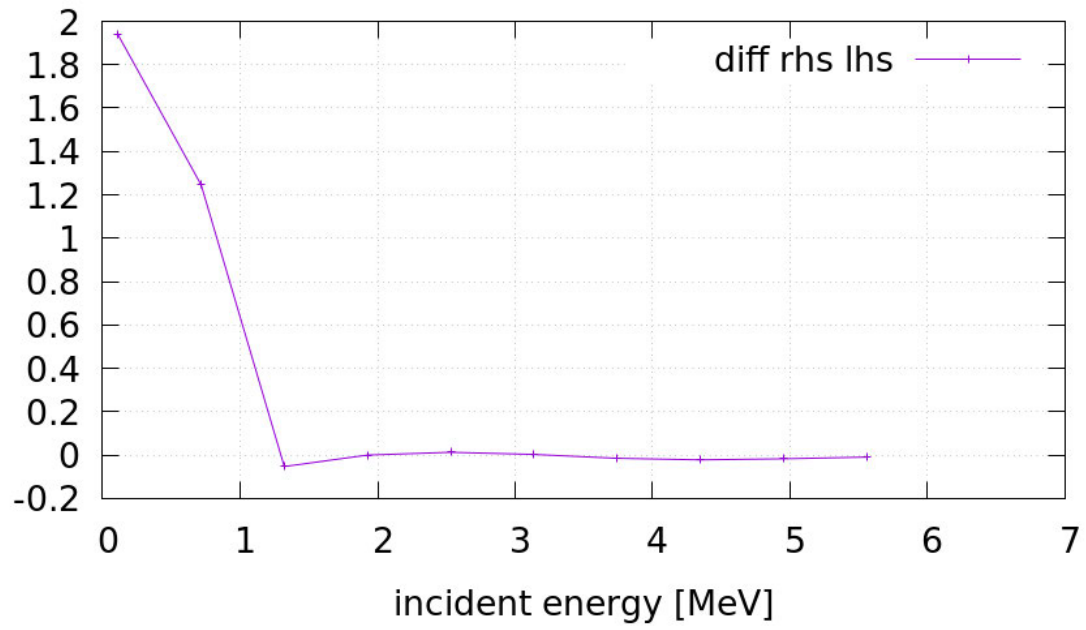


Figure 48: Total difference between left- and right-hand side of the optical theorem in Eq. (5.112)

8 Conclusion and Outlook

In light nuclear systems breakup channels with three or more fragments often occur even at low incident energies and can have a significant share on the total cross section. Consequently, approximative methods like the sequential approach are no longer appropriate to describe these channels. Hence, there was a need of a full quantum mechanical treatment of three-body processes in the frame of R -matrix theory.

Based on the Faddeev equations and the ideas of W. Glöckle [10] such a three-body R -matrix formalism was successfully developed for three arbitrary particles in [11]. In the present PhD thesis several essential modifications were elaborated and included into the formalism in order to make it applicable to nuclear systems. A numerical implementation was presented which is to our knowledge the first ever done for a three-body R -matrix formalism. The initial problem of an ill-conditioned system of linear equations for the expansion coefficients of the wave function in the interior region could be cured by introducing a regularization parameter.

We probed the novel formalism first on the neutron+deuteron system which is a genuine three-body system without any other nuclear structures. The results for the breakup cross section were impressively good and the calculated values as a function of the regularization parameter converged to the experimental data. A similar behavior was observed for the elastic cross section. However, in the energy range greater than 8 MeV the calculated results deviated significantly from the measured values. Studying this problem, we found an inherent deficiency of the three-body R -matrix formalism based on the Faddeev equations. The particles in the subsystem interact via a two-body potential which determines the matching radius a_i in the subsystem. However, the third particle is free and therefore exists no natural bound for the second matching radius A_i , which can be considered as a free parameter. In order to determine proper values for A_i we introduced the criterion of continuity of the first derivative of the wave function at the matching radius which was not included in the derivation of the formalism. Restoring the continuity of the three-body wave function for some areas of r (relative coordinate in the subsystem) we found values for A_i depending on the incident energy which led to a significant improvement of the elastic cross section. Finally, we obtained two energy regions with different values for the matching radii where a very good agreement of the calculated elastic and breakup cross section with experimental data was obtained.

The second system that was studied in the frame of the three-body R -matrix formalism is the $n+{}^9\text{Be}$ system which plays an important role as a neutron multiplier for tritium breeding in fusion reactors. The first breakup channel ${}^9\text{Be}(n,2n)({}^8\text{Be})$ energetically opens up at 1.664 MeV and was treated as an effective three-body channel by assuming that the α -particles form a long-lived resonance state (${}^8\text{Be}$). Because the three-body R -matrix formalism in its present form is elaborated for s-waves only, the problem of an $\ell = 1$ state in the $n+({}^8\text{Be})$ subsystem was solved by introducing the approximation of leaving the formalism unchanged, but using p-wave basis states for that subsystem which give the correct neutron density distribution. The numerical results for the breakup channel are in very good agreement with the experiment up to 4 MeV. The calculated elastic cross section shows similarities to the experimental data in shape although with problems below 1 MeV due to the appearance of the channel ${}^9\text{Be}(n,\alpha){}^6\text{He}$ which was not contained in the three-body structure of our model. For energies greater than 4 MeV we assume higher partial waves, which are not considered in the formalism, to contribute significantly.

Considering the optical theorem for both systems we observed a good fulfillment in case of the $n+{}^9\text{Be}$ system above 1 MeV. However, in the n +deuteron system there appear deviations. This may result from the fact that we use smaller matching radii in the n +deuteron system and the continuation of the asymptotic wave function to these small matching radii seems to be problematic. The consequence is a distortion of the phase in T -amplitudes which can be considered as an algorithm error. If the matching radii are increased the matching conditions between the interior and the asymptotic wave function improve which is reflected in a better fulfillment of the optical theorem as seen in the $n+{}^9\text{Be}$ system. However, increasing the matching radii implies a significant increase of the number of basis states for a fair reproduction of the interior wave function, which in turn extends the computation time dramatically.

In its present form the three-body R -matrix only exists as a calculable R -matrix, but not as a phenomenological one which is used for fitting procedures. For latter it is important to know its spectral representation which, however, is not yet established for the three-body case. Another task would be the extension of the formalism to higher partial waves than s-waves and hence making it applicable to higher energy regions.

In order to include this novel formalism into existing R -matrix evaluation processes one could insert T_i^b -amplitudes calculated, e.g. with the reduced R -matrix formalism elaborated in our group and then determine the breakup cross section via the three-

body R -matrix formalism. This would circumvent the problems appearing with the elastic channel in the three-body theory especially seen in case of the $n+{}^9\text{Be}$ system.

Acknowledgment

First I want to express gratitude to my supervisor Prof. Helmut Leeb. He spared no time and efforts to guide me through this thesis with great competence and experience. In many discussions we reviewed my ideas and I got new impulses and inspirations to proceed. It was quite challenging to elaborate and implement a novel formalism, but also very fulfilling and exciting to see your results getting better and better and finally approaching the experimental data. Doing something new is always a risk, but when you are successful it is a great satisfaction to know you could contribute to the progress in a scientific field.

Many thanks to my dear colleague and friend Thomas Srdinko who gave me lots of precious advices especially regarding computing and programming techniques. He is one of the most selfless and altruistic persons I have ever met. In addition I am very grateful for all the interesting things apart from physics that we did, discussed and I could learn from him not at least how to make the best Sacher cake in the world.

It was a great experience and pleasure to meet colleagues and friends during my studies coming from different countries of the world who expanded my horizons not only in scientific fields.

Finally I particularly want to thank my parents Maria and Franz and my brother Lukas for their great help and support in every sense during my time at Vienna University of Technology.

This work has been carried out within the framework of the EUROfusion Consortium and has received funding from the Euratom research and training programme 2014-2018 and 2019-2020 under grant agreement No 633053. The views and opinions expressed herein do not necessarily reflect those of the European Commission.

This work was also supported by the KKKÖ Matching Grant MG 2020-7 of the Austrian Academy of Sciences.

A Partial integration of Eq. (5.58)

In this section we consider the left hand side of Eq. (5.58) which reads,

$$\begin{aligned}
 & \iint_D dr dR \varphi_\mu(r, R) \left[-\frac{1}{2\mu_{jn}} \frac{d^2}{dr^2} + V(r) - \frac{1}{2\mu_{i(jn)}} \frac{d^2}{dR^2} - E \right] u(r, R) \\
 &= -\frac{1}{2\mu_{jn}} \int_0^A dR \int_0^a dr \varphi_\mu(r, R) \frac{d^2 u}{dr^2} - \frac{1}{2\mu_{i(jn)}} \int_0^a dr \int_0^A dR \varphi_\mu(r, R) \frac{d^2 u}{dR^2} \\
 &+ \int_0^a dr \int_0^A dR \varphi_\mu(r, R) [V(r) - E] u(r, R)
 \end{aligned} \tag{A.1}$$

and solve the occurring integrals via integration by parts. We can rewrite the terms containing second derivatives in Eq. (A.1) using the product rule twice (suppressing factors and the dependencies of the functions on spatial coordinates)

$$\frac{d^2}{dR^2}(\varphi_\mu u) = \frac{d}{dR} \left(\frac{d\varphi_\mu}{dR} u + \varphi_\mu \frac{du}{dR} \right) = \frac{d^2\varphi_\mu}{dR^2} u + \frac{d\varphi_\mu}{dR} \frac{du}{dR} + \frac{d\varphi_\mu}{dR} \frac{du}{dR} + \varphi_\mu \frac{d^2 u}{dR^2} \tag{A.2}$$

and isolate the term which occurs in Eq. (A.1),

$$\varphi_\mu \frac{d^2 u}{dR^2} = \frac{d^2}{dR^2}(\varphi_\mu u) - 2 \frac{d\varphi_\mu}{dR} \frac{du}{dR} - \frac{d^2\varphi_\mu}{dR^2} u. \tag{A.3}$$

Using relation (A.3), the integrals in the second line of Eq. (A.1) can be calculated beginning with the second one,

$$\begin{aligned}
& -\frac{1}{2\mu_{i(jn)}} \int_0^A dR \varphi_\mu(r, R) \frac{d^2 u}{dR^2} = -\frac{1}{2\mu_{i(jn)}} \int_0^A dR \left[\frac{d^2}{dR^2} [\varphi_\mu(r, R)u(r, R)] - 2 \frac{d\varphi_\mu}{dR} \frac{du}{dR} - \frac{d^2 \varphi_\mu}{dR^2} u \right] \\
& = -\frac{1}{2\mu_{i(jn)}} \frac{d}{dR} (\varphi_\mu(r, R)u(r, R)) \Big|_0^A + 2 \frac{1}{2\mu_{i(jn)}} \int_0^A dR \frac{d\varphi_\mu}{dR} \frac{du}{dR} + \frac{1}{2\mu_{i(jn)}} \int_0^A dR u(r, R) \frac{d^2 \varphi_\mu}{dR^2} \\
& = -\frac{1}{2\mu_{i(jn)}} \left(u(r, R) \frac{d\varphi_\mu}{dR} + \varphi_\mu(r, R) \frac{du}{dR} \right) \Big|_0^A \\
& \quad + 2 \frac{1}{2\mu_{i(jn)}} \left[\varphi_\mu(r, R) \frac{du}{dR} \Big|_0^A - \int_0^A dR \varphi_\mu(r, R) \frac{d^2 u}{dR^2} \right] + \frac{1}{2\mu_{i(jn)}} \int_0^A dR u(r, R) \frac{d^2 \varphi_\mu}{dR^2} \\
& = -\frac{1}{2\mu_{i(jn)}} \left[\underbrace{u(r, A) \frac{d\varphi_\mu}{dR} \Big|_{R=A}}_{=0} - \underbrace{u(r, 0) \frac{d\varphi_\mu}{dR} \Big|_{R=0}}_{=0} + \varphi_\mu(r, A) \frac{du}{dR} \Big|_{R=A} - \underbrace{\varphi_\mu(r, 0) \frac{du}{dR} \Big|_{R=0}}_{=0} \right] \\
& \quad + 2 \frac{1}{2\mu_{i(jn)}} \varphi_\mu(r, A) \frac{du}{dR} \Big|_{R=A} - \frac{1}{2\mu_{i(jn)}} \underbrace{\varphi_\mu(r, 0) \frac{du}{dR} \Big|_{R=0}}_{=0} - 2 \frac{1}{2\mu_{i(jn)}} \int_0^A dR \varphi_\mu(r, R) \frac{d^2 u}{dR^2} \\
& \quad + \frac{1}{2\mu_{i(jn)}} \int_0^A dR u(r, R) \frac{d^2 \varphi_\mu}{dR^2} \\
& = \frac{1}{2\mu_{i(jn)}} \varphi_\mu(r, A) \frac{du}{dR} \Big|_{R=A} - 2 \frac{1}{2\mu_{i(jn)}} \int_0^A dR \varphi_\mu(r, R) \frac{d^2 u}{dR^2} + \frac{1}{2\mu_{i(jn)}} \int_0^A dR u(r, R) \frac{d^2 \varphi_\mu}{dR^2}.
\end{aligned} \tag{A.4}$$

We integrated by parts in the second line of Eq. (A.4) and in the fifth and sixth line we made use of the boundary conditions (5.51),

$$\varphi_\mu(0, R) = \varphi_\mu(r, 0) = \frac{\partial \varphi_\mu(r, R)}{\partial r} \Big|_{r=a} = \frac{\partial \varphi_\mu(r, R)}{\partial R} \Big|_{R=A} = 0.$$

Additionally, $u(r, 0) = 0$ since we integrate over the domain D where

$$u(r, 0) = \sum_\mu c_\mu \varphi_\mu(r, 0) = 0. \tag{A.5}$$

Finally we get the result

$$\int_0^A dR \varphi_\mu(r, R) \frac{d^2 u}{dR^2} = \varphi_\mu(r, A) \left. \frac{du}{dR} \right|_{R=A} + \int_0^A dR u(r, R) \frac{d^2 \varphi_\mu}{dR^2} \quad (\text{A.6})$$

and analogously

$$\int_0^a dr \varphi_\mu(r, R) \frac{d^2 u}{dr^2} = \varphi_\mu(a, R) \left. \frac{du}{dr} \right|_{r=a} + \int_0^a dr u(r, R) \frac{d^2 \varphi_\mu}{dr^2}. \quad (\text{A.7})$$

Inserting them into Eq. (A.1) yields

$$\begin{aligned} & -\frac{1}{2\mu_{jn}} \int_0^A dR \varphi_\mu(a, R) \left. \frac{du}{dr} \right|_{r=a} - \frac{1}{2\mu_{jn}} \int_0^A dR \int_0^a dr u(r, R) \frac{d^2 \varphi_\mu}{dr^2} \\ & - \frac{1}{2\mu_{i(jn)}} \int_0^a dr \varphi_\mu(r, A) \left. \frac{du}{dR} \right|_{R=A} - \frac{1}{2\mu_{i(jn)}} \int_0^a dr \int_0^A dR u(r, R) \frac{d^2 \varphi_\mu}{dR^2} \\ & + \int_0^a dr \int_0^A dR \varphi_\mu(r, R) [V(r) - E] u(r, R) \\ = & -\frac{1}{2\mu_{jn}} \int_0^A dR \varphi_\mu(a, R) \left. \frac{du}{dr} \right|_{r=a} - \frac{1}{2\mu_{i(jn)}} \int_0^a dr \varphi_\mu(r, A) \left. \frac{du}{dR} \right|_{R=A} \\ & + \int_0^A dR \int_0^a dr u(r, R) \left[-\frac{1}{2\mu_{jn}} \frac{d^2}{dr^2} + V(r) - \frac{1}{2\mu_{i(jn)}} \frac{d^2}{dR^2} - E \right] \varphi_\mu(r, R) \\ = & -\frac{1}{2\mu_{jn}} \int_0^A dR \varphi_\mu(a, R) \left. \frac{du}{dr} \right|_{r=a} - \frac{1}{2\mu_{i(jn)}} \int_0^a dr \varphi_\mu(r, A) \left. \frac{du}{dR} \right|_{R=A} \\ & + \int_0^A dR \int_0^a dr (E_\mu - E) u(r, R) \varphi_\mu(r, R) \\ = & -\frac{1}{2\mu_{jn}} \int_0^A dR \varphi_\mu(a, R) \left. \frac{du}{dr} \right|_{r=a} - \frac{1}{2\mu_{i(jn)}} \int_0^a dr \varphi_\mu(r, A) \left. \frac{du}{dR} \right|_{R=A} + (E_\mu - E) c_\mu \end{aligned} \quad (\text{A.8})$$

In the third equality we applied Eq. (5.50),

$$\left[-\frac{1}{2\mu_{jn}} \frac{d^2}{dr^2} + V(r) - \frac{1}{2\mu_{i(jn)}} \frac{d^2}{dR^2} - E_\mu \right] \varphi_\mu(r, R) = 0$$

and in the last line we used the definition of the expansion coefficients (5.53) for the interior wave function,

$$c_\mu = \iint_D dr dR \varphi_\mu(r, R) u(r, R).$$

B Experimental data for the neutron+deuteron system

B.1 Breakup cross section

incident energy [MeV]	Δ incident energy [MeV]	$\sigma_{breakup}$ [mbarn]	$\Delta\sigma_{breakup}$ [mbarn]	Ref
5.54	0.080	57.6	3.3	[24]
5.81	0.090	60.5	3.4	[24]
6.34	0.100	74.9	4.2	[24]
6.83	0.100	74.6	4.2	[24]
6.83	0.150	82.6	11.2	[24]
7.23	0.150	85.5	6.2	[24]
7.75	0.150	98.6	7.2	[24]
20.2	0.4	172.4	14.1	[24]
21.2	0.4	153.7	11.8	[24]
21.6	0.4	128.9	10.9	[24]
21.8	0.3	142.6	11	[24]
21.8	0.3	136.3	10.1	[24]
21.8	0.4	131.8	12.1	[24]
22.4	0.3	134.1	10.9	[24]
23	0.3	132.1	11.5	[24]
23.5	0.3	154.4	12.2	[24]
24.1	0.3	141.6	13.8	[24]
24.7	0.3	141.8	11	[24]
7.41	0.165	109	17	[25]
7.93	0.15	138	15	[25]
8.44	0.135	127	13	[25]
8.94	0.125	137	10	[25]
9.44	0.115	149	11	[25]
9.93	0.11	120	10	[25]
10.42	0.1	142	19	[25]
10.91	0.095	146	10	[25]
11.4	0.09	165	10	[25]
11.88	0.085	148	10	[25]
12.36	0.085	155	13	[25]
12.85	0.08	165	14	[25]
13.33	0.075	165	14	[25]
13.8	0.075	175	14	[25]
14.28	0.07	168	14	[25]
14.76	0.065	180	14	[25]

incident energy [MeV]	Δ incident energy [MeV]	$\sigma_{breakup}$ [mbarn]	$\Delta\sigma_{breakup}$ [mbarn]	Ref
14.8	-	145	15	[26]
8.2	-	103	10	[27]
12.17	-	176	14	[27]
13.66	-	181	13	[27]
14	-	172	12	[27]
14.8	-	176	14	[27]
16.05	-	181	12	[27]
17.4	-	172	12	[27]
18.8	-	180	17	[27]
20.02	-	179	16	[27]
21.07	-	180	17	[27]
22	-	176	16	[27]
14.1	0.075	183	3	[28]
14.46	-	158	16	[29]
4.10	-	13	8	[30]
4.40	-	17	7	[30]
4.60	-	25	6	[30]
4.90	-	34	6	[30]
5.20	-	45	6	[30]
5.85	-	61	7	[30]
6.30	-	60	7	[30]
6.55	-	64	7	[30]
14.1	0.075	180	7	[31]
14.1	0.2	107	20	[32]
6.11	-	67	6.7	[33]
6.55	-	73	7.3	[33]
7.32	-	88	8.8	[33]
8.26	-	110	9.9	[33]
10.2	-	140	15.4	[33]
14.1	-	180	19.8	[34]
14.1	0.075	128	2	[35]

B.2 Elastic cross section

incident energy [MeV]	$\sigma_{breakup}$ [mbarn]	$\Delta\sigma_{breakup}$ [mbarn]	Ref
0.000000027743	3440	60	[36]
2.5	2375	140	[37]
3	2149	129	[37]
3.5	1985	119	[37]
4	1863	112	[37]
4.5	1723	103	[37]
5	1608	96	[37]
6	1448	87	[37]
7	1254	75	[37]
8	1120	67	[37]
9	1028	62	[37]
10.25	938	56	[37]
12	819	49	[37]
14	694	42	[37]
16	607	36	[37]
18	523	31	[37]
20	463	28	[37]
22.5	395	32	[37]
25	334	27	[37]
27.5	299	24	[37]
30	264	26	[37]
2.480	2450	15	[38]
3.270	2145	13	[38]
5.55	1480	0	[39]
7	1267	0	[39]
8	1127	0	[39]
9	1002	0	[39]
18.55	486	39	[39]
20.5	442	36	[39]
23	399	35	[39]
0.135	4800	340	[40]
0.280	3790	220	[40]
0.446	3100	290	[40]
0.588	3140	200	[40]
0.780	3180	170	[40]
0.914	3290	200	[40]

References

- [1] <https://www-nds.iaea.org/exfor>
- [2] D. A. Brown et al., Nuclear Data Sheets **148**, p. 1-142 (2018)
- [3] A. J. N. Plompen et al., Europ. Phys. J. A **56**, 181 (2020)
- [4] K. Shibata et al., Journal of Nuclear Science and Technology 48, p 1-30 (2011)
- [5] A. Trkov and D.A. Brown, <https://www.osti.gov/biblio/1425114> (2018)
- [6] B. Raab, Th. Srdinko, H. Leeb, EPJ Web of Conferences 211, 07006 (2019)
- [7] E.P. Wigner, L. Eisenbud, Phys. Ref. **72**, 29 (1947)
- [8] A.M. Lane, R.G. Thomas, Rev.Modern Phys. **30**, 257 (1958)
- [9] L.D. Faddeev, Soviet Phys. JETP **12**, 1014 (1961)
- [10] W. Glöckle, Z. Phys. **271**, 31 (1974)
- [11] B. Raab, *A Faddeev based R-matrix method*, (Master thesis, TU Wien, 2017)
- [12] P. Descouvemont, D. Baye, Rep. Prog. Phys. **73**, 036301 (2010)
- [13] B. Raab, Th. Srdinko, H. Leeb, EPJ Web of Conferences 239, 03002 (2020)
- [14] C.W. Reich and M.S. Moore, Phys. Rev. **111**, 929 (1958)
- [15] H. Leeb, private communications (2021)
- [16] Th. Srdinko, T. Stary, private communications (2021)
- [17] C. Bloch, Nucl. Phys. **4**, 503 (1957)
- [18] W. Glöckle, "The Quantum Mechanical Few-Body Problem", Springer Verlag, ISBN-13:978-3-642-82083-0
- [19] W. Glöckle, Nucl. Phys. **A141**, 620 (1970)
- [20] P. Fröbrich and R. Lipperheide "Theory of Nuclear Reactions", Clarendon Press, Oxford 1996 ISBN 0 19 853783 2
- [21] E.W. Schmid, H. Ziegelmann, "The Quantum Mechanical Three-Body Problem", Vieweg, ISBN 3 528 08337 9
- [22] V. G. J. Stoks, R. A. M. Klomp, M. C. M. Rentmeester and J. J. de Swart, Phys. Rev. C **48** 792 (1993)
- [23] A. Koning et al., "The JEFF-3.1 Nuclear Data Library", Report 21, OECD (2006)

- [24] J.-M.Laborie et al., European Physical Journal A: Hadrons and Nuclei Vol.48, p.87 (2012)
- [25] J. Frehaut et al., Radiation Effects Vol.96, p.219 (1986)
- [26] K. Gul et al., Jour. of Physics, Part G (Nucl.and Part.Phys.) Vol.5, Issue.8, p.1107 (1979)
- [27] G. Pauletta, F.D.Brooks, Nuclear Physics, Section A Vol.255, p.267 (1975)
- [28] N. Koori, Journal of the Physical Society of Japan Vol.32, p.306 (1972)
- [29] E.R. Graves, J.D. Seagrave, U.S.AEC Nucl.Cross Sections Advisory Comm. Repts No.42, p.158 (1971)
- [30] M. Holmberg, Nuclear Physics, Section A Vol.129, p.327 (1969)
- [31] S. Shirato, N. Koori, Nuclear Physics, Section A Vol.120, p.387 (1968)
- [32] G. Vedrenne, D.Blanc, F. Cambou, Journal de Physique Vol.24, p.801 (1963)
- [33] H.C. Catron et al., Physical Review Vol.123, p.218 (1961)
- [34] V.J. Ashby et al., Physical Review Vol.111, p.616 (1958)
- [35] N. Koori, Journal of the Physical Society of Japan Vol.32, p.306 (1972)
- [36] E. Fermi, L. Marshall, Physical Review Vol.75, p.578 (1949)
- [37] P. Schwarz, et al., Nuclear Physics, Section A Vol.398, Issue.1, p.1 (1983)
- [38] P. Chatelain et al., Nuclear Physics, Section A Vol.319, p.71 (1979)
- [39] J.D. Seagrave et al., Annals of Physics (New York) Vol.74, p.250 (1972)
- [40] P.R. Tunncliffe, Physical Review Vol.89, p.1247 (1953)

Curriculum vitæ

Name	Benedikt Raab
Address	██
Date of birth	██████████
Nationality	Austrian
Religion	██████████
Marital status	██████████
Mobile	██████████
E-mail	benedikt.raab@tuwien.ac.at

PROFESSIONAL EXPERIENCE

Jan. 2018 - May 2022	Project assistant at the Atominstitut, <i>Vienna University of Technology</i> in the project "Nuclear data evaluation and processing", partly supported by EUROfusion grant agreement 633053 and KKKÖ grant of the Austrian Academy of Sciences
-----------------------------	---

EDUCATION

Jan. 2018 - present	PhD student at the Atominstitut, <i>Vienna University of Technology</i> , PhD thesis: "A novel three-body <i>R</i> -matrix formalism for breakup reactions in light nuclear systems"
November 2017	Master of Science (MSc) in Technical physics with distinction, <i>Vienna University of Technology</i>
Oct. 2014 - Nov. 2017	Master studies Technical physics, <i>Vienna University of Technology</i> , Master's thesis: "A Faddeev based <i>R</i> -Matrix Theory"

July 2014	Bachelor of Science (BSc) in Technical physics with distinction, <i>Vienna University of Technology</i>
Oct. 2010 - July 2014	Bachelor studies Technical physics, <i>Vienna University of Technology</i>
Sep. 2009 - Mar. 2010	Military service in the Austrian army
June 2009	Final exam (Matura) with distinction (1.0)
2001 - 2009	Secondary school (Gymnasium) in Gmünd, Lower Austria
1997 - 2001	Primary school in Weitra, Lower Austria

LANGUAGES

German	first language
English	fluent written and spoken
Latin	good reading and writing skills

PUBLICATIONS

B. Raab, Th. Srdinko, H. Leeb:
”*Formulation of Model Defects Suitable for the Resonance Regime*”;
In Proc. WONDER-2018 – 5th International Workshop On Nuclear
Data Evaluation for Reactor applications, Aix-en-Provence 2018;
EPJ Web Conf., Volume 211, 2019

B. Raab, Th. Srdinko, H. Leeb:
”*Developments regarding three-body reaction channels
within the R-matrix formalism*”;
In Proc. Int. Conference on Nuclear Data for Science and Technology
(ND 2019), Beijing 2019;
EPJ Web Conf., Volume 239, 2020